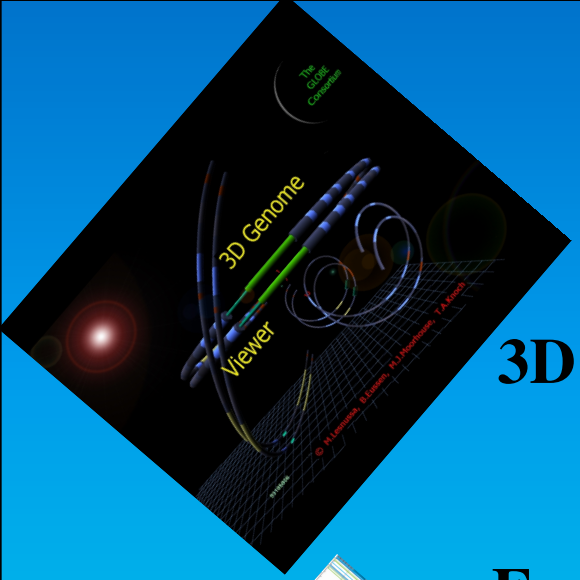

The Detailed 3D Multi-Loop Aggregate/Rosette Chromatin Architecture and Functional Dynamic Organization of the Human and Mouse Genomes

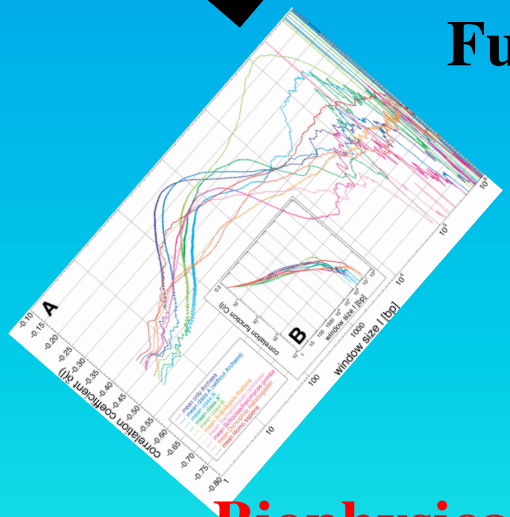

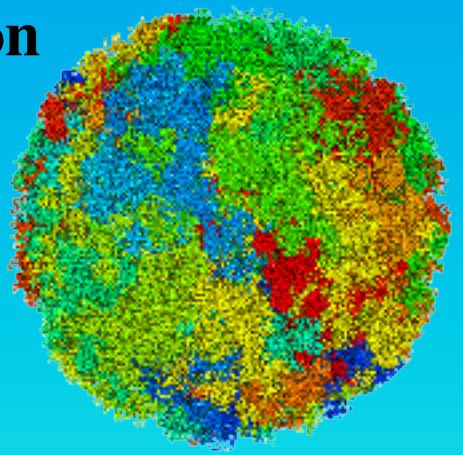

Tobias A. Knoch

Biophysical Genomics & Erasmus Computing Grid

Erasmus Medical Center

TA.Knoch@taknoch.org

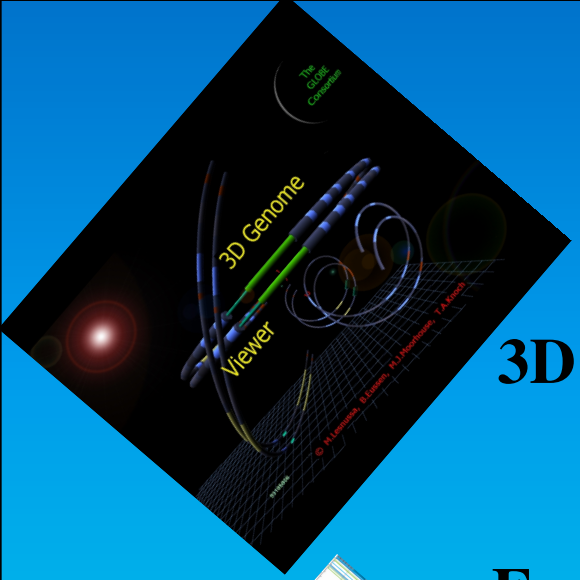

The Detailed 3D Multi-Loop Aggregate/P… Chromatin Archit… and Functional Dyn… …tion

Hum… …Genomes

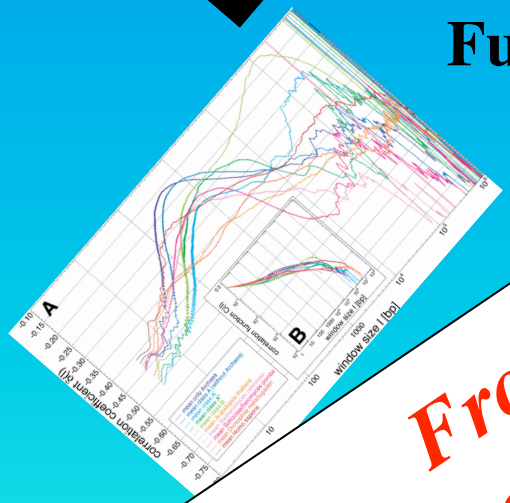

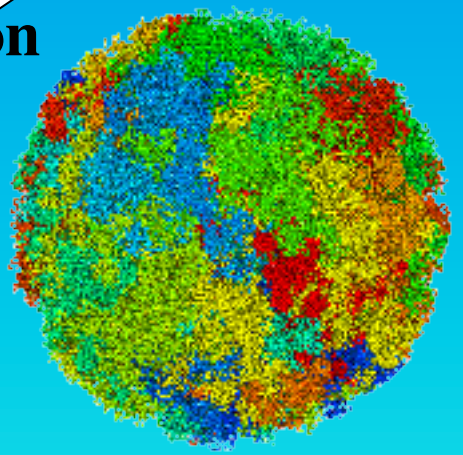

From Sequence to Morphology: Towards a Holistic Understanding of Genomes!

…bias A. Knoch

…enomics & Erasmus Computing Grid

Erasmus Medical Center

TA.Knoch@taknoch.org

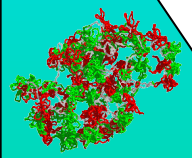

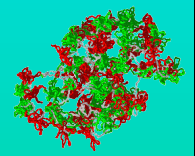

Dynamic and Hierarchical Genome Organization

The different organization levels of genomes bridge several orders of magnitude concerning space and time. How all of these organization levels connect to processes like gene regulation, replication, embryogeneses, or cancer development is still unclear?

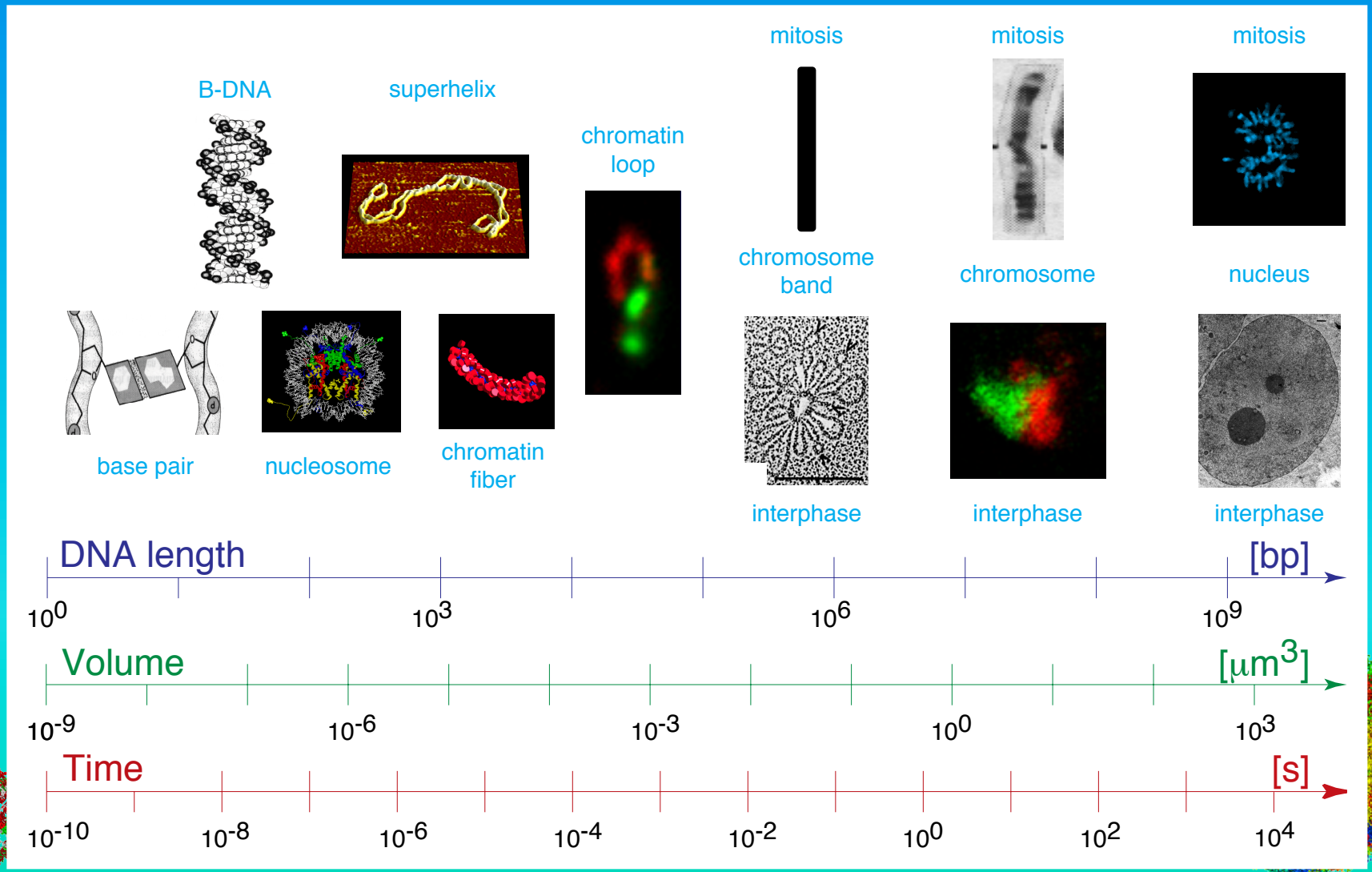

Chromatin Conformation and Higher-Order Topologies

It becomes increasingly clearer, that the chromatin conformation is a random organization of nucleosomes, which depending on external or modification conditions has different condensation degrees, with a prevalence for the 30nm fiber with ~6nucleosomes per 11nm. This seems to make loops which further cluster to form aggregates more or less rosette-like which then constitute the chromosome.

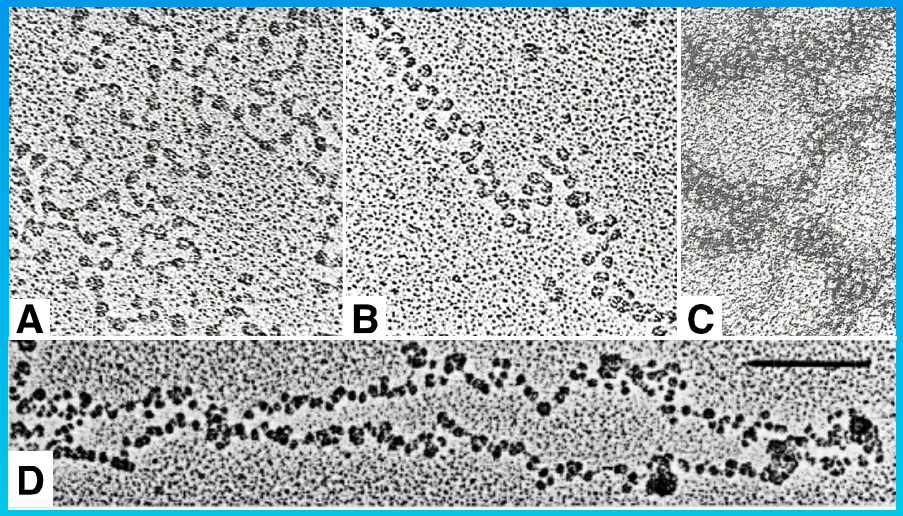

A-C: Voet & Voet D: Reznik *et al.*

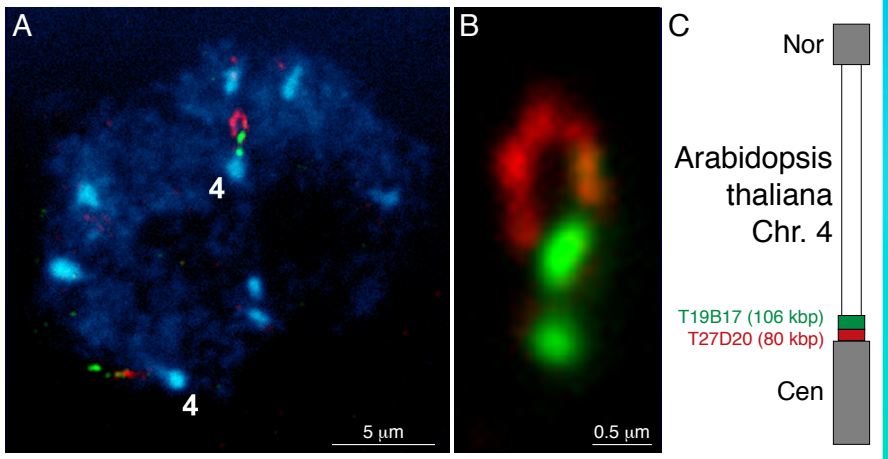

Courtesy P. Fransz, Amsterdam

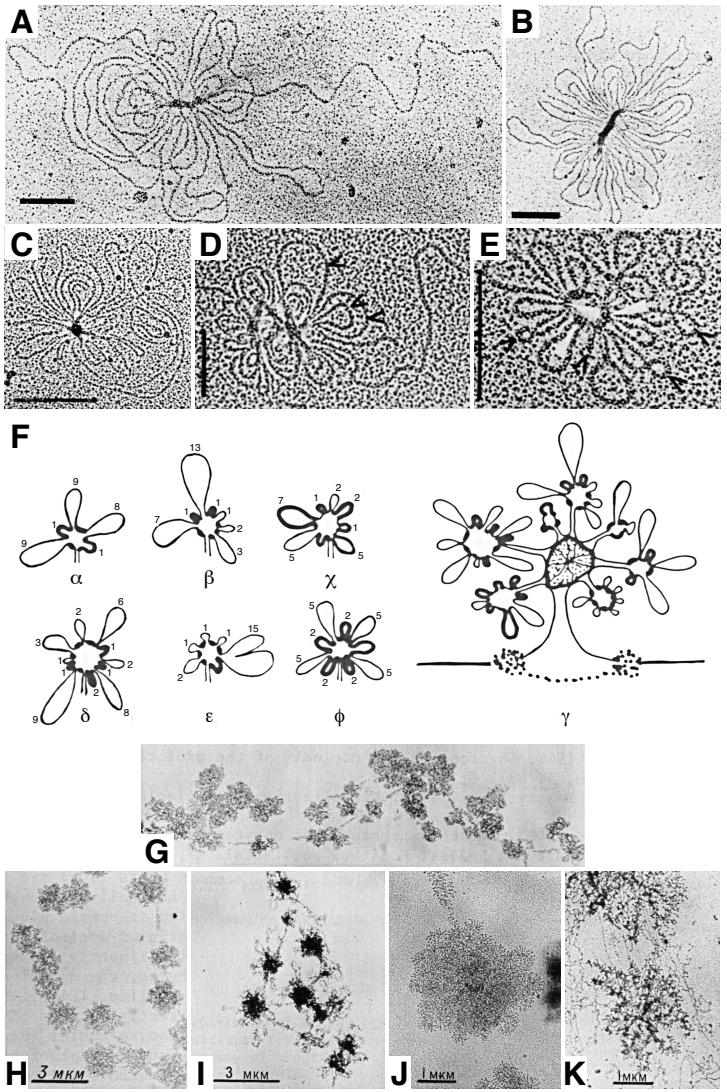

A, B: Avramova *et al.*; C: Salganik *et al.*; D-G:Frznik *et al.*; G-K: Tsvetkov & Parvenov.

Integral Models of Cell Nuclear Organization I

Already Rabl and Boveri were aware of the obvious fact that the organization of genomes has to be consistent from the sequence level to the morphology of the whole cell nucleus. Although they might be different in detail their common seem is recursive folding and clustering thereof with variation/ modification and dynamics accounting for different nuclear states and function.

Rabl & Boveri

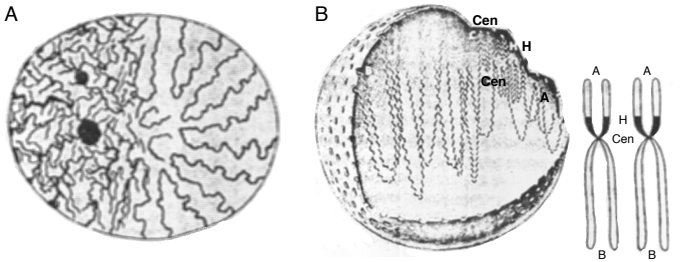

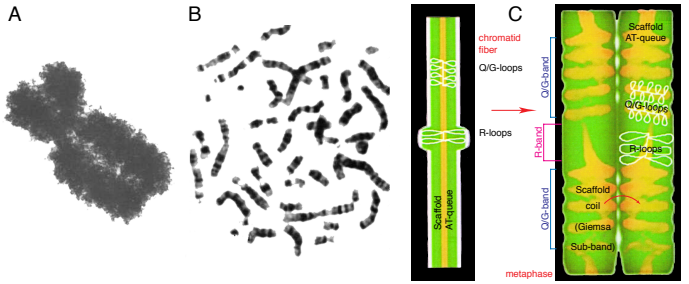

A: Bloom & Fawcett
B: Alberts *et al.*
C: Paulson & Laemmli

A, B: Pienta & Coffey; C: Alberts *et al.*; D: Belmont & Bruce

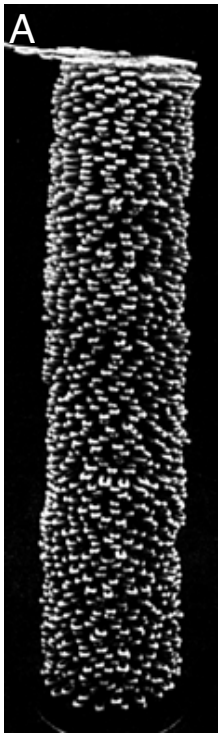

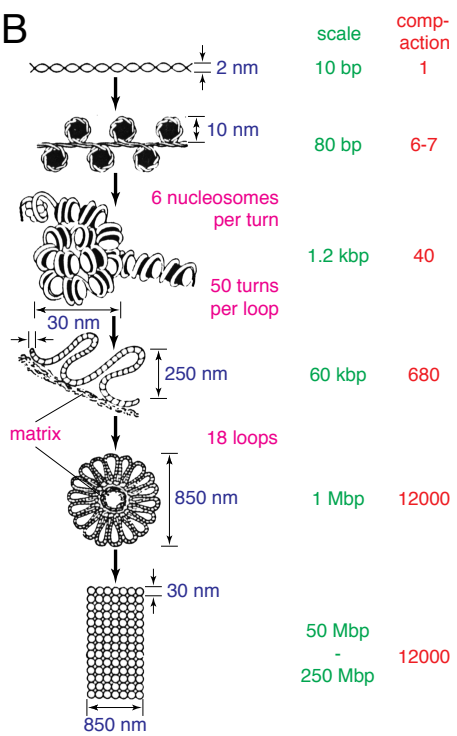

scale	comp-action
10 bp	1
80 bp	6-7
1.2 kbp	40
60 kbp	680
1 Mbp	12000
50 Mbp - 250 Mbp	12000

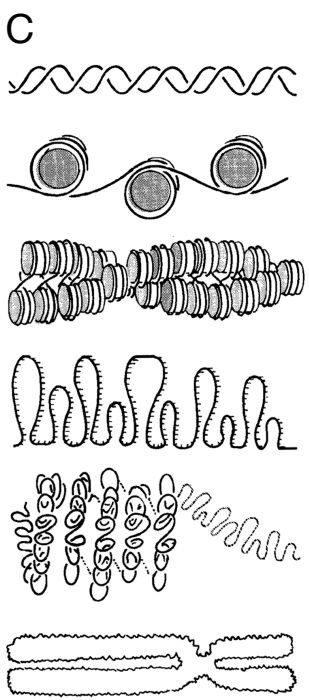

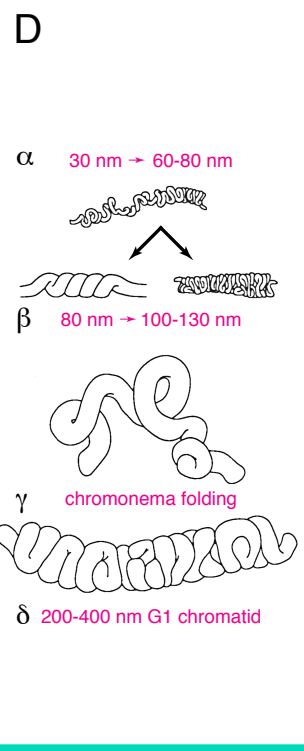

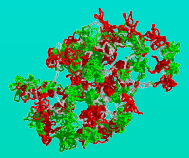

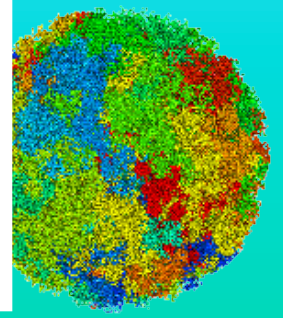

Integral Models of Cell Nuclear Organization

The biggest advantage of integral models is the again obvious and simple fact, that they allow the validation from the consistency of different levels of organization from the other levels. Thus, e.g. the so called Interchromosmal Domain Model can be ruled out by simple volumenous thought…

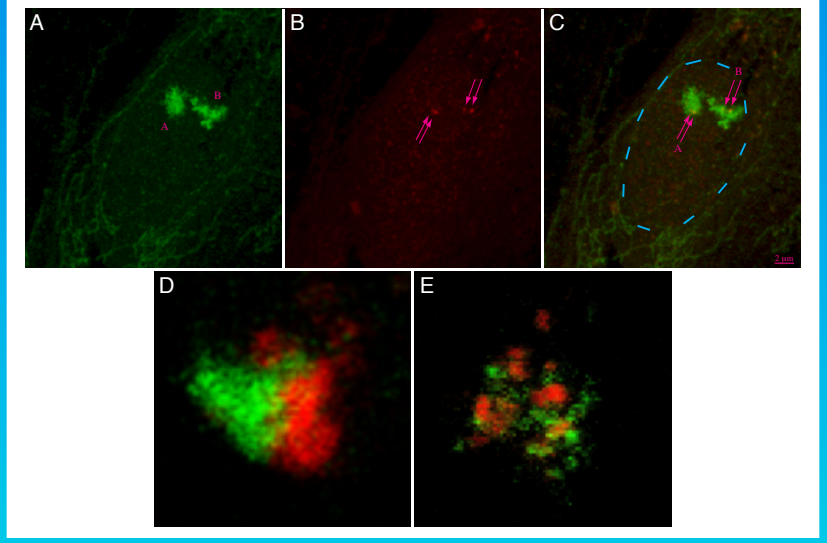

D: courtesy S. Dietzel; E: courtesy D. Zink

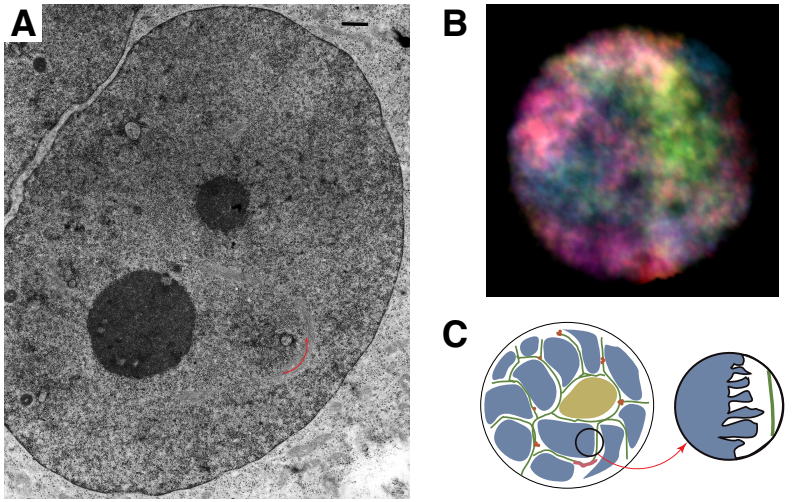

A: courtesy K. Richter; B: courtesy K. Greulich-Bode

Random-Walk/Giant-Loop Multi-Loop-Subcompatment Model

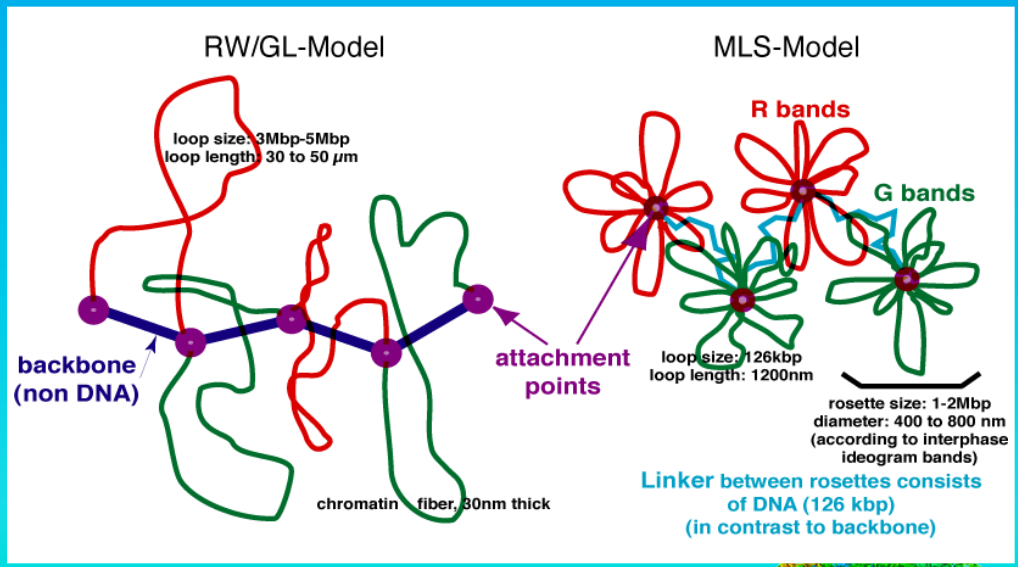

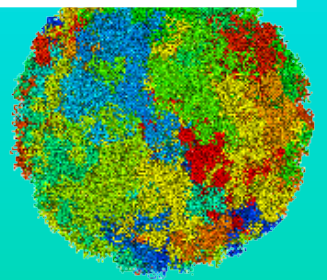

Selective Chromosome Interaction Capture (T2C)

T2C is a novel selective high-resolution high-throughput chromosome interaction capture, in which the relation between, region size, resolution, interaction frequency range, and sequencing depth can be designed towards the goal of the experiment. T2C reaches the limit of the “genomic” uncertainty principle and statistical mechanics.

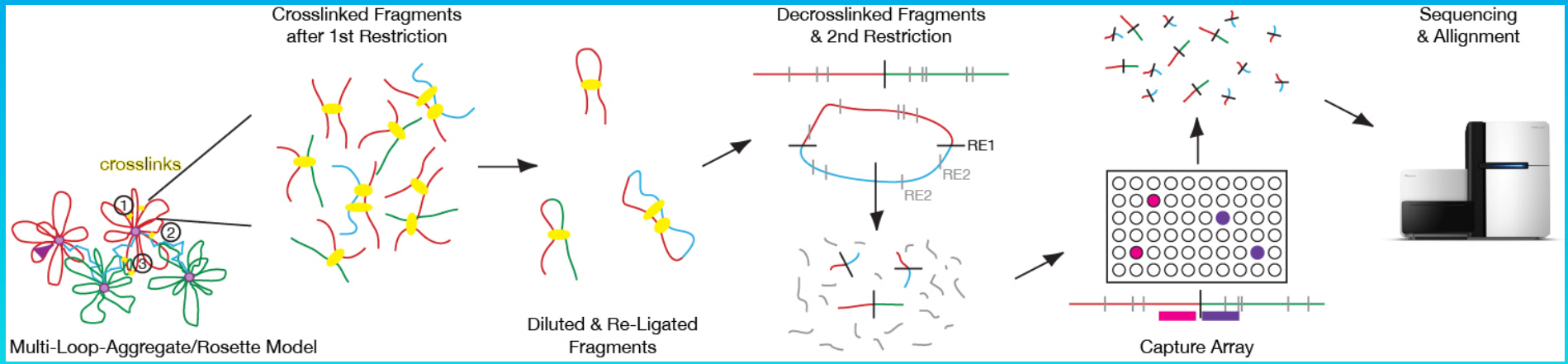

Selective Chromosome Interaction Capture (T2C)

T2C is a novel selective high-resolution high-throughput chromosome interaction capture, in which the relation between, region size, resolution, interaction frequency range, and sequencing depth can be designed towards the goal of the experiment. T2C reaches the limit of the "genomic" uncertainty principle and statistical mechanics.

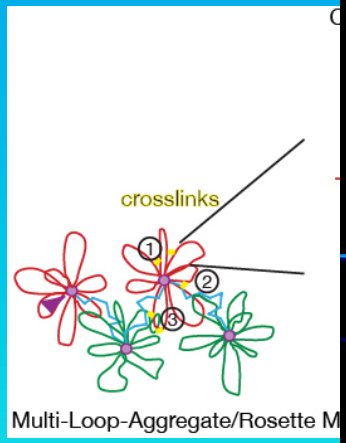

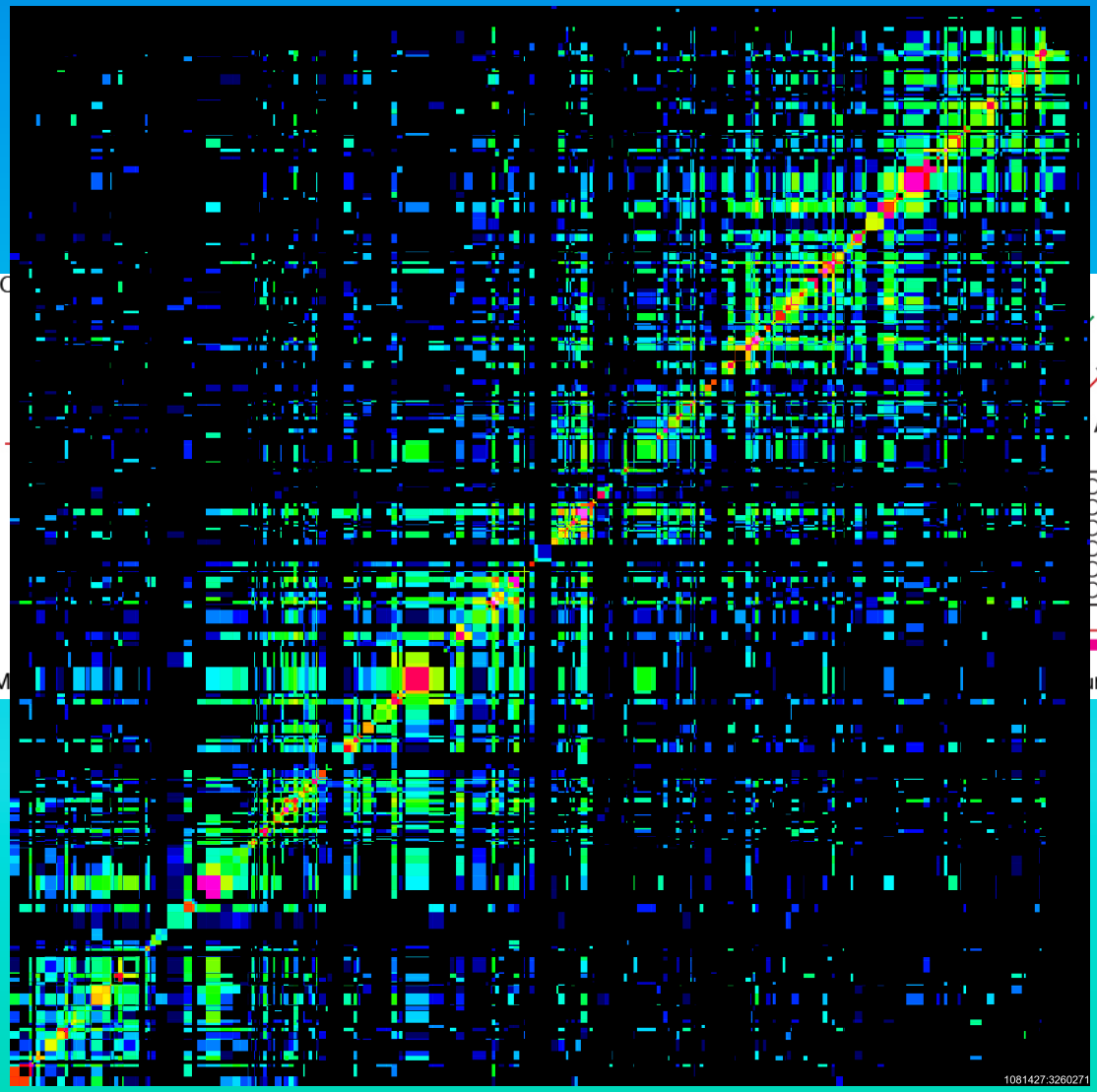

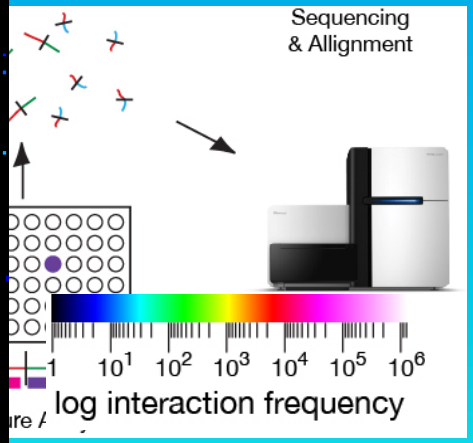

HS IGF locus
~2.1 Mbp

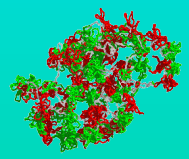

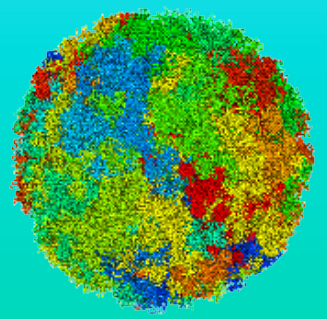

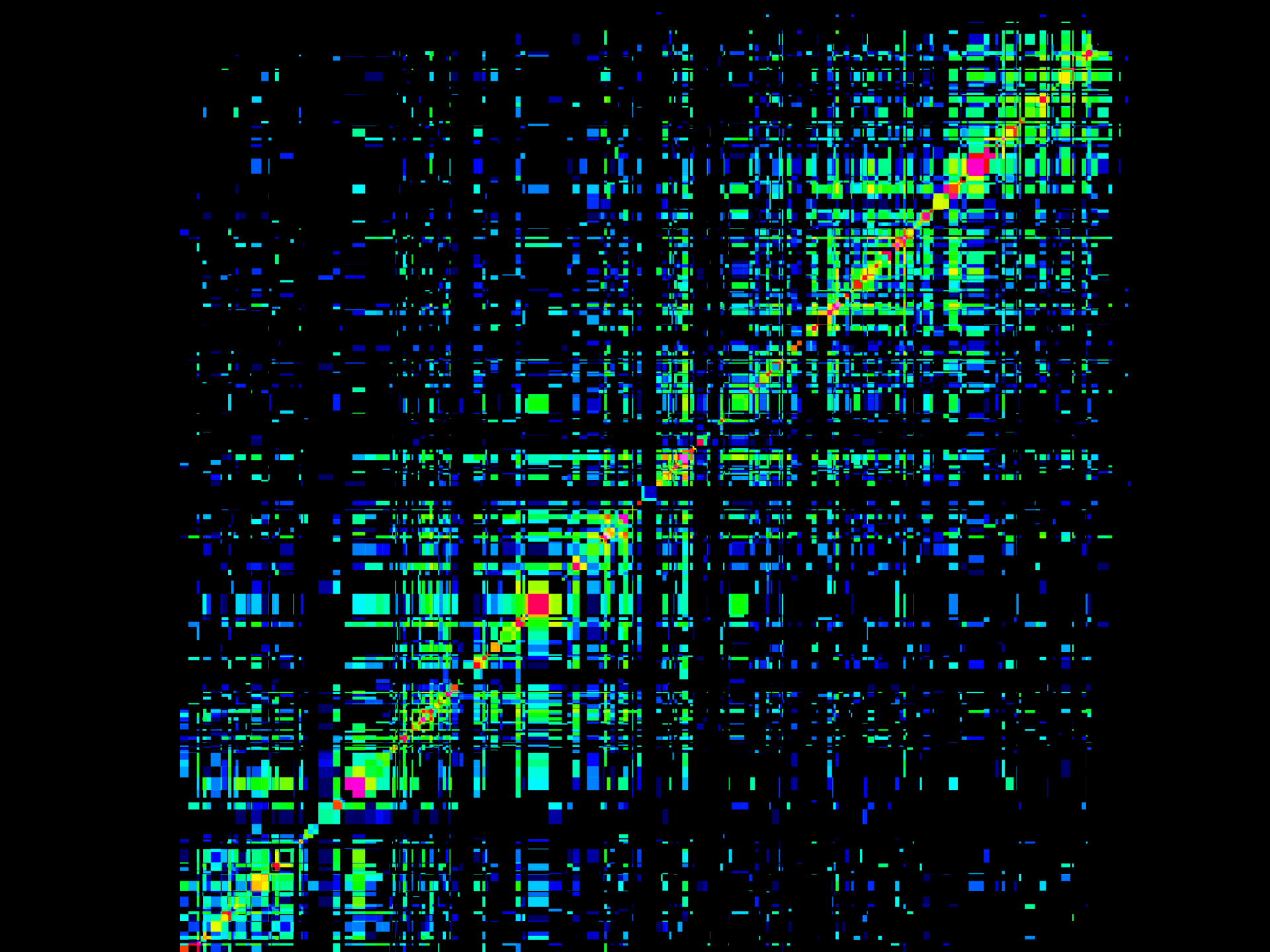

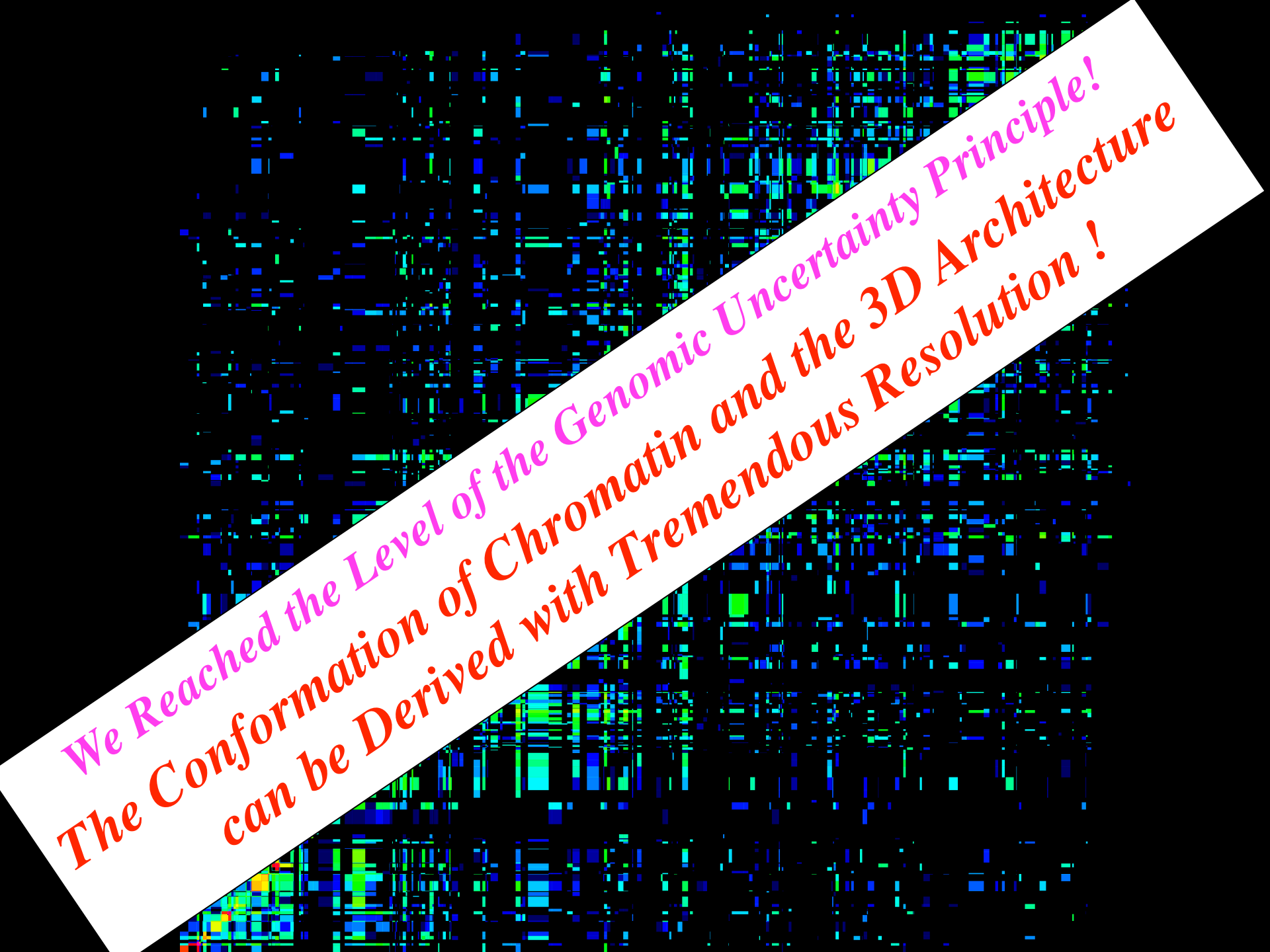
We Reached the Level of the Genomic Uncertainty Principle!
The Conformation of Chromatin and the 3D Architecture
can be Derived with Tremendous Resolution !

Stable Consensus Architecture of Genomes

Due to the high signal-to-noise ratio of T2C reaching 5-6 orders of magnitude interaction maps reveal definitely an extremely high degree of similarity between different species, cell types, or functional states, thus functional differences are variation of a stable theme persisting through the cell cycle

HB2

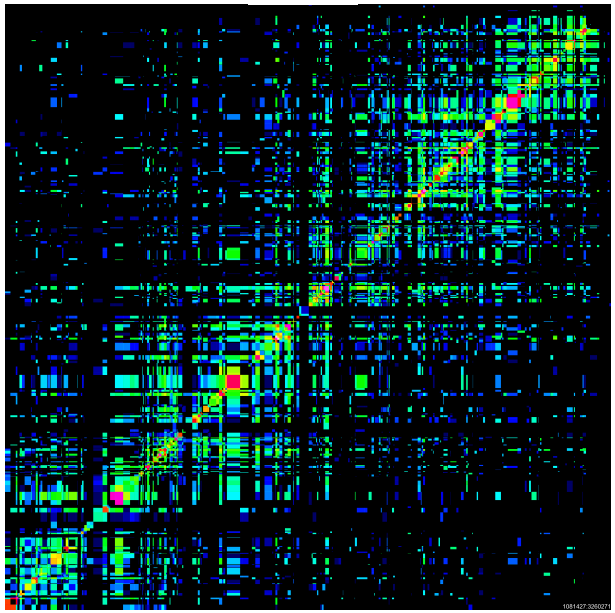

TEV-HEK293T cohesin intact

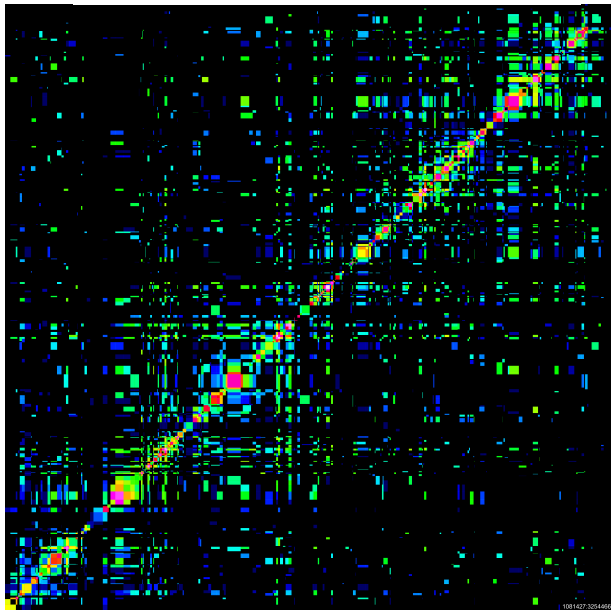

HRV-HEK293T cohesin cleaved

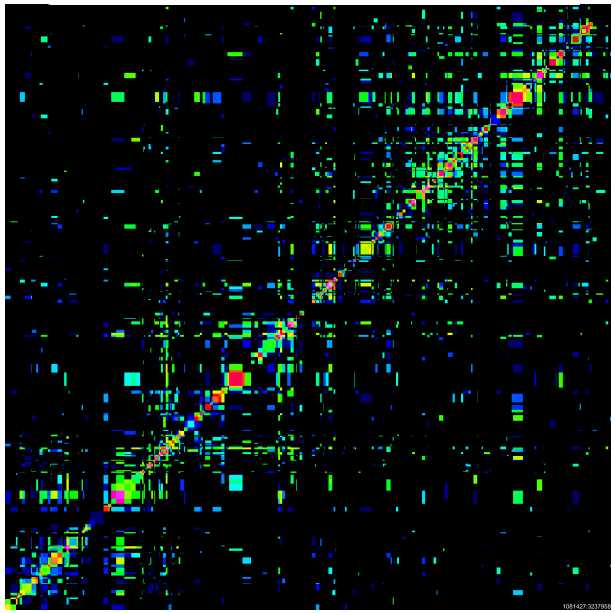

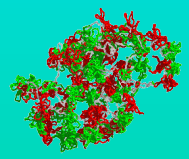

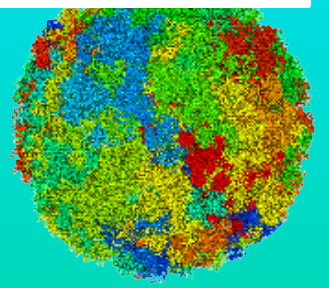

Stable Consensus Architecture of Genomes

Due to the high signal-to-noise ratio of T2C reaching 5-6 orders of magnitude interaction maps reveal definitely an extremely high degree of similarity between different species, cell types, or functional states, thus functional differences are variation of a stable theme persisting through the cell cycle

Fetal Brain (inactive β-Globin)

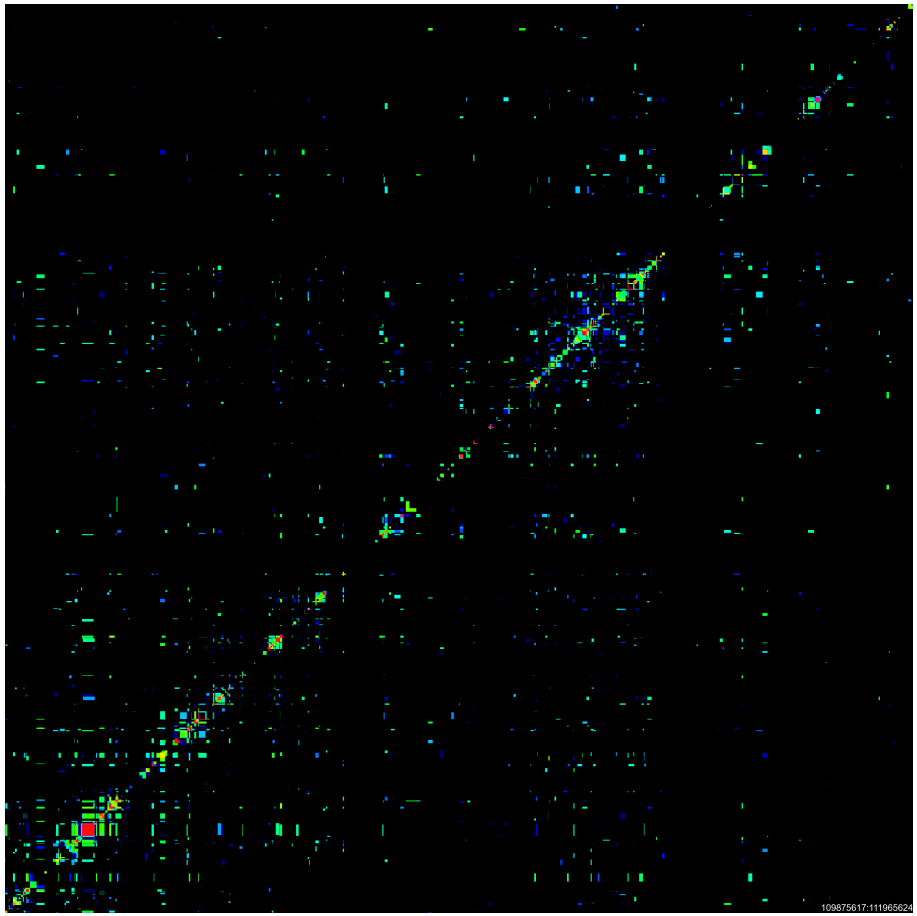

Fetal Liver (active β-Globin)

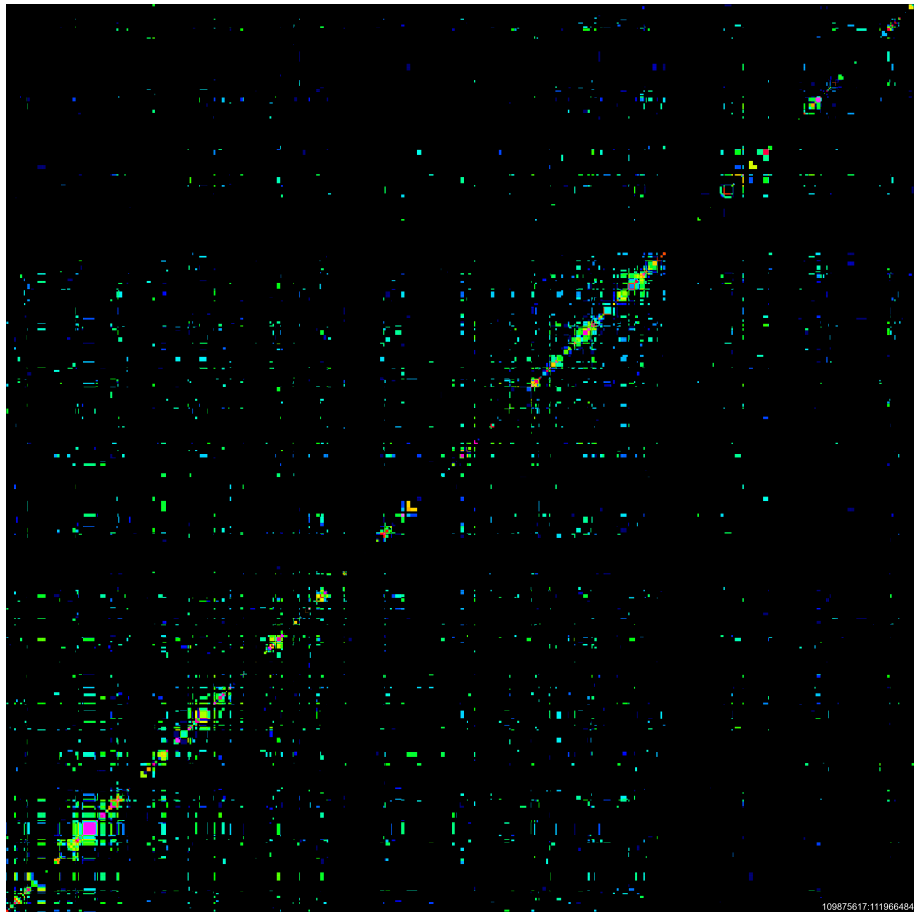

MM β-Globin 2.1 Mbp

Fine Structure of Loop Aggregates/Rosettes

Depending on the resolution, the loops within a domain an their arrangement in loop aggregates/rosettes can be shown as well as the details of how the loops are organized at their base as well as their aggregated rosette core: parallel loop fibres exist at the loop base with ~6kbp and these form the core.

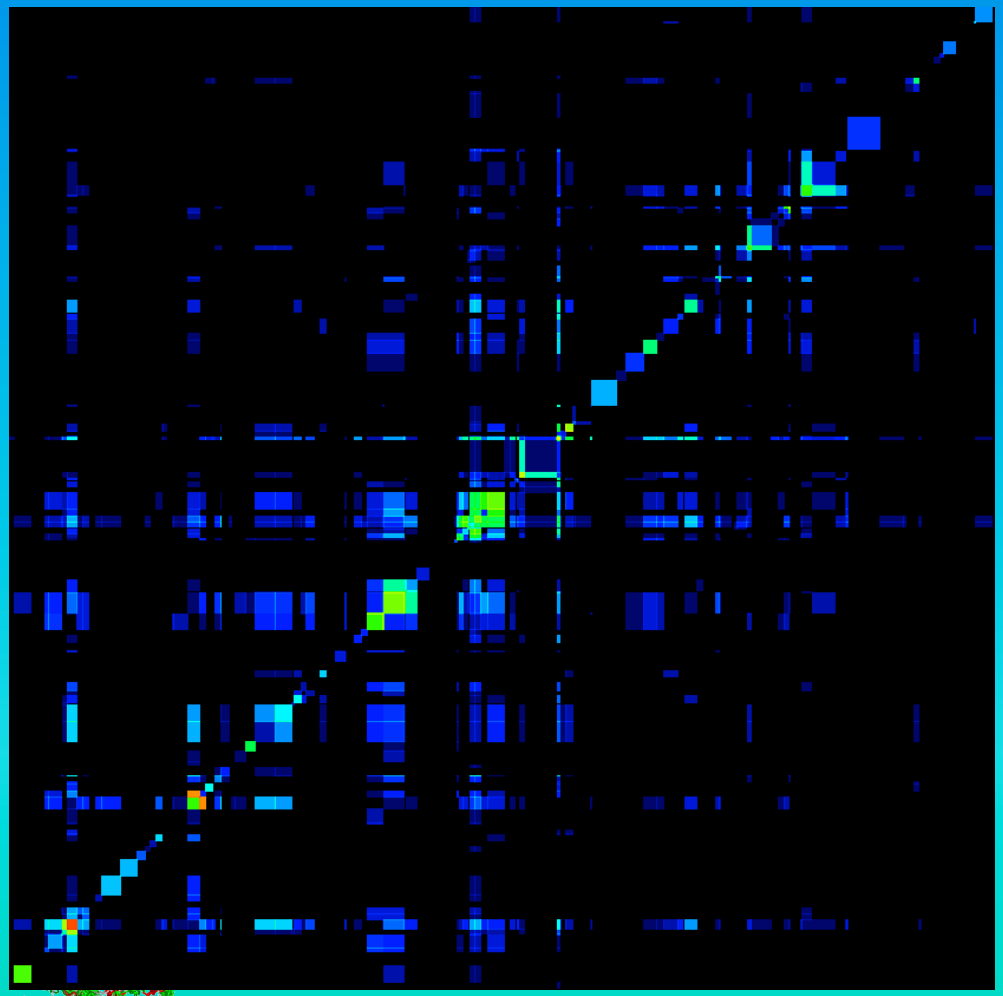

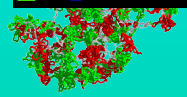

~ 800 kbp

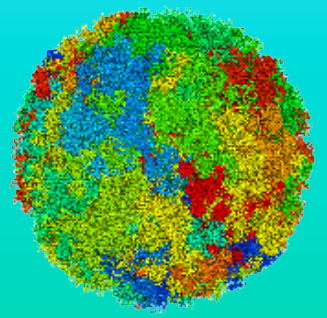

Fine Structure of Loop Aggregates/Rosettes

Depending on the resolution, the loops within a domain an their arrangement in loop aggregates/rosettes can be shown as well as the details of how the loops are organized at their base as well as their aggregated rosette core: parallel loop fibres exist at the loop base with ~6kbp and these form the core.

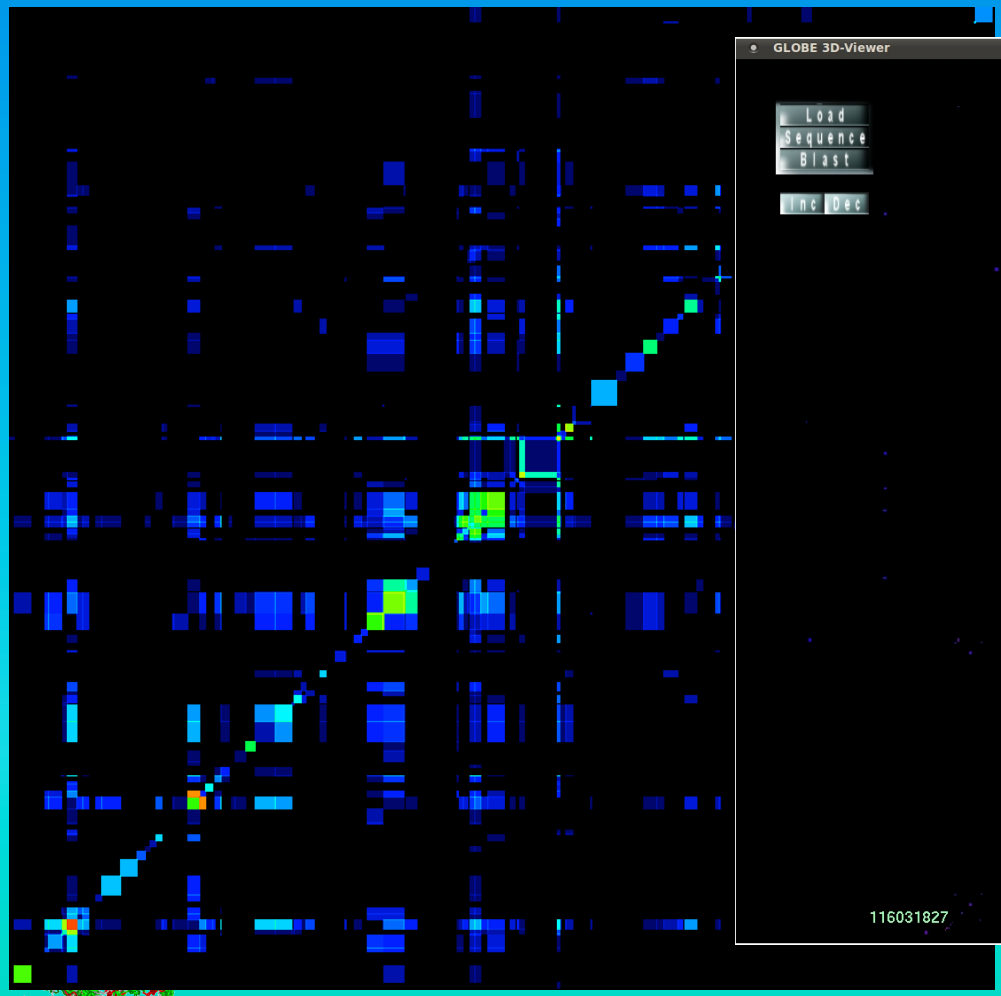

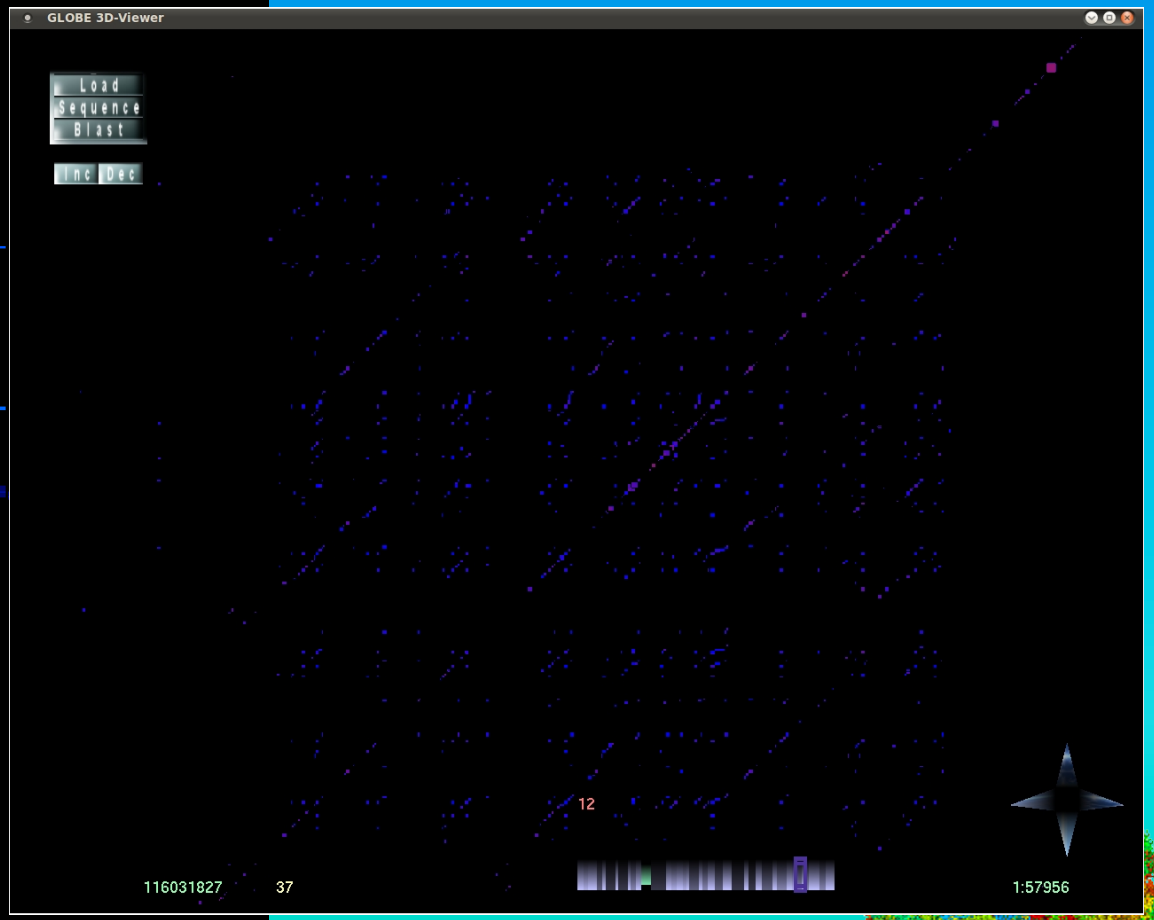

~ 800 kbp

Fine Structure of Loop Aggregates/Rosettes

Depending on the resolution, the loops within a domain an their arrangement in loop aggregates/rosettes can be shown as well as the details of how the loops are organized at their base as well as their aggregated rosette core: parallel loop fibres exist at the loop base with ~6kbp and these form the core.

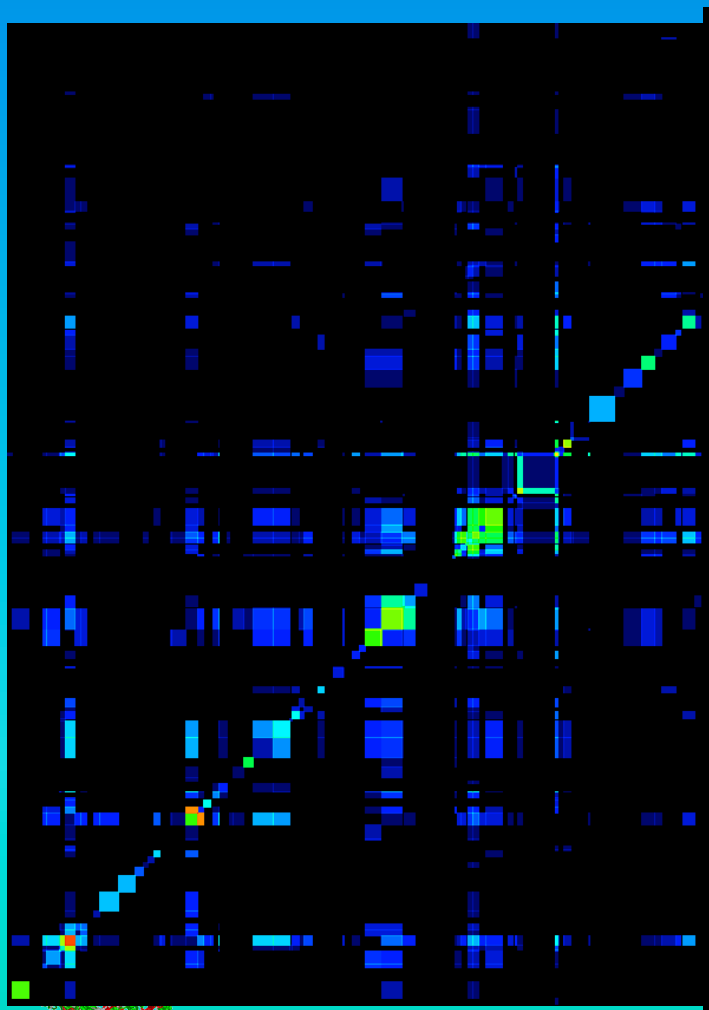

~ 800 kbp

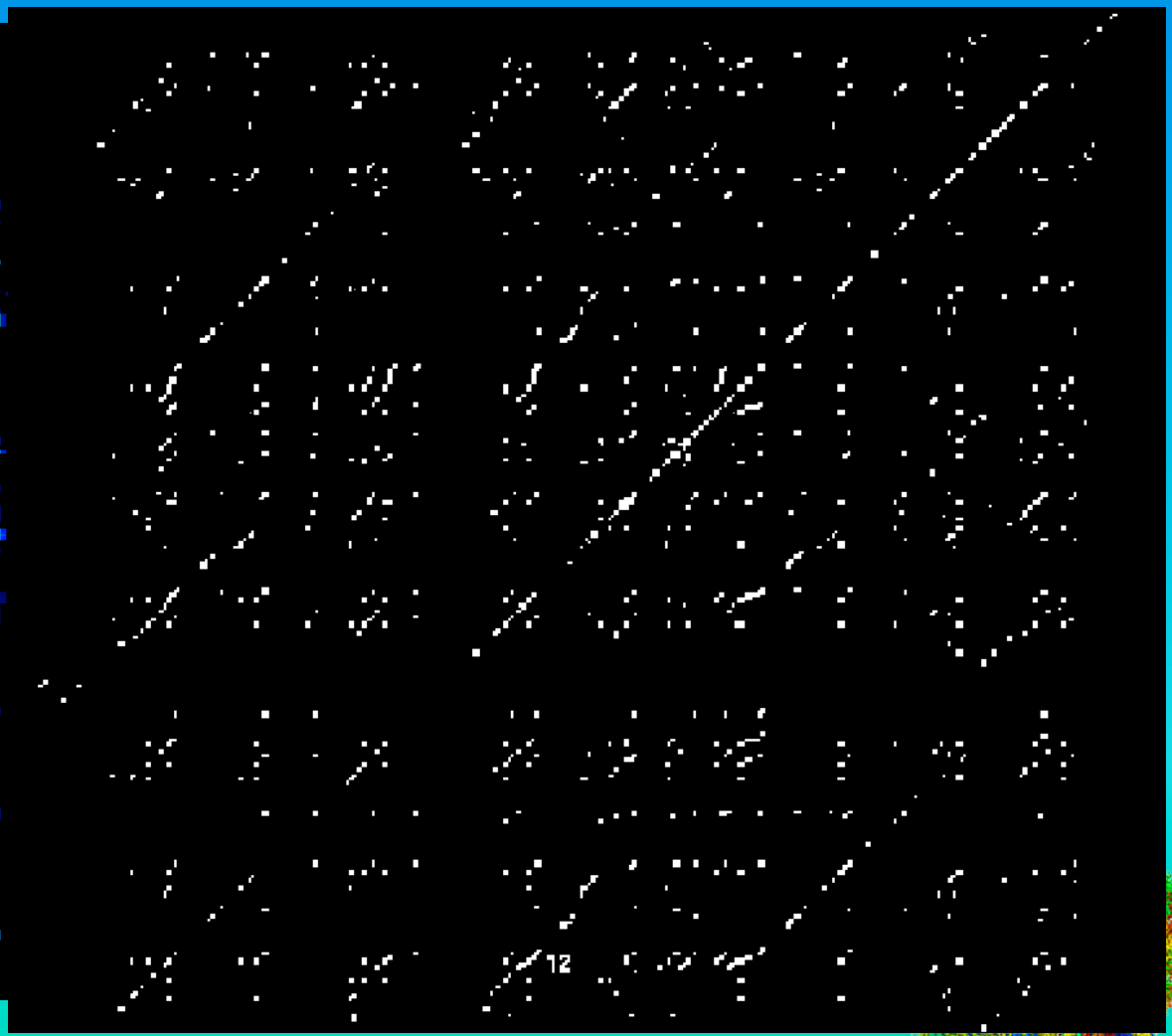

~ 380 kbp

Fine Structure of Loop Aggregates/Rosettes

Depending on the resolution, the loops within a domain an their arrangement in loop aggregates/rosettes can be shown as well as the details of how the loops are organized at their base as well as their aggregated rosette core: parallel loop fibres exist at the loop base with ~6kbp and these form the core.

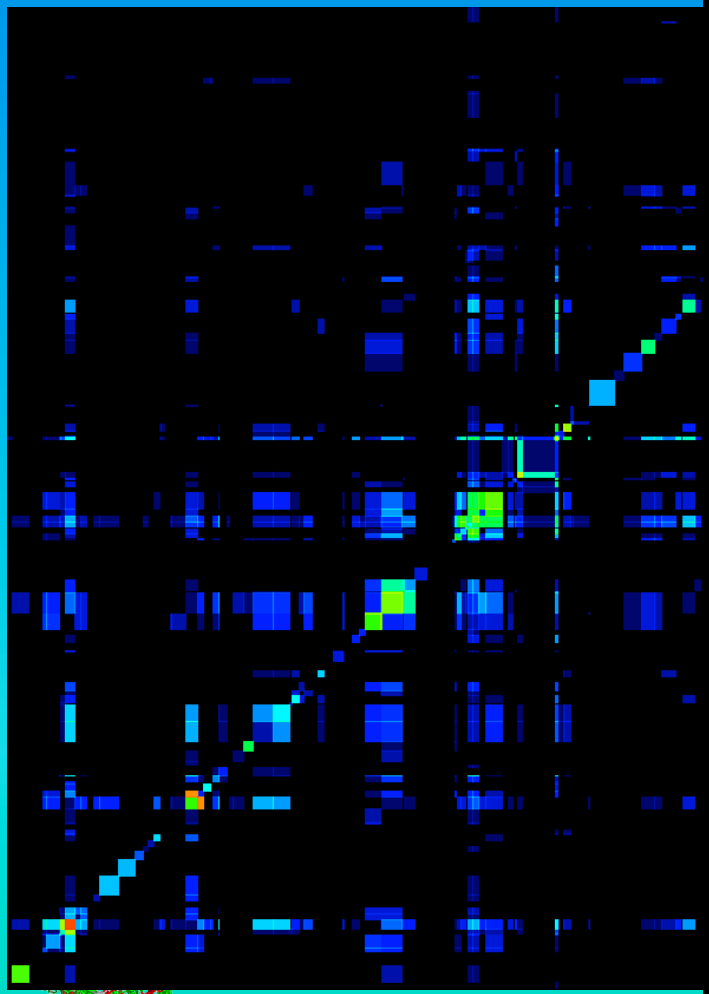

~ 800 kbp

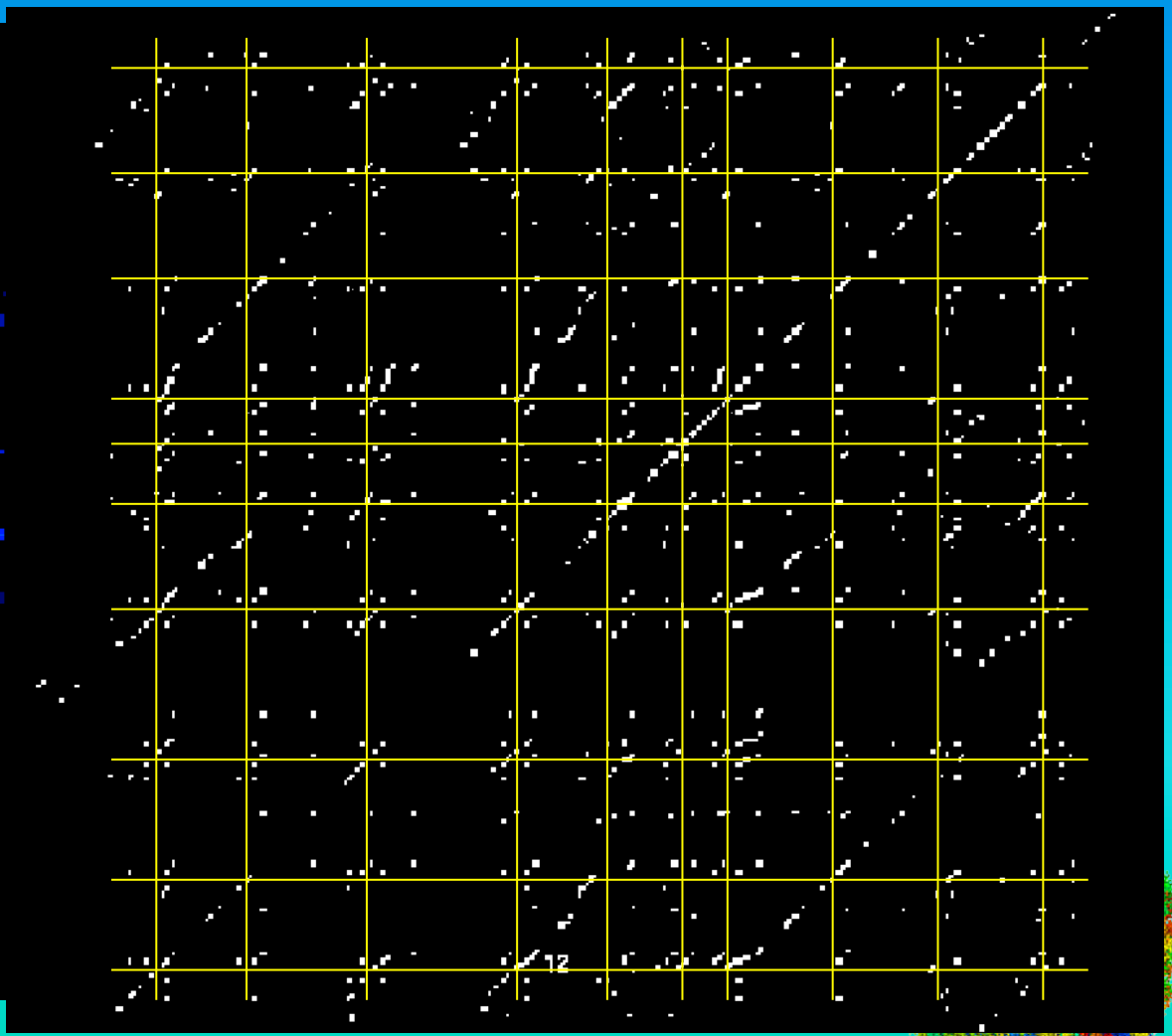

~ 380 kbp

Fine Structure of Loop Aggregates/Rosettes

Depending on the resolution, the loops within a domain an their arrangement in loop aggregates/rosettes shown as well as the details of how the loops are organized at their base as well as their aggregated core: parallel loop fibres exist at the loop base with ~6kbp and these form the core

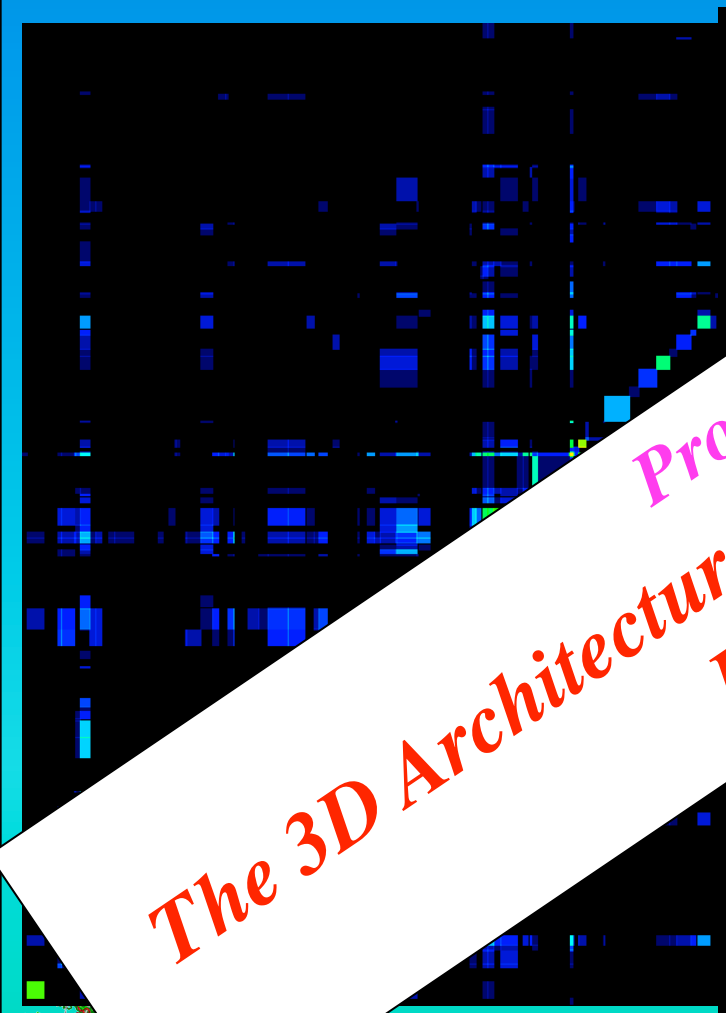

~ 800 kbp

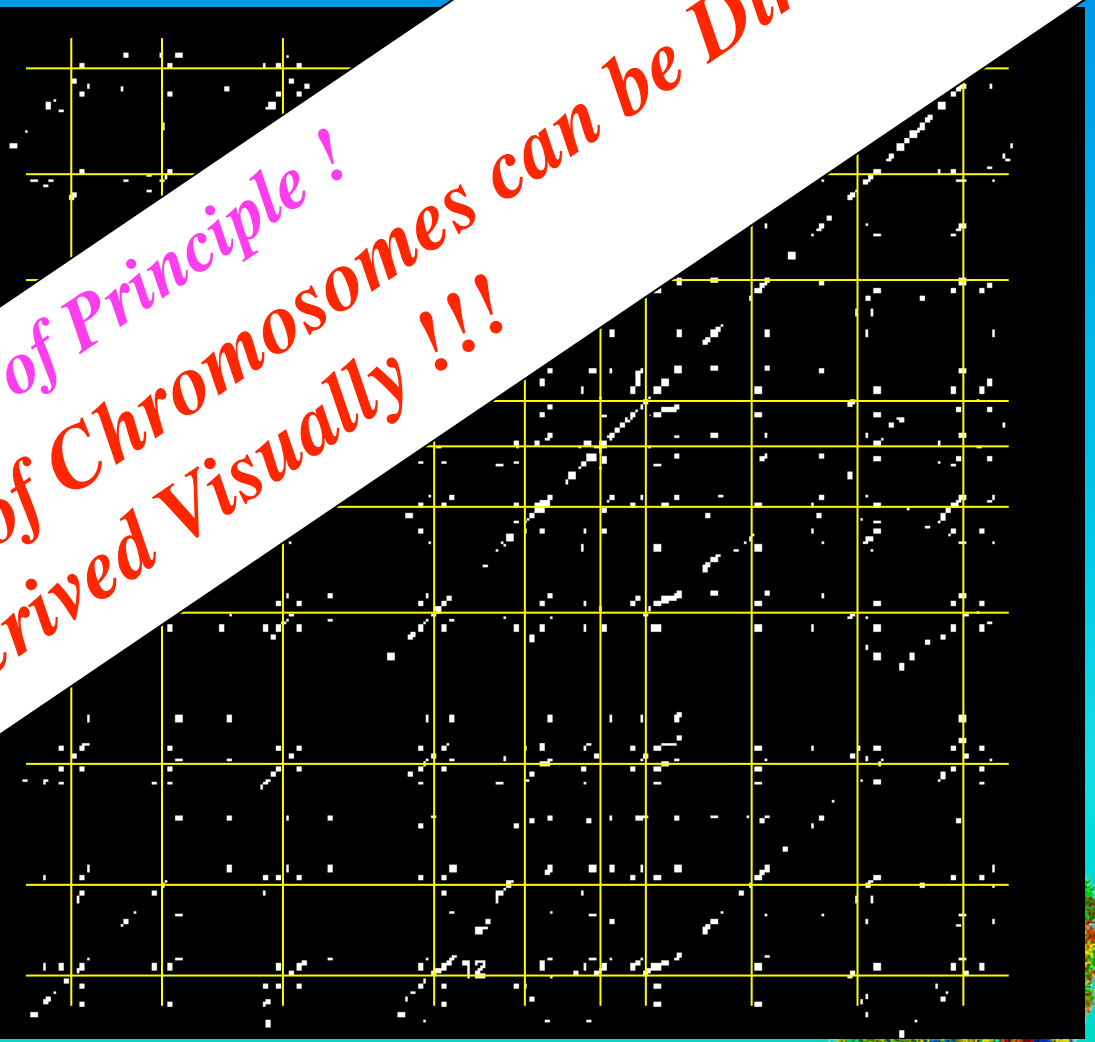

~ 380 kbp

Proof of Principle !

The 3D Architecture of Chromosomes can be Directly Derived Visually !!!

Simulation of Single Chromosomes

The 30 nm chromatin fiber is modeled as a polymer chain with stretching, bending, and excluded volume interactions. Monte Carlo and Brownian Dynamic methods lead to thermodynamical equilibrium configurations.

All models form chromosome territories with big voids and different chromatin morphologies. Experimental territory and subcompartment diameters agree best with an MLS model with 80 to 120 kbp loops and linkers.

Metaphase starting configuration with ideogram bands in red/green, linker in grey.

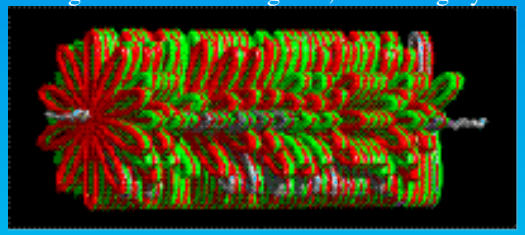

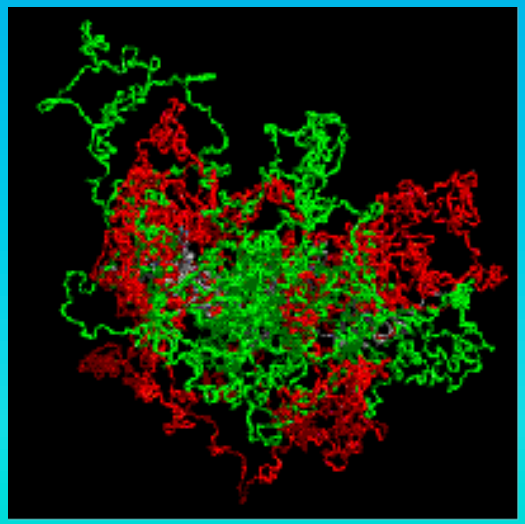

RW/GL model, loop size 5 Mbp, after ~80.000 MC and 1000 relaxing BD steps. Large loops intermingle freely and reach out of the chromsome territory, thus forming no distinct features like in MLS model.

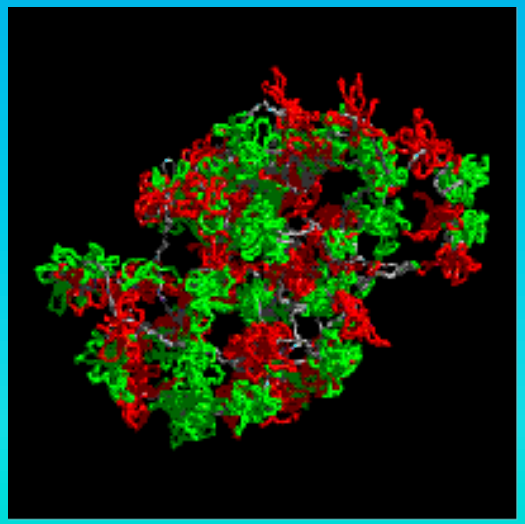

MLS model, loop size 126kbp, linker size 126 kbp, after ~50.000 MC and 1000 relaxing BD steps. Here rosettes form subcompartments as separated organizational and dynamic entities.

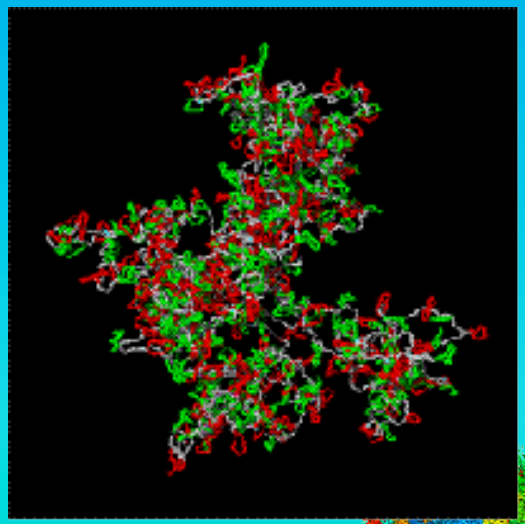

RW/GL model, loop size 126 kbp, after ~80.000 MC and 1000 relaxing BD steps. Large loops intermingle freely thus forming no distinct features like in MLS model.

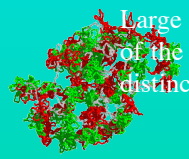

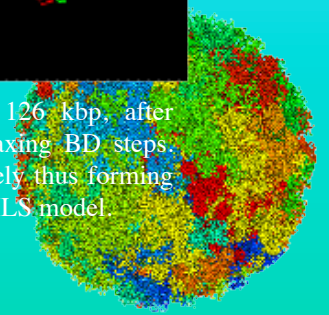

Simulation of Single Chromosomes

The 30 nm chromatin fiber is modeled as a polymer chain with stretching, bending, and excluded volume interactions. Monte Carlo and Brownian Dynamic methods lead to thermodynamical equilibrium configurations.

All models form chromosome territories with big voids and different chromatin morphologies. Experimental territory and subcompartment diameters agree best with an MLS model with 80 to 120 kbp loops and linkers.

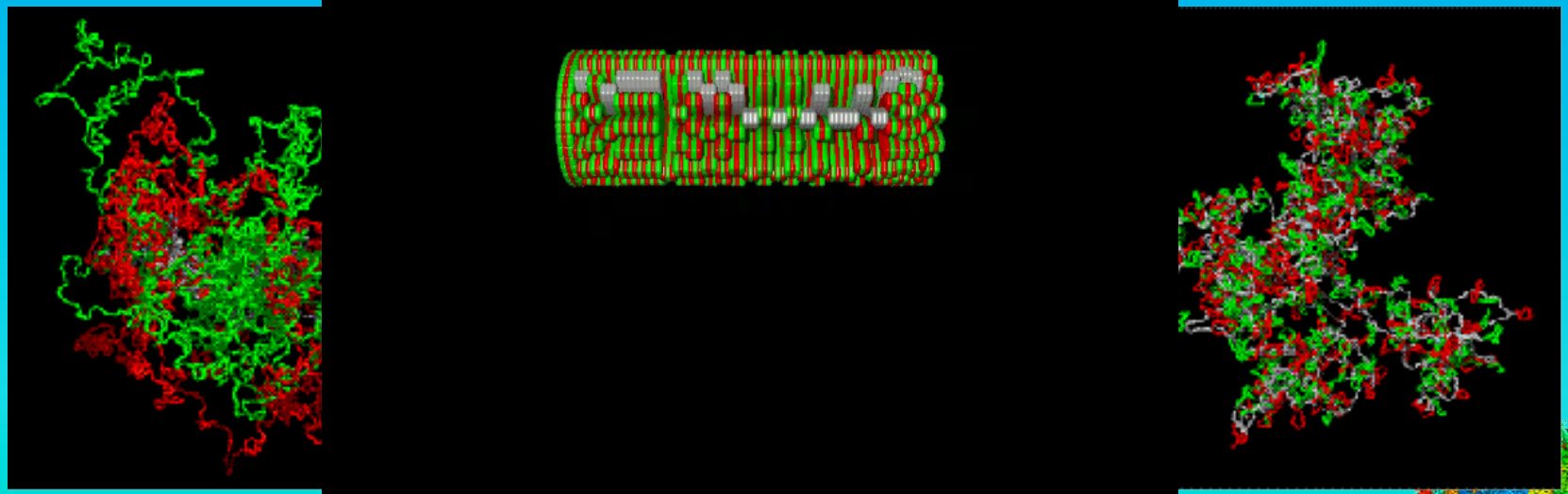

RW/GL model, loop size ~80.000 MC and 1000 relaxing BD steps. Large loops intermingle freely and reach out of the chromsome territory, thus forming no distinct features like in MLS model.

120 kbp, after ~50.000 MC and 1000 relaxing BD steps. Here rosettes form subcompartments as separated organizational and dynamic entities.

model, loop size 126 kbp, after ~80.000 MC and 1000 relaxing BD steps. Large loops intermingle freely thus forming no distinct features like in MLS model.

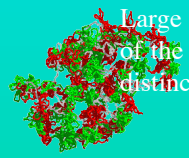

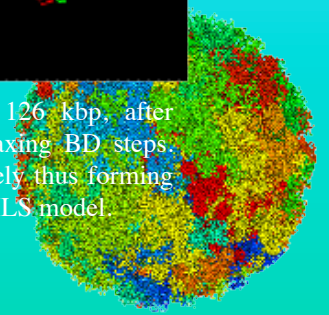

Simulation of Whole Nuclei with all 46 Chromosomes

Starting with some metaphase arrangement of cylindrical chromosomes, interphase nuclei with a 30 nm fiber resolution and at thermodynamical equilibrium are created in 4 steps using simulated annealing and Brownian Dynamics methods with stretching, bending, excluded volume and a spherical boundary interactions.

The chromosome territory position depends on their metaphase position and is reasonably stable.

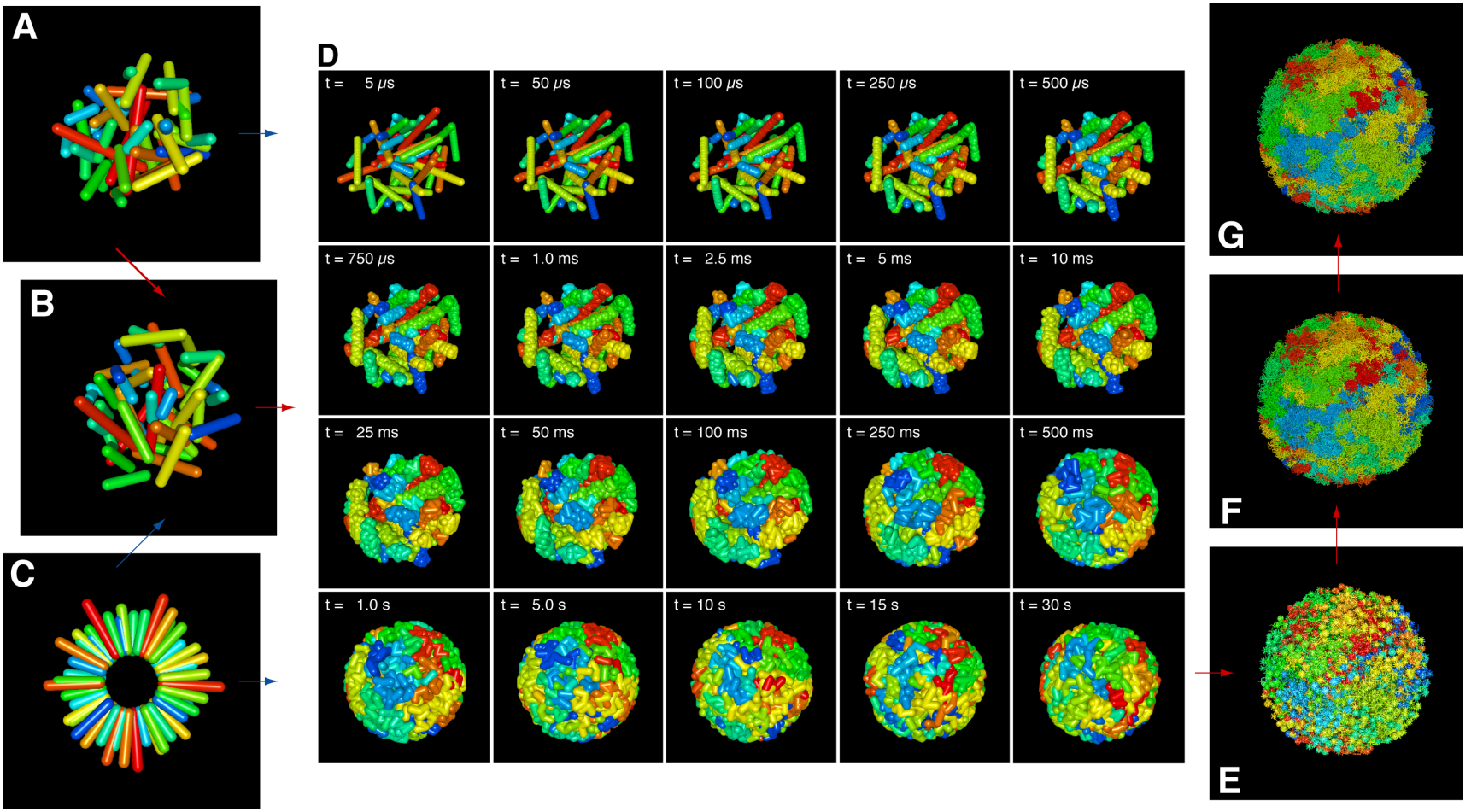

Simulation of Whole Nuclei with all 46 Chromosomes

Starting with some metaphase arrangement of cylindrical chromosomes, interphase nuclei with a 30 nm fiber resolution and at thermodynamical equilibrium are created in 4 steps using simulated annealing and Brownian Dynamics methods with stretching, bending, excluded volume and a spherical boundary interactions.

The chromosome territory position depends on their metaphase position and is reasonably stable.

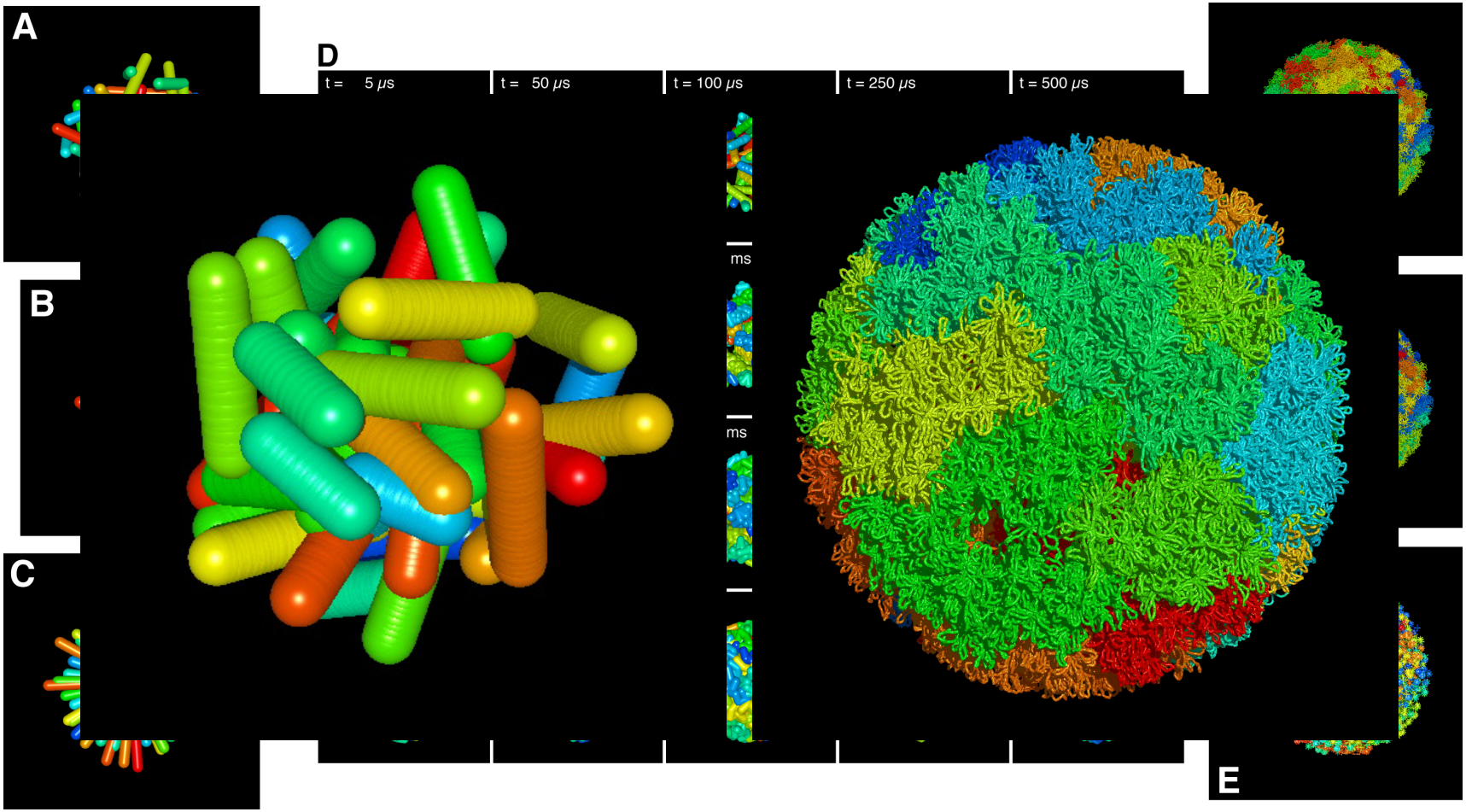

Simulation of Whole Nuclei with all 46 Chromosomes

Starting with some metaphase arrangement of cylindrical chromosomes, interphase nuclei with a 30 nm fiber resolution and at thermodynamical equilibrium are created in 4 steps using simulated annealing and Brow Dynamics methods with stretching, bending, excluded volume and a spherical boundary interacti

The chromosome territory position depends on their metaphase position and is reasonably

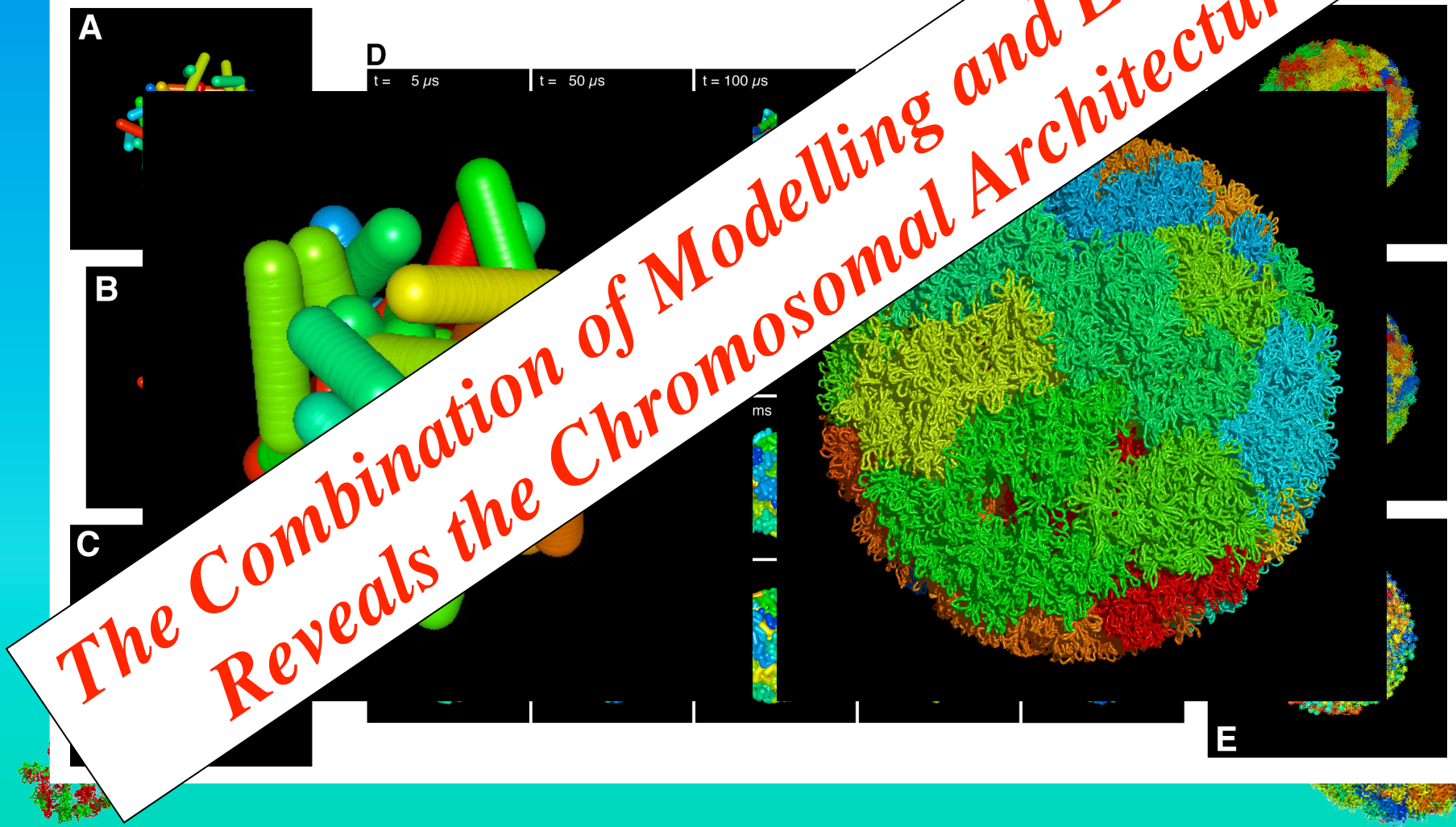

The Combination of Modelling and Experiment Reveals the Chromosomal Architecture !

Simulated Interaction Maps

Simulated spatial distance maps as well as simulated interaction maps result in the representation of every parameter variation, and also exhibit the fine-structure describing the loop base as well as rosette core. Thus from the quasi-fibre to the entire chromosome the architecture can be understood in detail.

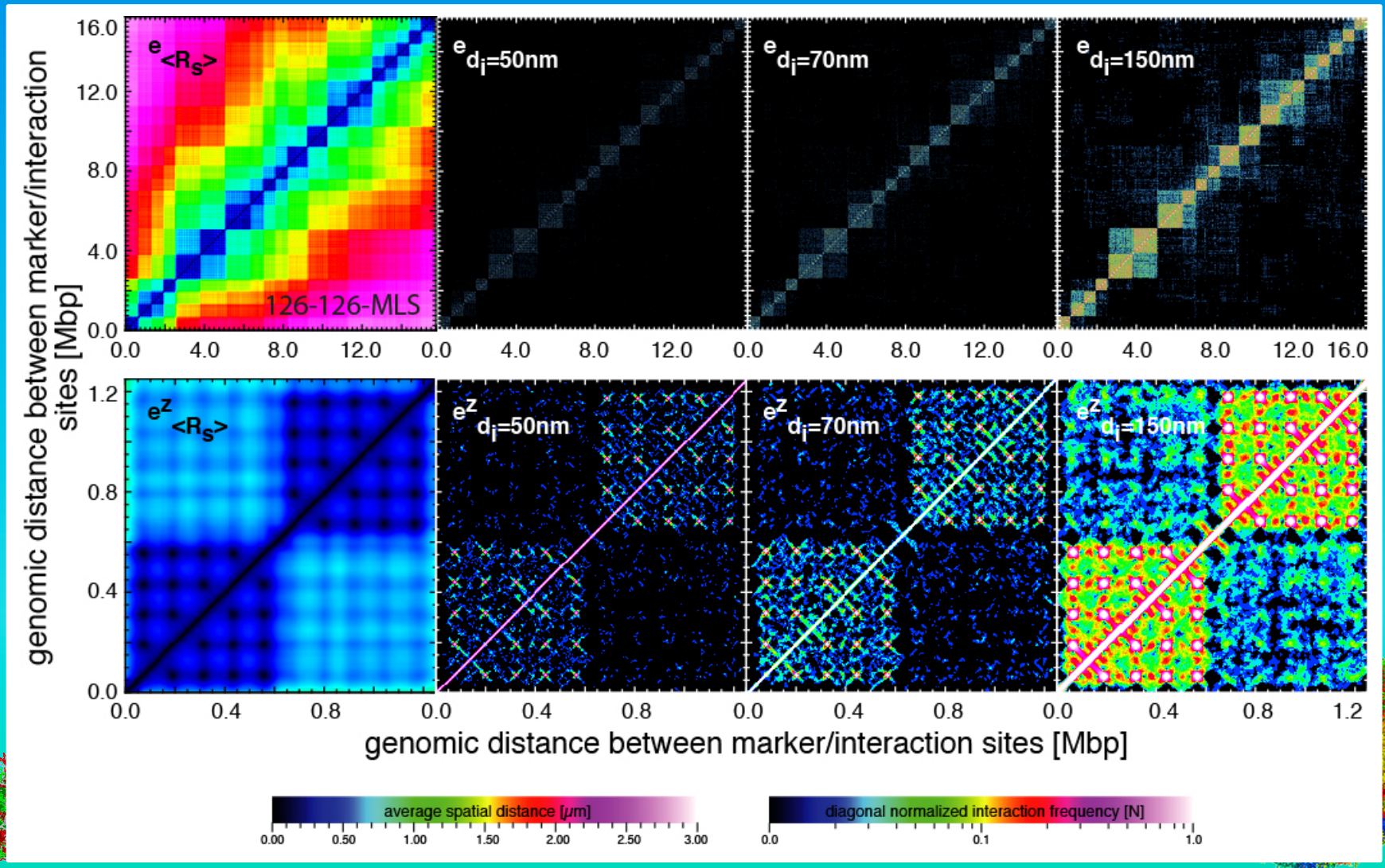

Simulated Interaction Maps

Simulated spatial distance maps as well as simulated interaction maps result in the representation of every parameter variation, and also exhibit the fine-structure describing the loop base as well as rosette core. Thus from the quasi-fibre to the entire chromosome the architecture can be understood in detail.

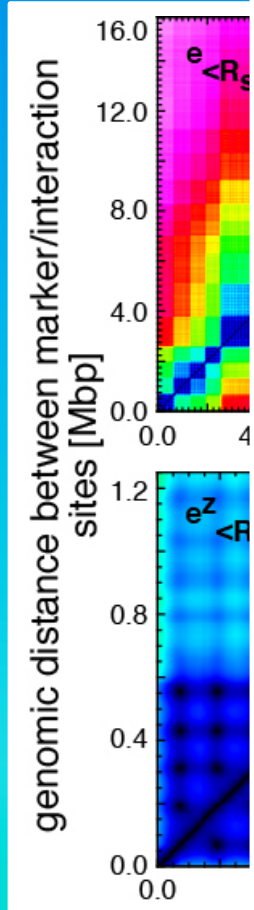

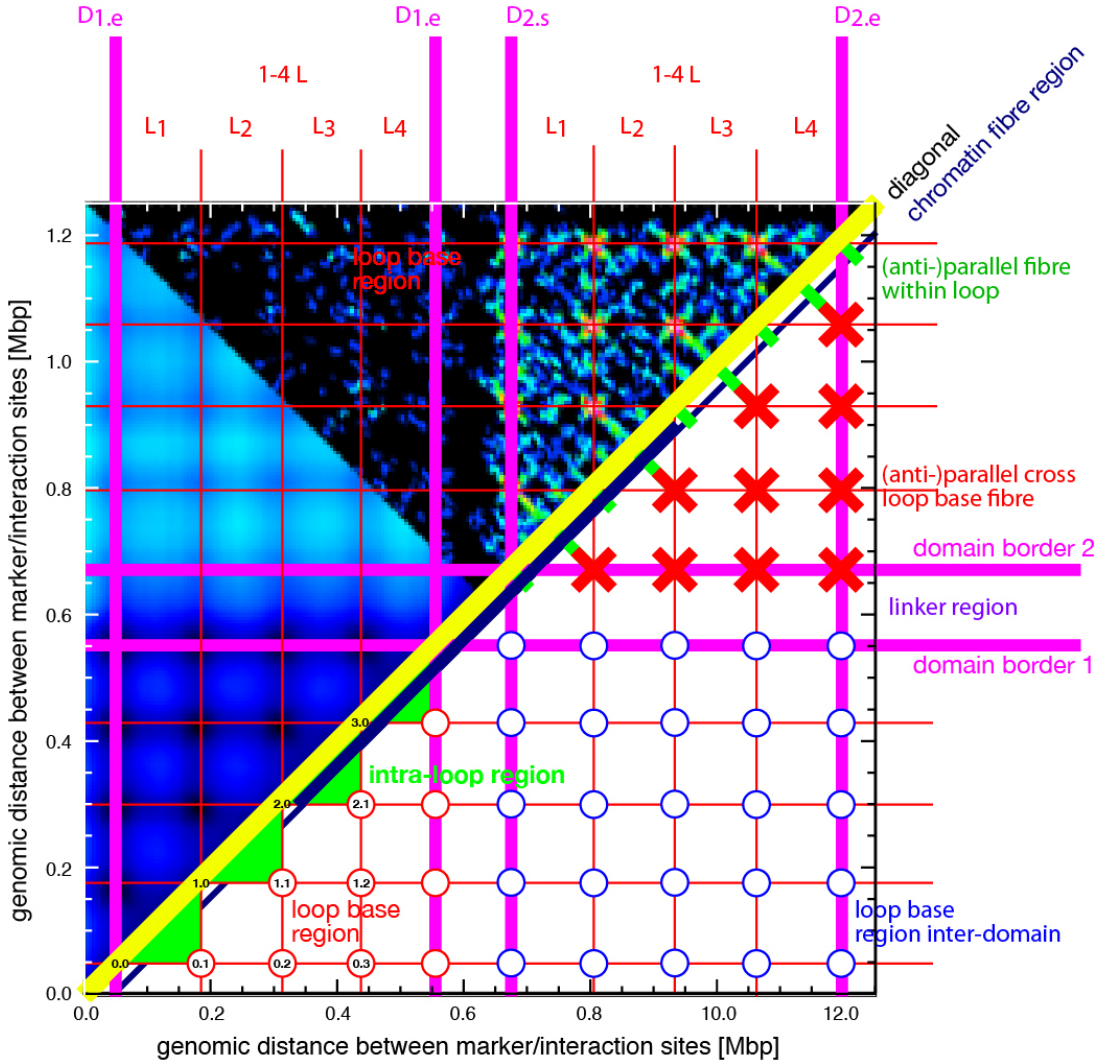

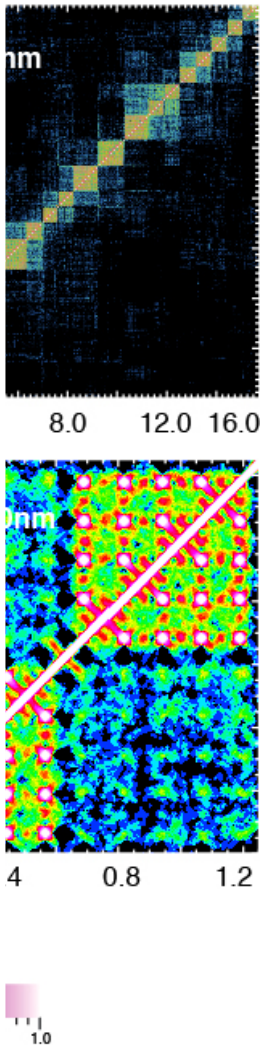

Variation of a Consensus Architecture Scheme

The difference between different cell types, functional states or even species is minor despite depending on the region. From this, the chromatin fibre conformation, loop position, and their association into loop aggregates/ rosettes can be derived, simulated by polymer models and finally visualized.

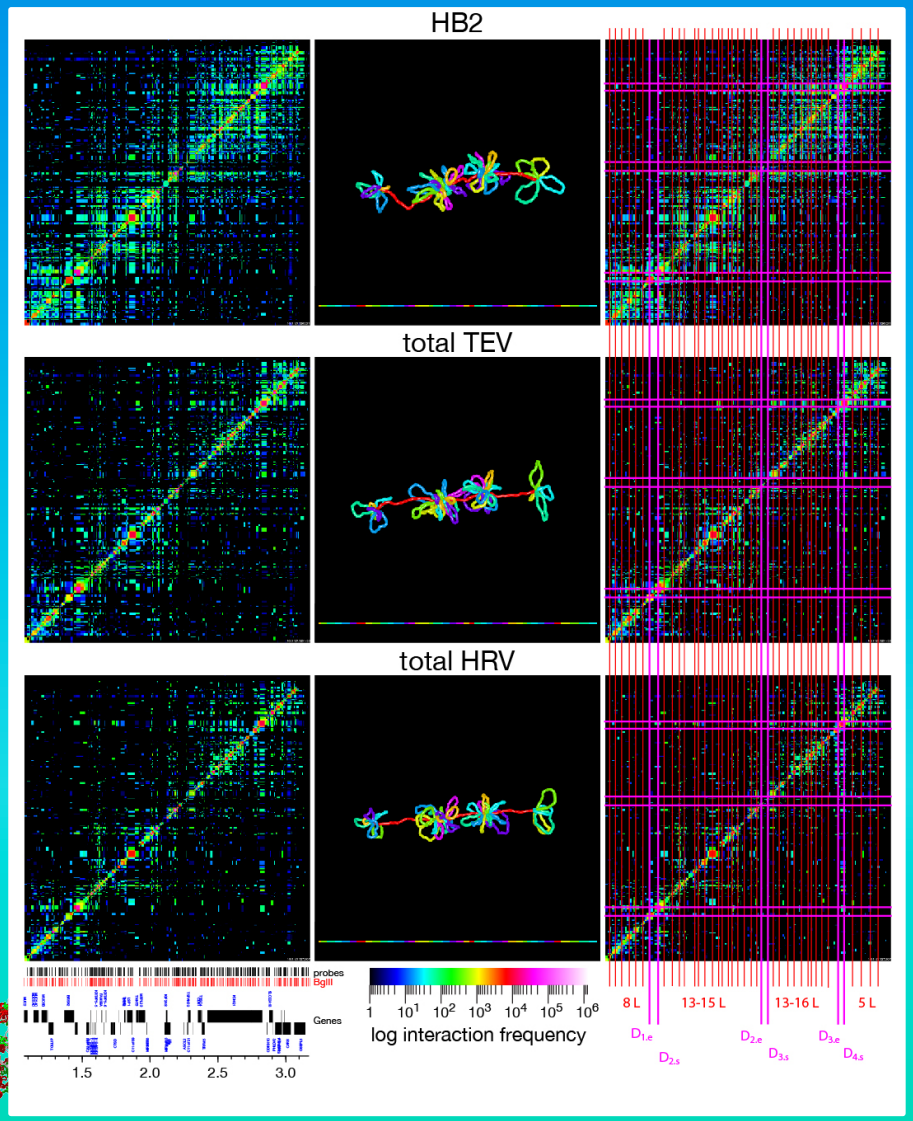

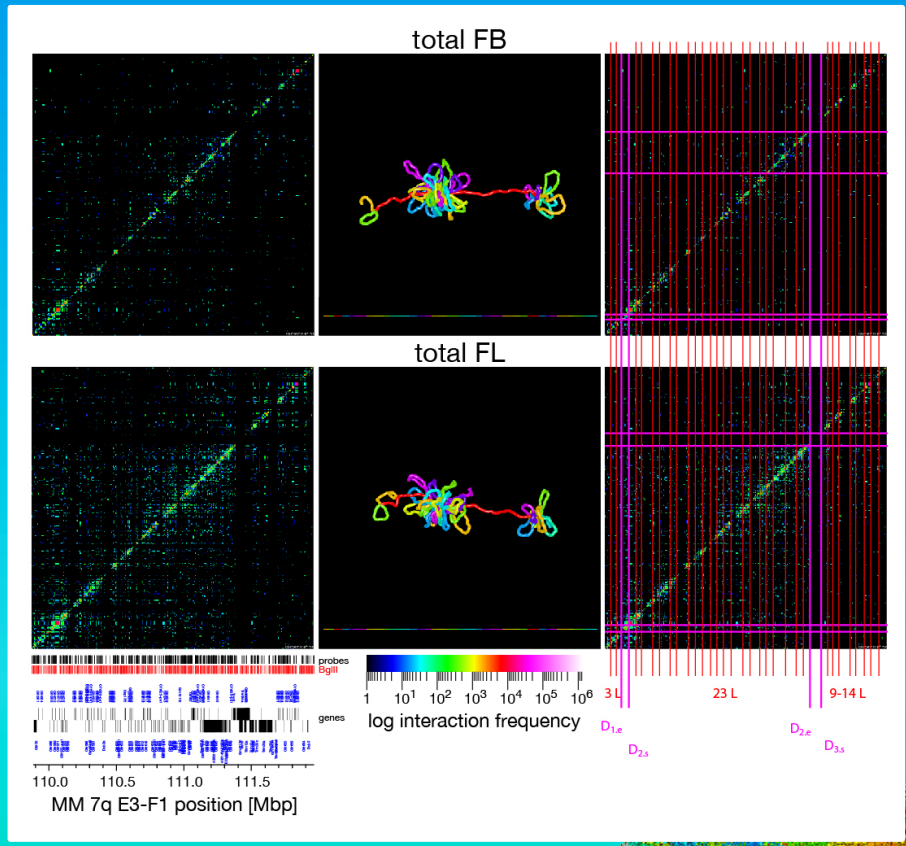

Variation of a Consensus Architecture Scheme

The difference between different cell types, functional states or even species is minor despite depending on the region. From this, the chromatin fibre conformation, loop position, and their association into loop aggregates/ rosettes can be derived, simulated by polymer models and finally visualized.

3D Architecture of the Prader-Willi Region

Fluorescence *in situ* hybridization with various protocols of small probes within the Prader-Willi region combined with spectral precision distance confocal laser scanning microscopy and comparison with large-scale computer simulations shows a Multi-Loop Subcompartiment organization of the Prader-Willi region.

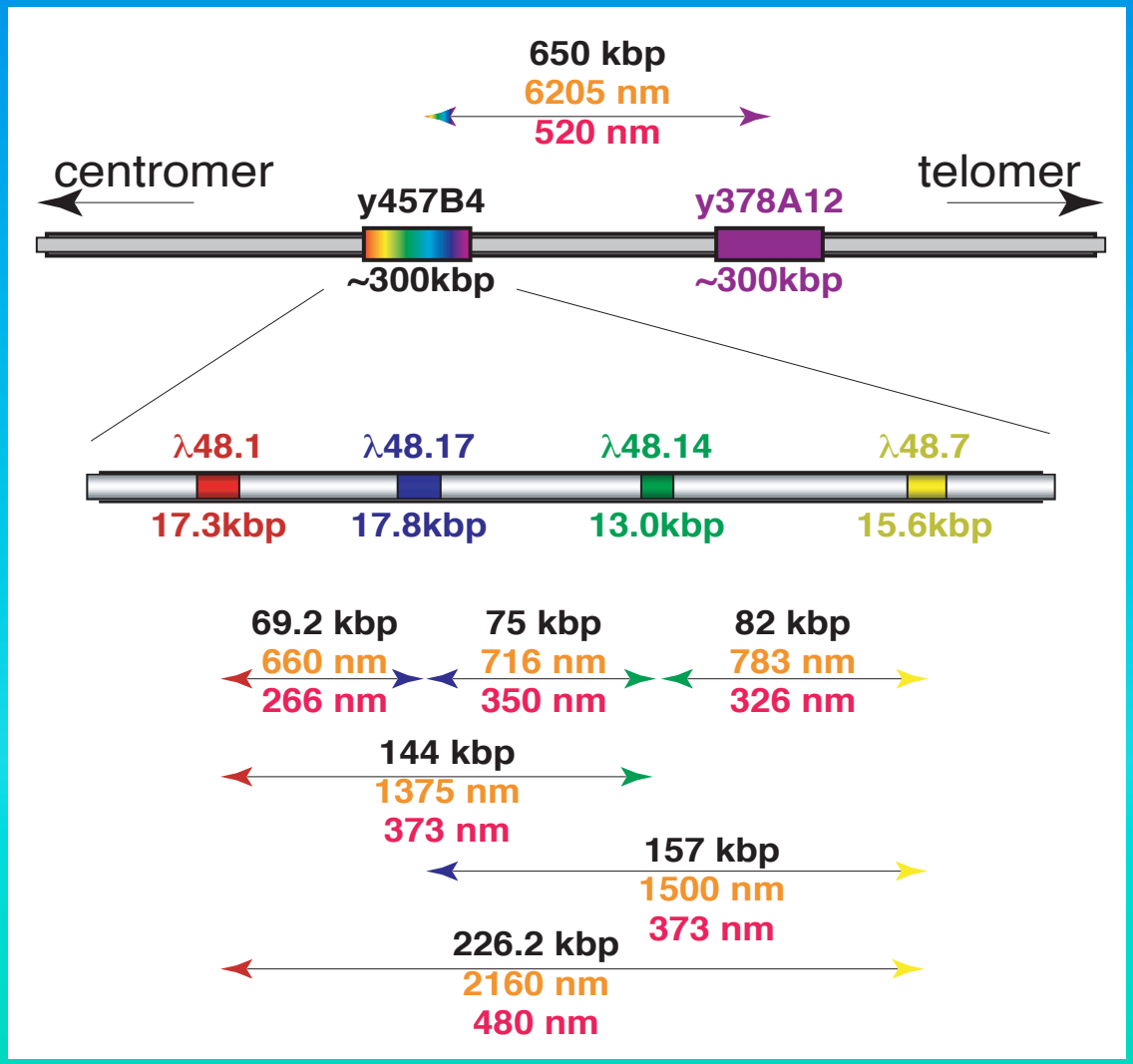

3D Architecture of the Prader-Willi Region

Fluorescence *in situ* hybridization with various protocols of small probes within the Prader-Willi region combined with spectral precision distance confocal laser scanning microscopy and comparison with large-scale computer simulations shows a Multi-Loop Subcompartiment organization of the Prader-Willi region.

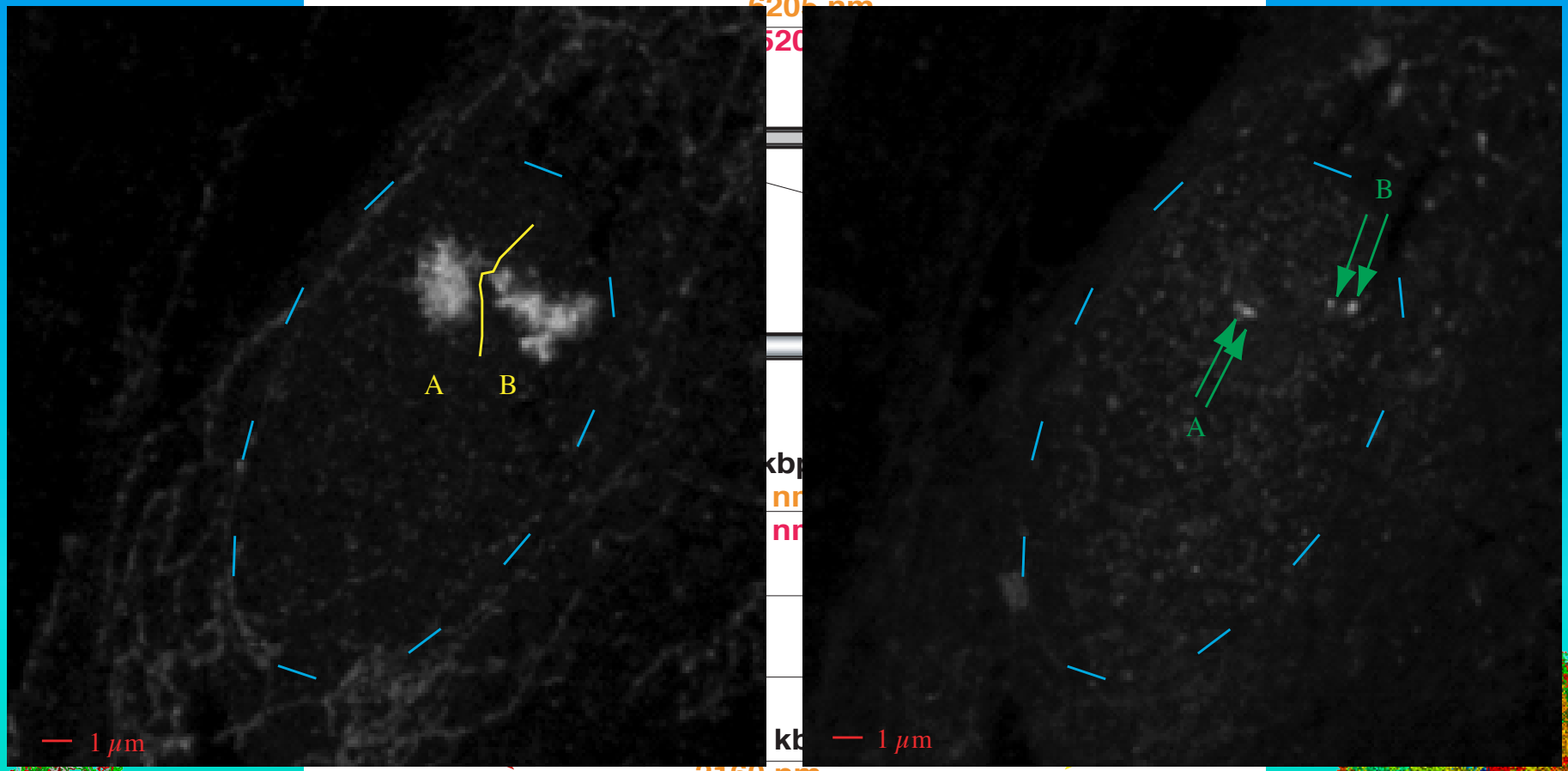

3D Architecture of the Prader-Willi Region

Fluorescence *in situ* hybridization with various protocols of small probes within the Prader-Willi region combined with spectral precision distance confocal laser scanning microscopy and comparison with large-scale computer simulations shows a Multi-Loop Subcompartiment organization of the Prader-Willi region.

650 kbp

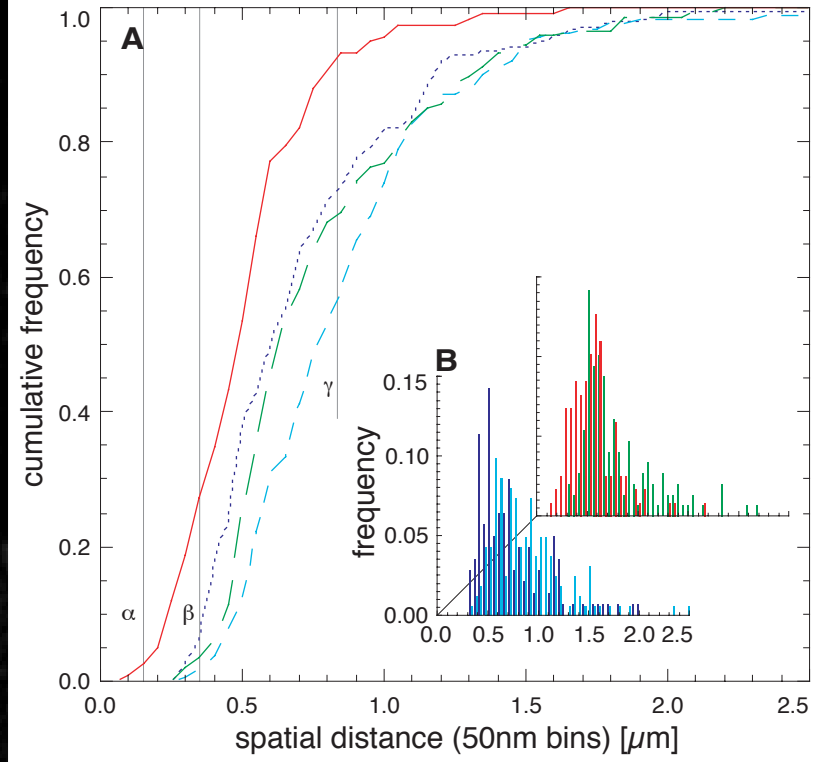

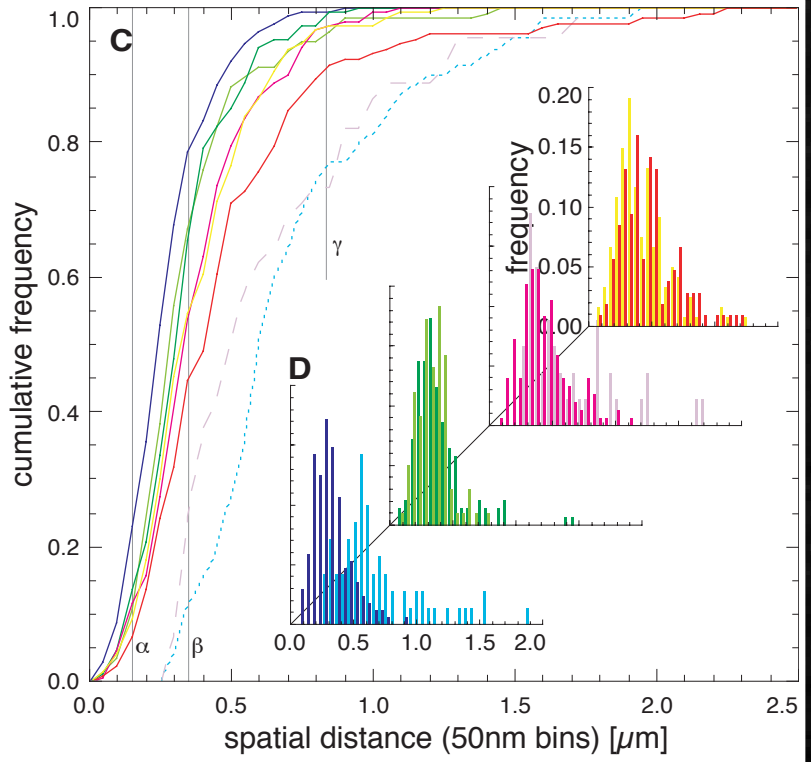

1 μm

1 μm

2160 nm

480 nm

3D Architecture of the Prader-Willi Region

Fluorescence *in situ* hybridization with various protocols of small probes within the Prader-Willi region combined with spectral precision distance confocal laser scanning microscopy and comparison with large-scale computer simulations shows a Multi-Loop Subcompartiment organization of the Prader-Willi region.

650 kbp

6205 nm

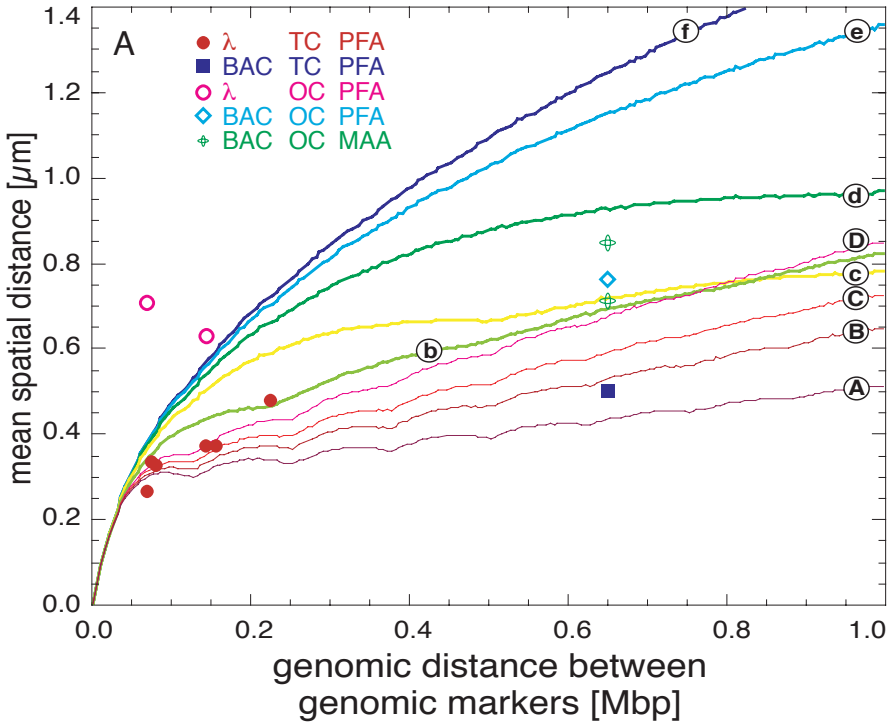

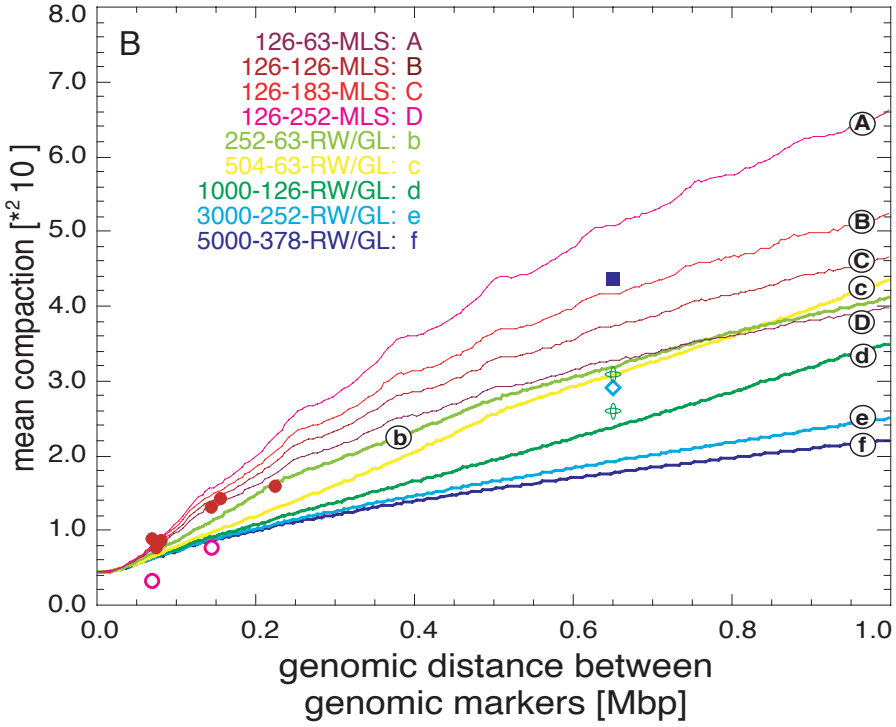

2160 nm

480 nm

3D Archticture & Function of the IgH Locus

Fluorescence *in situ* hybridization of the IgH locus combined with spectral precision distance epifluorescence microscopy, analytical trilateration and comparison with computer simulations shows again a Multi-Loop Subcompartiment organization of the IgH locus with functional relevant distances.

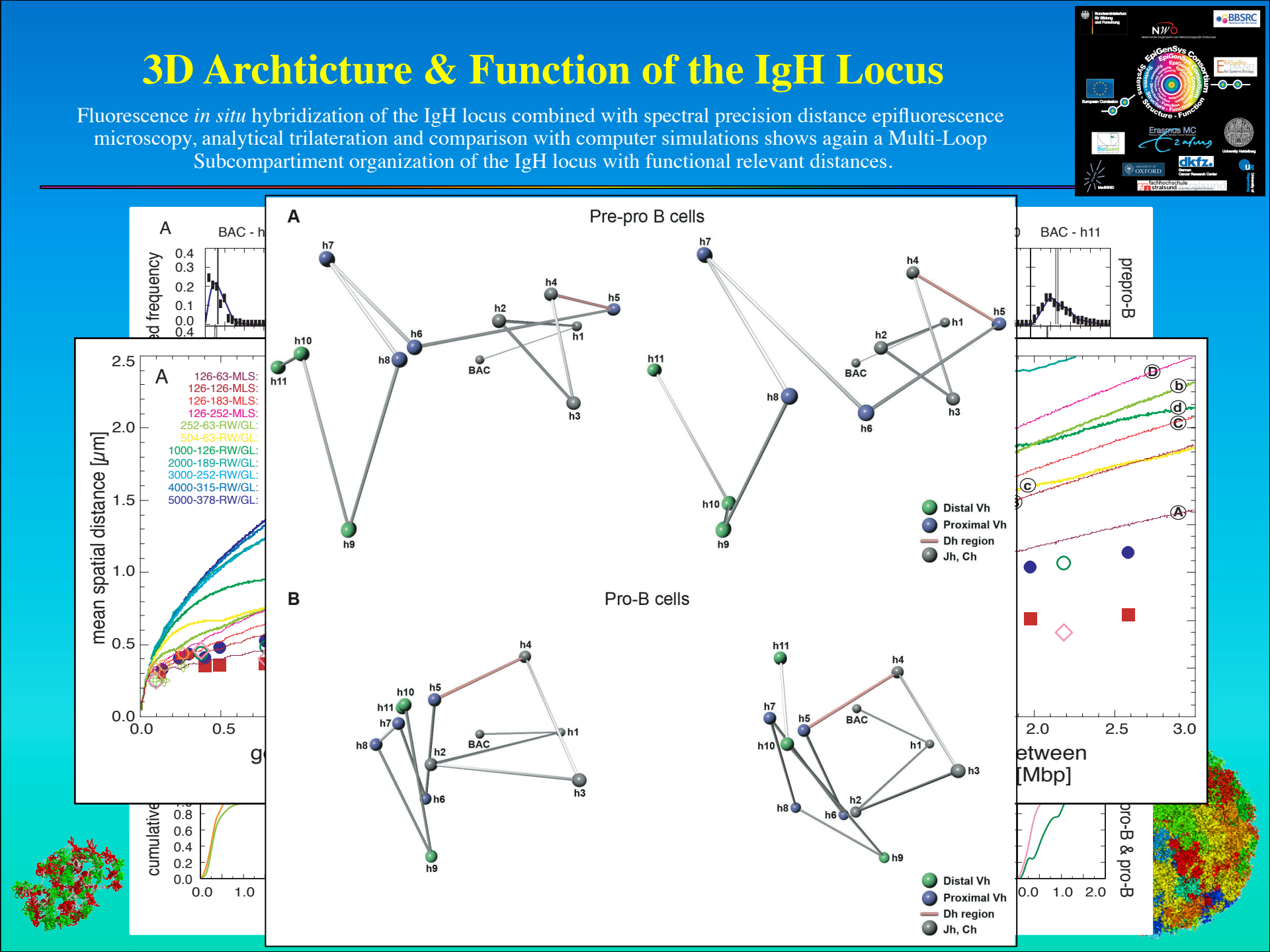

“Synoptic” 3D Architecture of Various Loci

A history “synoptic” comparison of the spatial distance mapping from their original background and aim, FISH methodological protocols, via microscopic imaging and restoration analysis procedures, to their interpretation, reveals that with time Multi-Loop Subcompartment models are fovoured.

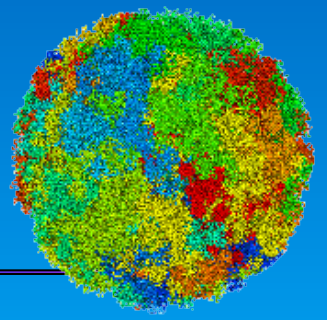

Study	Location	Preparation of Cells			FISH			Microscopy		Fit to model
		Cell cycle	KCl [nM]	Fix-ative	Melt-ing	Label	Col-ours	# of nuclei	Image acquisi-tion	
Fig. 3B, Trask ’89	DHFR	UA41 G1-cf	75 dropped	MAA 3:1	FM 50 %	Biotin	1	20-37	photo, wall	RWGL 0.08-J RWGL 1.0
Fig. 3B, Lawrence’90	Dystro-phin	WI38F G1	75 dropped	MAA 3:1	FM 50 %	Biotin	1	20-60	photo, wall	RWGL 0.5-1
Fig. 3A, Trask ’91	Xq28	F G1-cf	75 dropped	MAA 3:1	FM 50 %	Biotin	1	30-60	photo, wall	RWGL 0.7 J RWGL 2.0->5.0
Fig. 3B, Trask ’91	Xq28	F G1-cf	75 dropped	MAA 3:1	FM 50 %	Biotin Dig	2	30-60	photo, wall	RWGL 1.0-3.0
Fig. 3, v.d. Engh ’92 or Fig. 5A, Trask ’93	4p16.3	F G1-cf	75 dropped	MAA 3:1	FM 50 %	Biotin Dig	2	?	photo, d-board	L_S <=0.1 for GS < 0.5 < RWGL >5.0
Fig. 5B, Trask ’93	6p21	F G1-cf	75	MAA 3:1	FM 50-70 %	Biotin Dig	2	?	photo, d-board	L_S <=0.1 for GS < 1.0 < RWGL 1.0-5.0
Fig. 5, Senger ’93	MHC 6p21.31	HFF G1-cf	?	?	FM 50 %	Biotin	1	> 30	photo, wall	MLS L_S&LI_S= 0.12-0.25 RWGL 0.1-0.5
Fig. 5, Senger ’93	MHC 6p21.31	HFF G1-cf	?	?	FM 50 %	Biotin Dig	2	> 30	photo, wall	MLS L_S=0.1 LI_S=0.18 RWGL 0.1-0.5
Fig. 1, Warrington ’94	4p16.3	F G1-cf	75	MAA 3:1	FM 50 %	Biotin Dig	2	?	?	RWGL > 5.0
Tab. 1, Warrington ’94	5q31-33	L	?	?	?	?	?	?	CLSM BioRad	RWGL > 5.0
Fig. 2B, Yokota ’95	4p16.3	F G1-cf	40 dropped	MAA 3:1	FM 70 %	Biotin Dig	2	40-360	photo, d-board	RWGL 2.0-4.0
Fig. 3B, Yokota ’95	4p16.3	F G1-cf	-	PFA 4 %	FM 70 %	Biotin Dig	2	40-350	photo, d-board	MLS L_S&LI_S= 0.1-0.125

Study	Location	Preparation of Cells			FISH			Microscopy		Fit to model
		Cell cycle	KCl [nM]	Fix-ative	Melt-ing	Label	Col-ours	# of nuclei	Image acquisi-tion	
Fig. 2A, Yokota ’97	4p16.3 R-band	F G1-cf	40 dropped	MAA 3:1	FM 70 %	Biotin Dig	2	37-178	photo, d-board	RWGL 2.0-3.0
Fig. 2B, Yokota ’97	6p21.3 R-band	F G1-o	40 dropped	MAA 3:1	FM 70 %	Biotin Dig	2	37-178	photo, d-board	RWGL 4.0-5.0
Fig. 2C, Yokota ’97	21q22.2 G-band	F G1-o	40 dropped	MAA 3:1	FM 70 %	Biotin Dig	2	37-178	photo, d-board	RWGL 1.0-2.0
Fig. 2D, Yokota ’97	Xp21.3 G-band	F G1-o	40 dropped	MAA 3:1	FM 70 %	Biotin Dig	2	37-178	photo, d-board	RWGL 0.5-0.9
Fig. 2D, Yokota ’97	Xq28 R-band	F G1-of	40 dropped	MAA 3:1	FM 70 %	Biotin Dig	2	37-178	photo, d-board	RWGL 1.0-5.0j
Fig. 2A, Yokota ’97	Xp21.3 G-band	F	-	PFA 4 %	FM 70 %	Biotin Dig	2	37-178	photo, d-board	RWGL 0.25 MLS L_S=0.126 LI_S=0.200
Fig. 2A, Yokota ’97	Xq28 R-band	F	-	PFA 4 %	FM 70 %	Biotin Dig	2	37-178	photo, d-board	RWGL 1.0
Fig. 4B, Yokota ’97	Xp21.3 G-band	HeLa	40 dropped	MAA 3:1	FM 70 %	Biotin Dig	2	37-178	photo, d-board	RWGL 0.25 MLS L_S=0.126 LI_S=0.200
Fig. 4B, Yokota ’97	Xq28 R-band	HeLa	40 dropped	MAA 3:1	FM 70 %	Biotin Dig	2	37-178	photo, d-board	RWGL 1.0
Monier ’97	11q13	F	-	PFA 4%	FM 70 %	Biotin Dig	1	22-69	CLSM	MLS L_S=0.126 LI_S=180
Monier ’97	11q13	L	-	PFA 4%	FM 70 %	Biotin Dig	1	22-69	CLSM	MLS L_S=0.1 LI_S=0.18-0.24
Knoch ’98/ Rauch ’99	15q11-21	F	-	PFA 4%	FM 70 %	Biotin Dig	1 & 2	60-120	CLSM	MLS L_S=0.1 LI_S=0.06-0.125

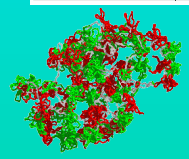

“Synoptic” 3D Architecture of Various Loci

A history “synoptic” comparison of the spatial distance mapping from their original background and aim, FISH methodological protocols, via microscopic imaging and restoration analysis procedures, to their interpretation, reveals that with time Multi-Loop Subcompartment models are favoured.

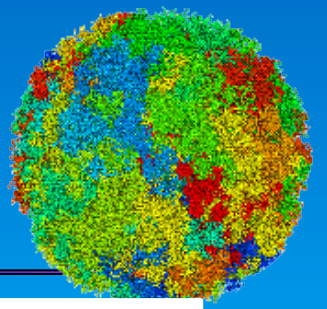

Study	to model
Fig. 3B, Tr ’89	L 2.0-3.0
Fig. 3B, Lawrence’	L 4.0-5.0
Fig. 3A, Tr ’91	L 1.0-2.0
Fig. 3B, Tr ’91	L 0.5-0.9
Fig. 3, v.d. ’92 or Fig. Trask ’93	L 1.0-5.0j
Fig. 5B, Tr ’93	L 0.25 L_S=0.126 0.200
Fig. 5, Senger ’93	L 1.0
Fig. 5, Senger ’93	L 0.25 L_S=0.126 0.200
Fig. 1, Warrington	L 1.0
Tab. 1, Warrington	L_S=0.126 180
Fig. 2B, Yo ’95	L_S=0.1 0.18-0.24
Fig. 3B, Yo ’95	L_S=0.1 0.06-0.125

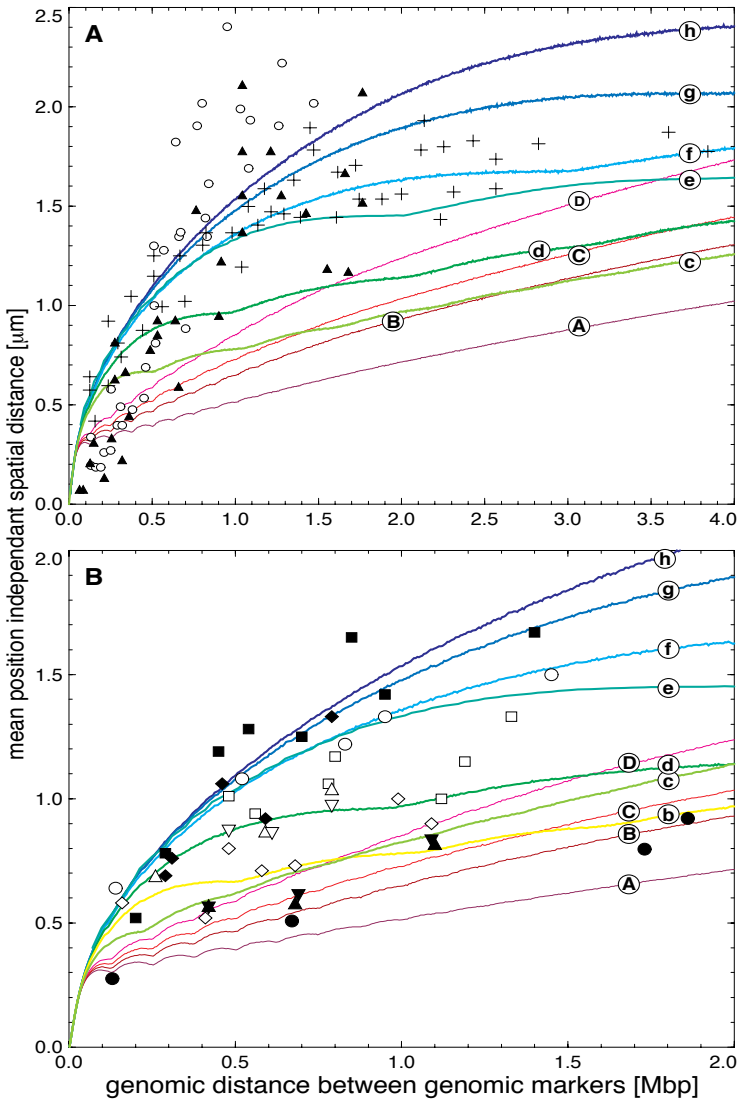

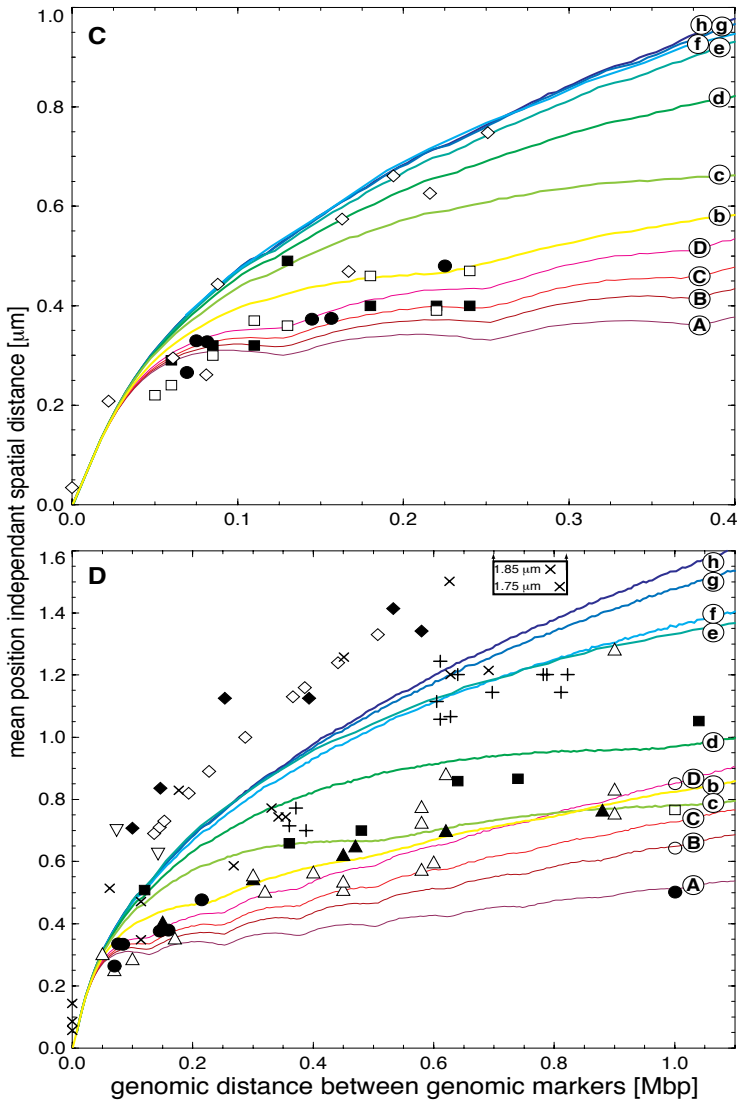

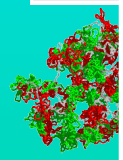

"Synoptic" 3D Architecture of Various Loci

A history "synoptic" comparison of the spatial distance mapping from their original background and aim, FISH methodological protocols, via microscopic imaging and restoration analysis procedures, to their interpretation, reveals that with time Multi-Loop Subcompartment models are favoured.

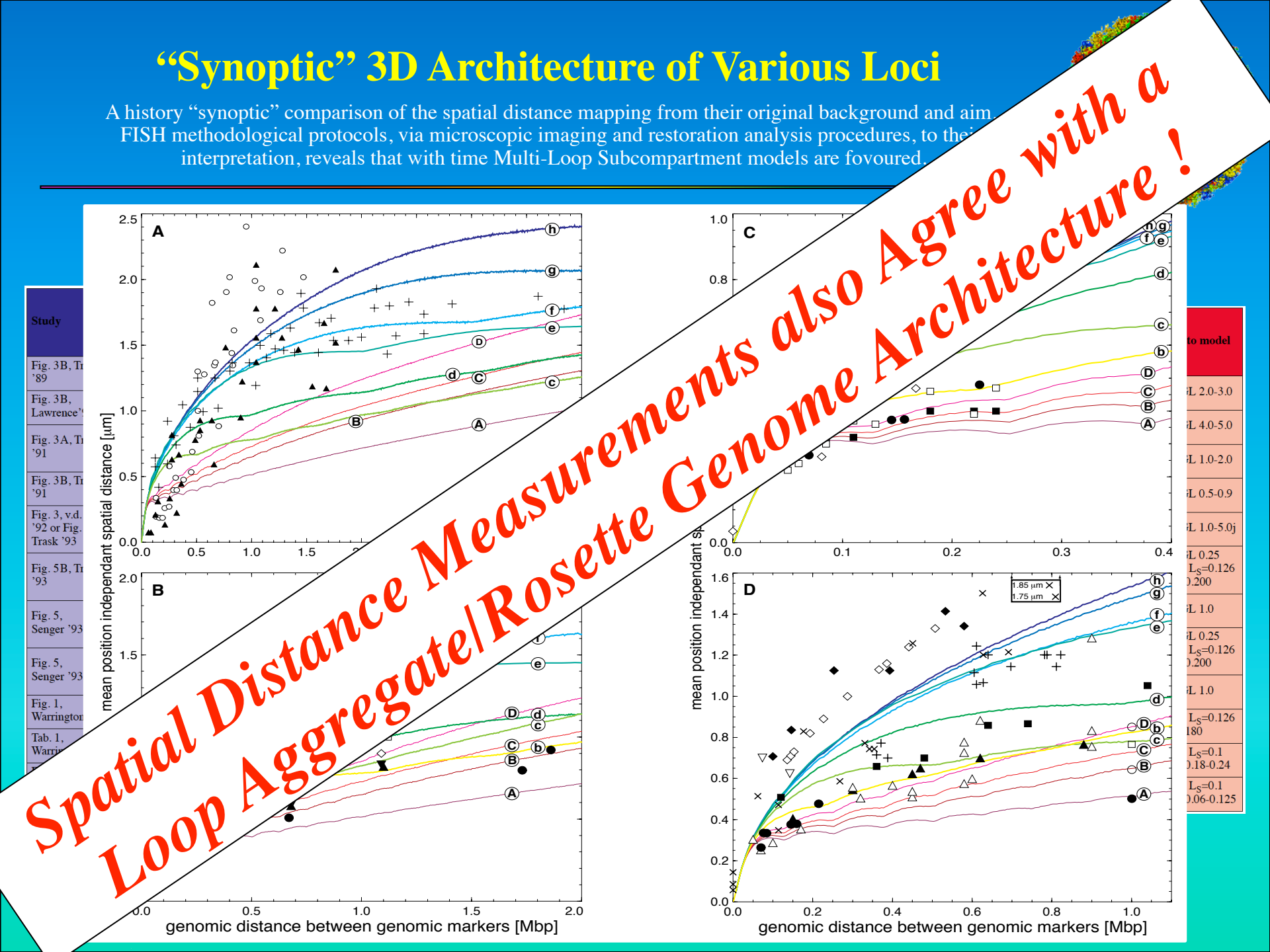

Study	to model
Fig. 3B, Tr '89	L 2.0-3.0
Fig. 3B, Lawrence'	L 4.0-5.0
Fig. 3A, Tr '91	L 1.0-2.0
Fig. 3B, Tr '91	L 0.5-0.9
Fig. 3, v.d. '92 or Fig. Trask '93	L 1.0-5.0j
Fig. 5B, Tr '93	L 0.25 L_S=0.126 0.200
Fig. 5, Senger '93	L 1.0
Fig. 5, Senger '93	L 0.25 L_S=0.126 0.200
Fig. 1, Warrington	L 1.0
Tab. 1, Warri	L_S=0.126 180
	L_S=0.1 0.18-0.24
	L_S=0.1 0.06-0.125

DNA Sequence Organization

Determination of the concentration fluctuation function $C(l)$ and its local slope the correlation coefficient $\delta(l)$ are an indication for the i) degree of long-rang scaling behaveour, ii) general multi-scaling, and iii) fine-structure features, which all are connected to all levels of genome organization and especially also the three-dimensional genome architecture.

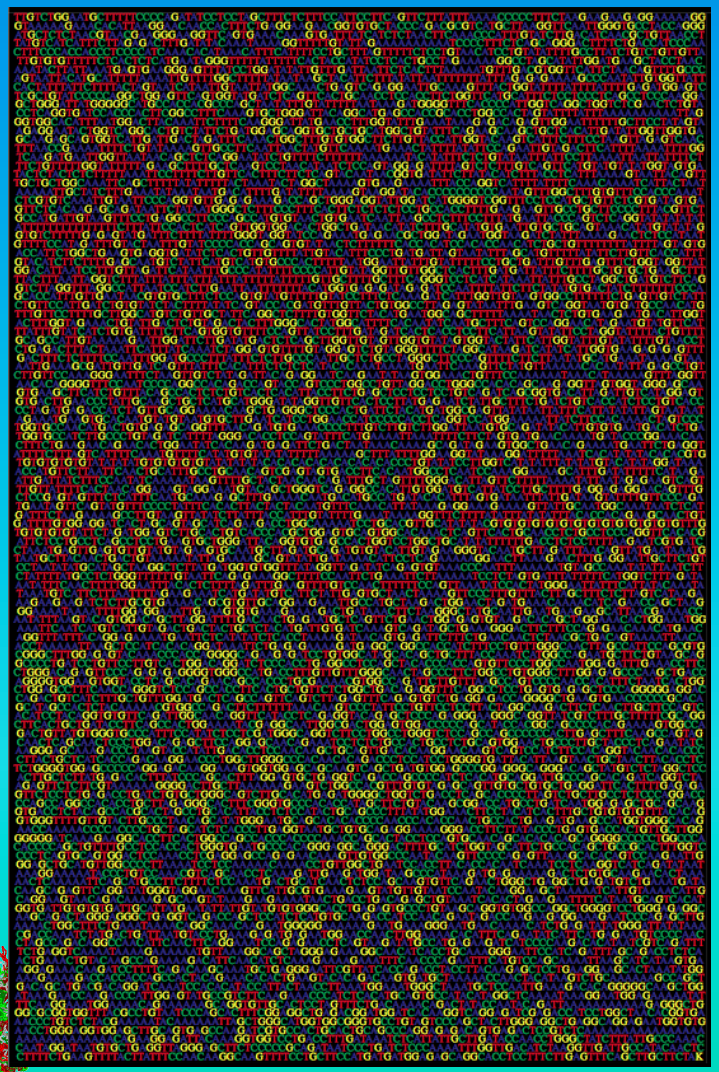

$$C(l) = \sqrt{\left\langle (c_l - \bar{c}_L)^2 \right\rangle_s}$$

$$C(l) = \sqrt{\frac{1}{L-l+1}\sum_{s=1}^{L-l}\left(\frac{1}{l}\sum_{k=1}^{l} n - \frac{1}{L}\sum_{k=1}^{L} N\right)^2}$$

$$C(l) = \frac{1}{Ll}\sqrt{\frac{1}{L-l}\sum_{s=1}^{L-l}\left[\left(\sum_{k=1}^{l} Ln\right) - \left(\sum_{k=1}^{L} lN\right)\right]^2}$$

DNA Sequence Organization

Determination of the concentration fluctuation function $C(l)$ and its local slope the correlation coefficient $\delta(l)$ are an indication for the i) degree of long-rang scaling behaveour, ii) general multi-scaling, and iii) fine-structure features, which all are connected to all levels of genome organization and especially also the three-dimensional genome architecture.

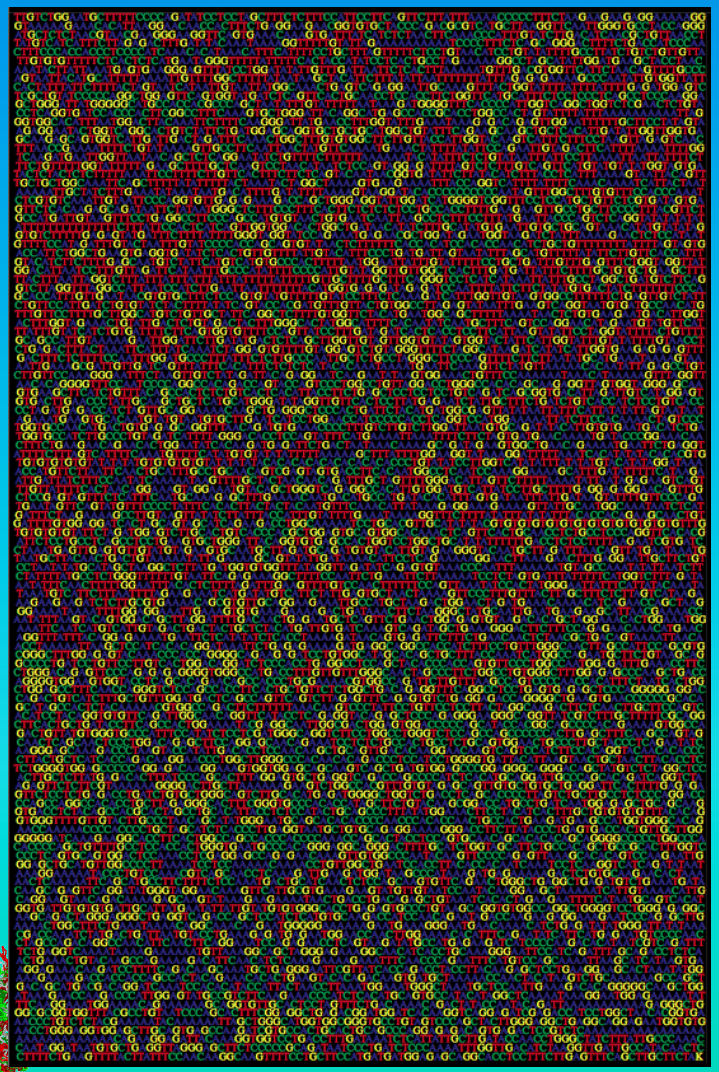

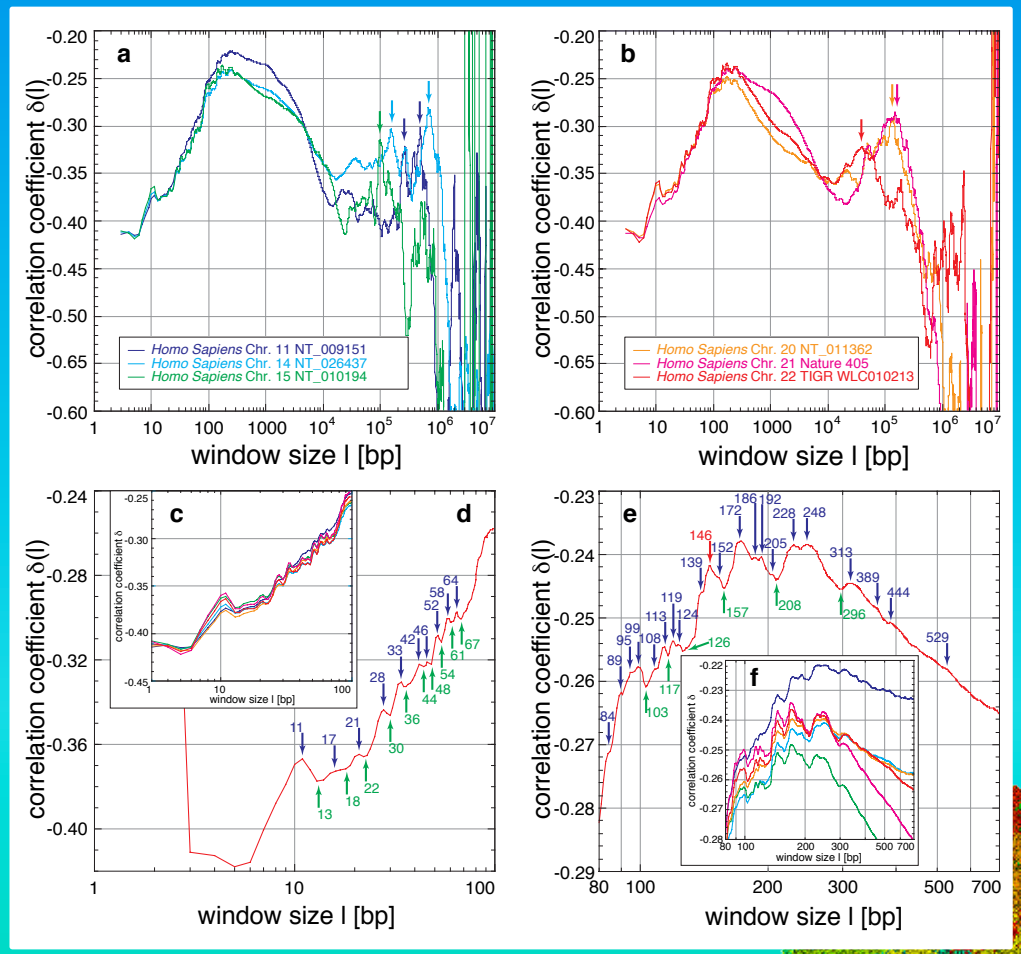

DNA Sequence Organization

Determination of the concentration fluctuation function $C(l)$ and its local slope the correlation coefficient $\delta(l)$ are an indication for the i) degree of long-rang scaling behaveour, ii) general multi-scaling, and iii) fine-structure features, which all are connected to all levels of genome organization and especially also the three-dimensional genome architecture.

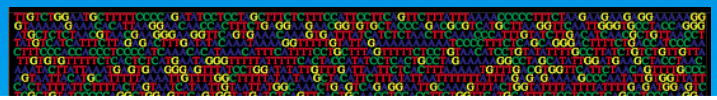

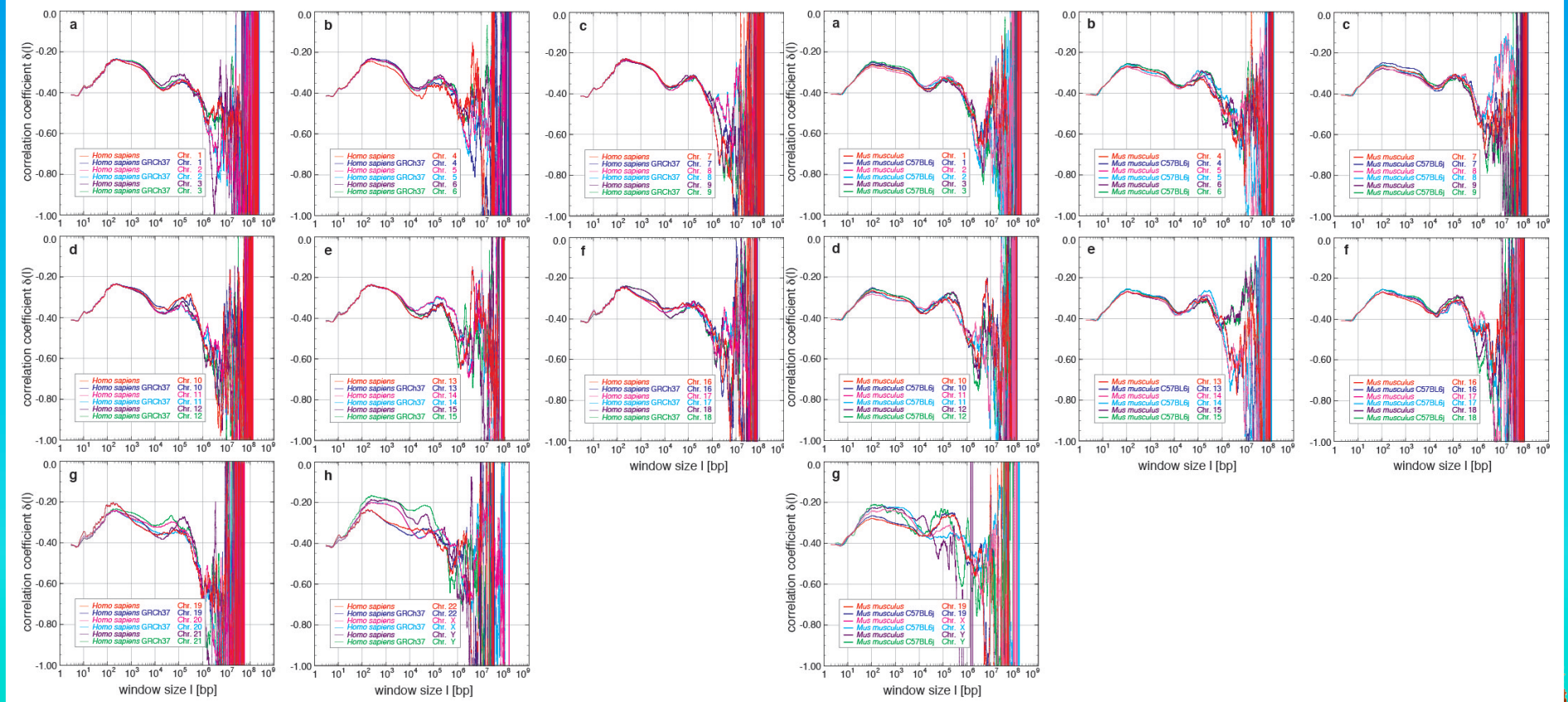

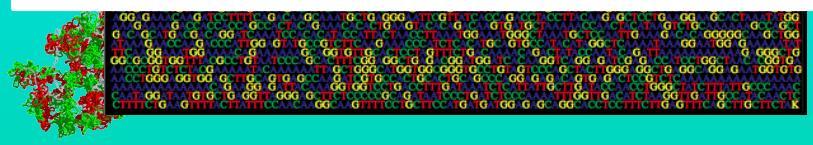

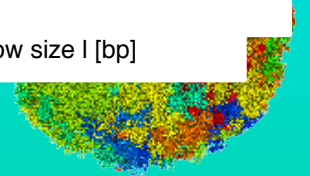

DNA Sequence Organization

Determination of the concentration fluctuation function $C(l)$ and its local slope the correlation coefficient $\delta(l)$ are an indication for the i) degree of long-rang scaling behaveour, ii) general multi-scaling, and iii) fine-structure features, which all are connected to all levels of genome organization and especially also the three-dimensional genome architecture.

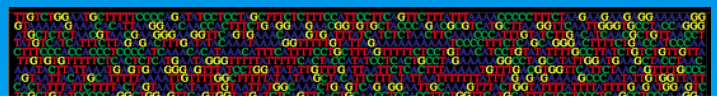

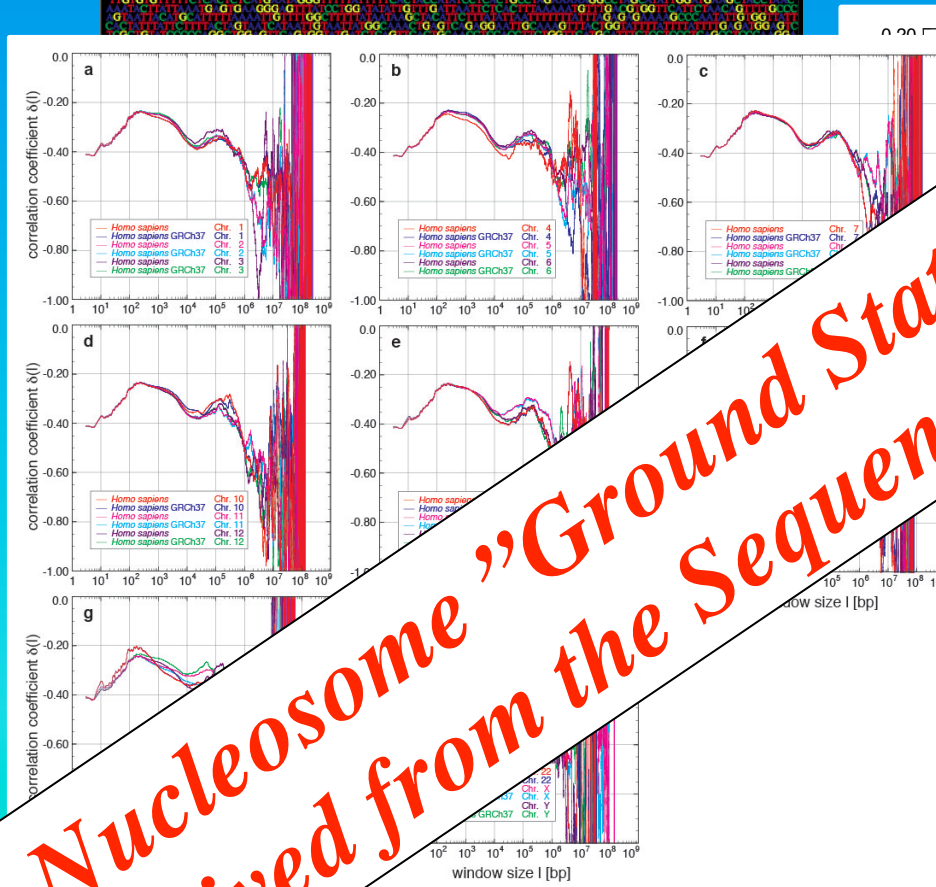

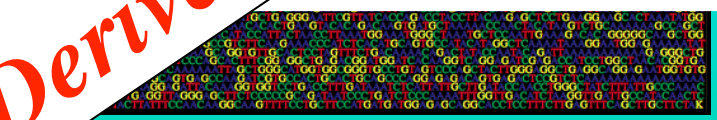

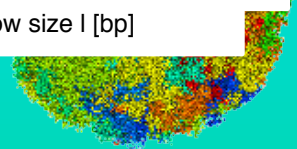

window size l [bp]

window size l [bp]

Nucleosome "Ground States" and Rosettes can be Derived from the Sequence and Show the Holistics !

Scaling Analysis

Scaling analysis show again the entire bandwidth of architectural effects in an aggregated manner. Beyond, they show the scale bridging of the structures and the evolutionary holistic entanglement between the 3D architecture and the DNA sequence organization itself.

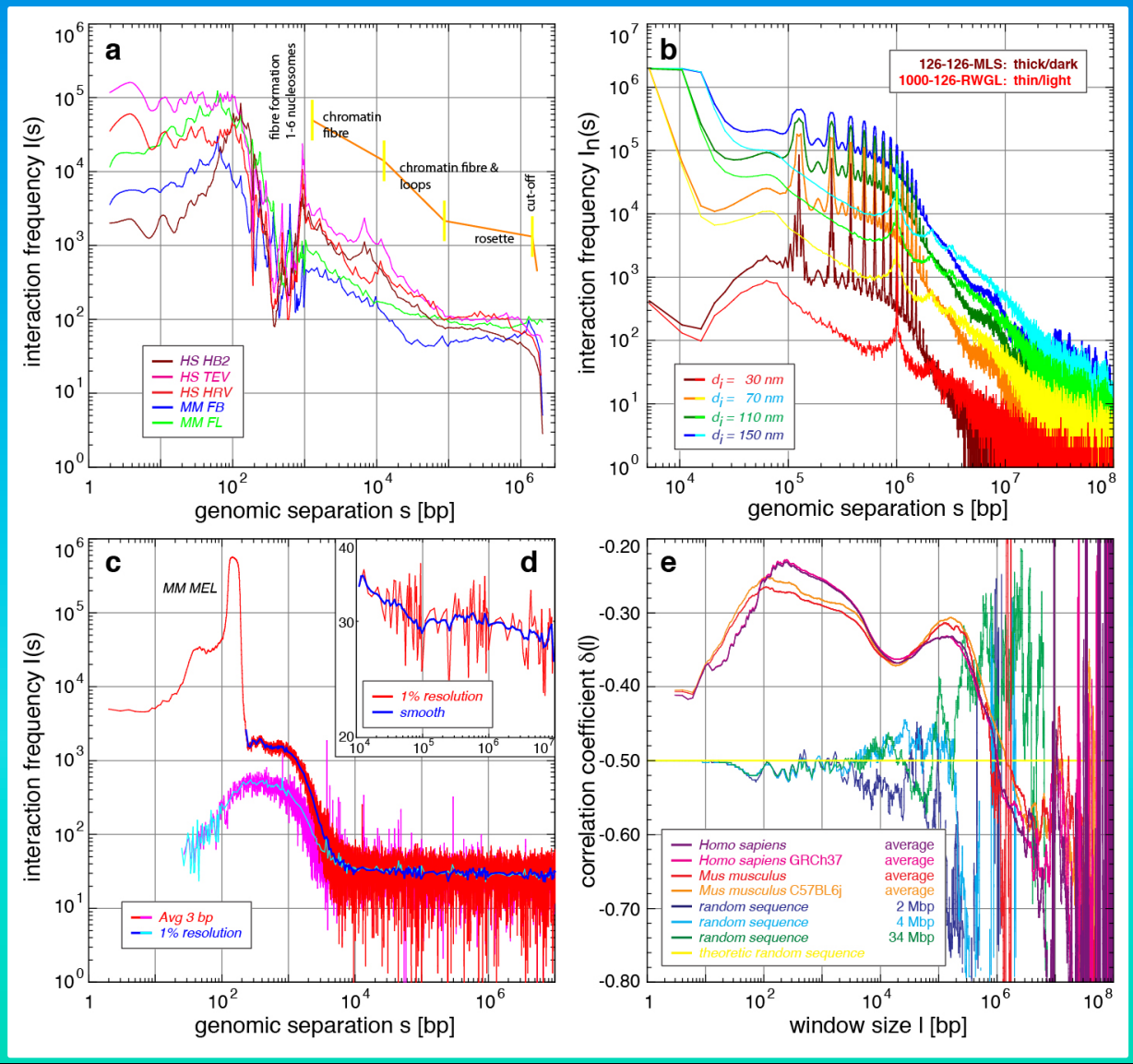

Scaling Analysis

Scaling analysis show again the entire bandwidth of architectural effects in an aggregated manner. Beyond they show the scale bridging of the structures and the evolutionary holistic entanglement between the 3 architecture and the DNA sequence organization itself.

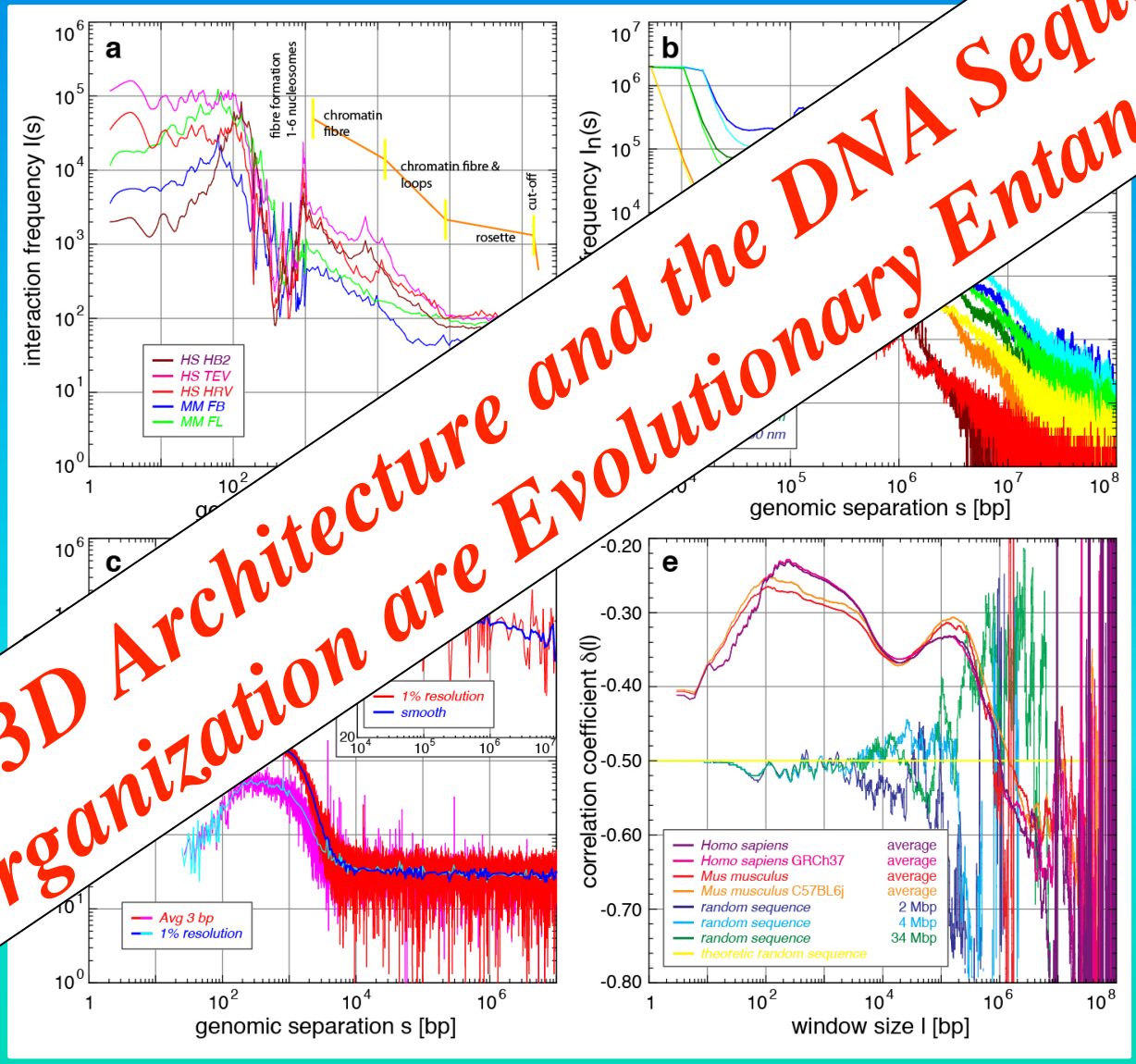

The 3D Architecture and the DNA Sequence Organization are Evolutionary Entangled !

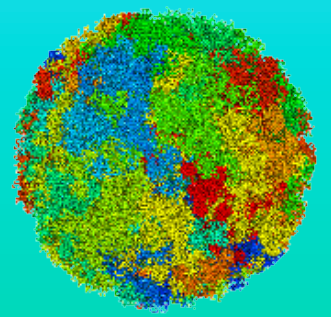

Scaling of the Chromatin Fiber Topology

The spatial-distance and exact yard-stick dimension distinguish between the simulated models in detail.The MLS model shows a globular and fine-structured multi scaling behaviour due to the loops froming rosettes. This agrees with DNA fragmentation by Carbon ion irradiation and the appearance of fine-structured multi-scaling long-range correlations found in the sequential organization of genomes.

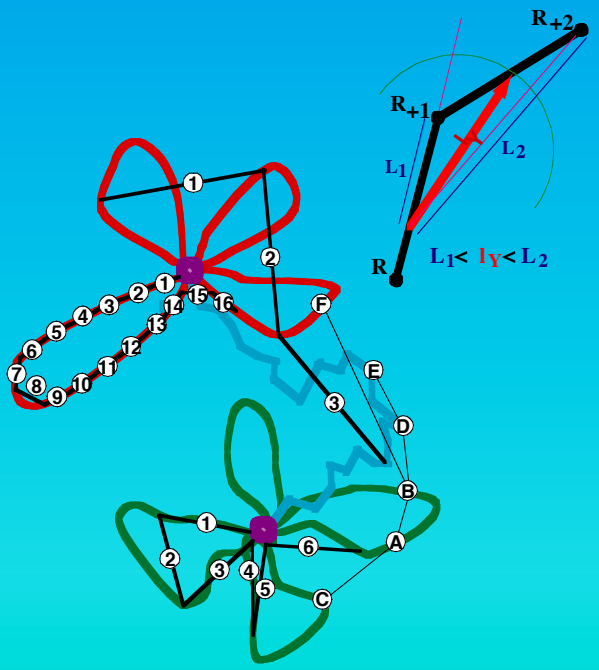

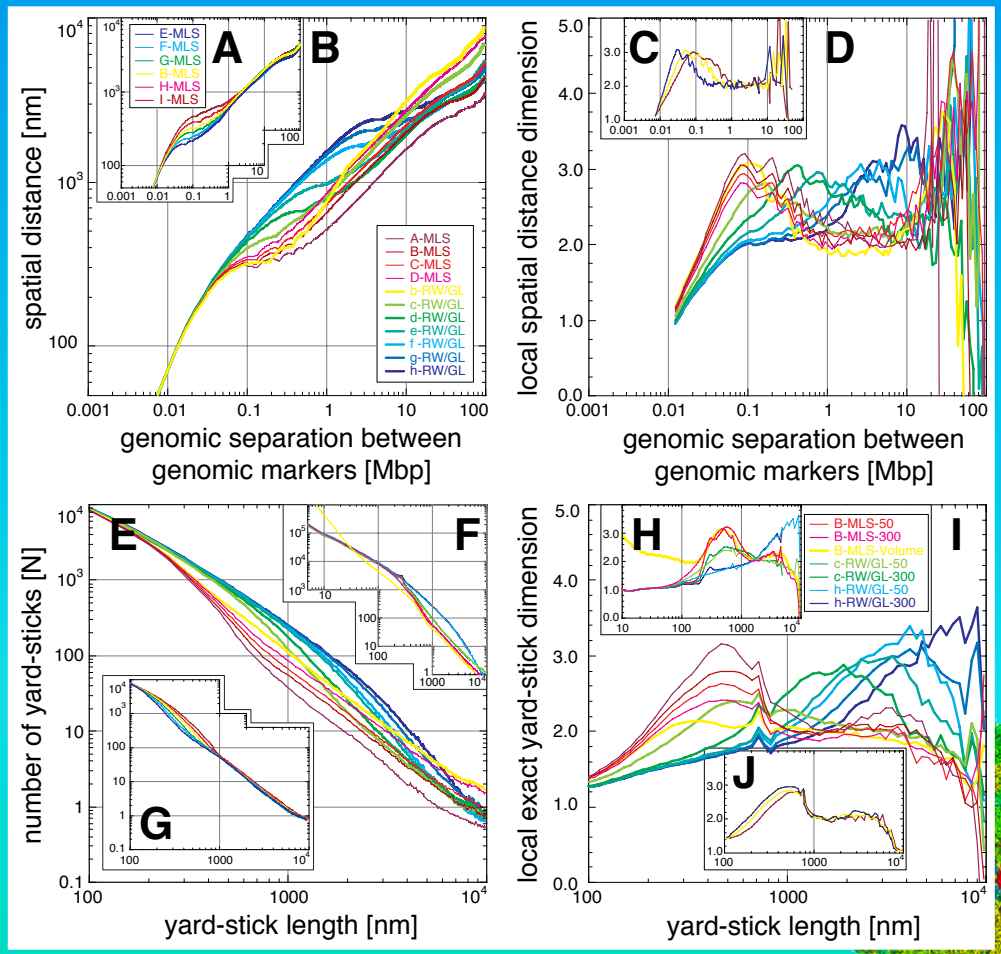

From Fiber Topology to Nuclear Morphology

Chromosome territories form in the RW/GL and the MLS model. However, only the MLS model leads distinct subcompartments and low chromosome and subcompartment overlap. Best agreement is reached for an MLS model with 80 to 120 kbp loops and linkers in nuclei with 8 to 10 μm diameter.

The simulated nuclear morphology reflects the chromosome fiber topology of different models in detail.

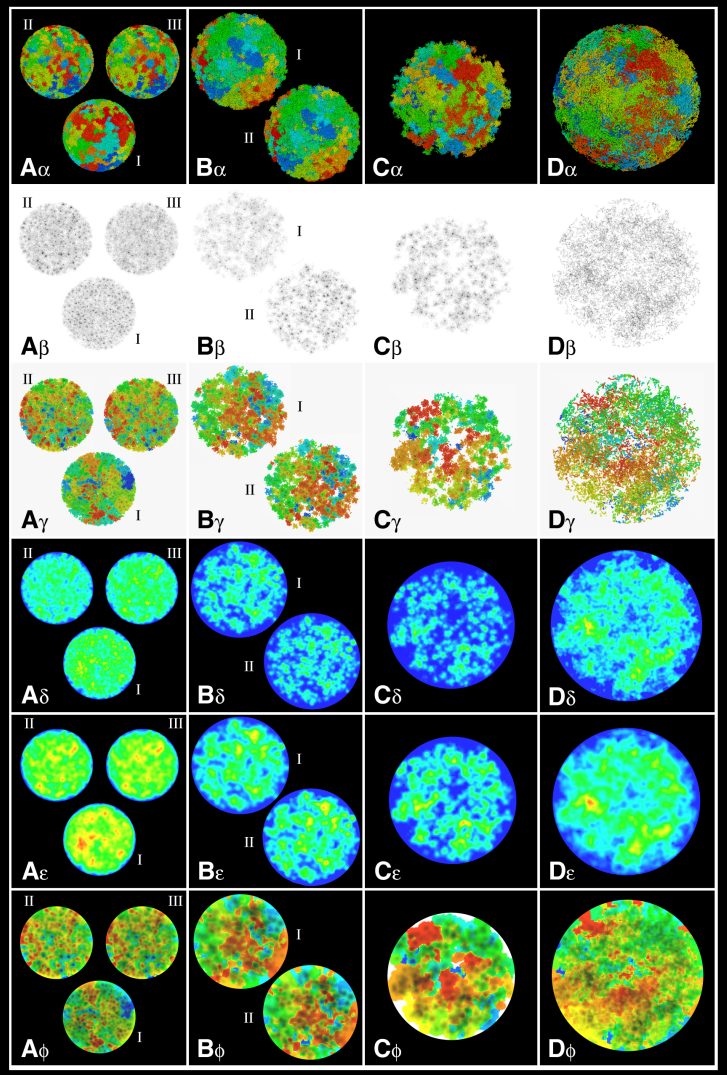

A: MLS in 6 μm nucleus
I: 63 kbp loops, 63 kbp linkers
II: 63 kbp loops, 252 kbp linkers
III: 126 kbp loops, 252 kbp linkers

B: MLS in 8 μm nucleus
I: 126 kbp loops, 126 kbp linkers
II: 84 kbp loops, 126 kbp linkers

C: MLS in 10 μm nucleus
126 kbp loops, 126 kbp linker,
not totally relaxed

D: RW/GL in 12 μm nucleus
5 Mbp loops
not totally relaxed

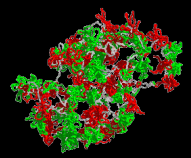

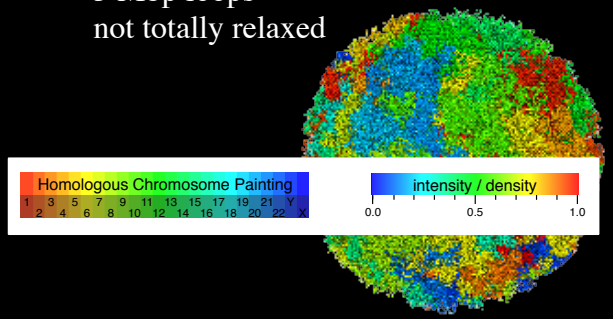

Fine Morphology of Nuclei

High resolution rendering and simulated electron microscopy including territory painting reveal not only again the model details but also that any location in the nucleus is accessible to biological molecules <15 nm in diameter and that even the Extended Interchromosomal Domain hypothesis is oversimplified.

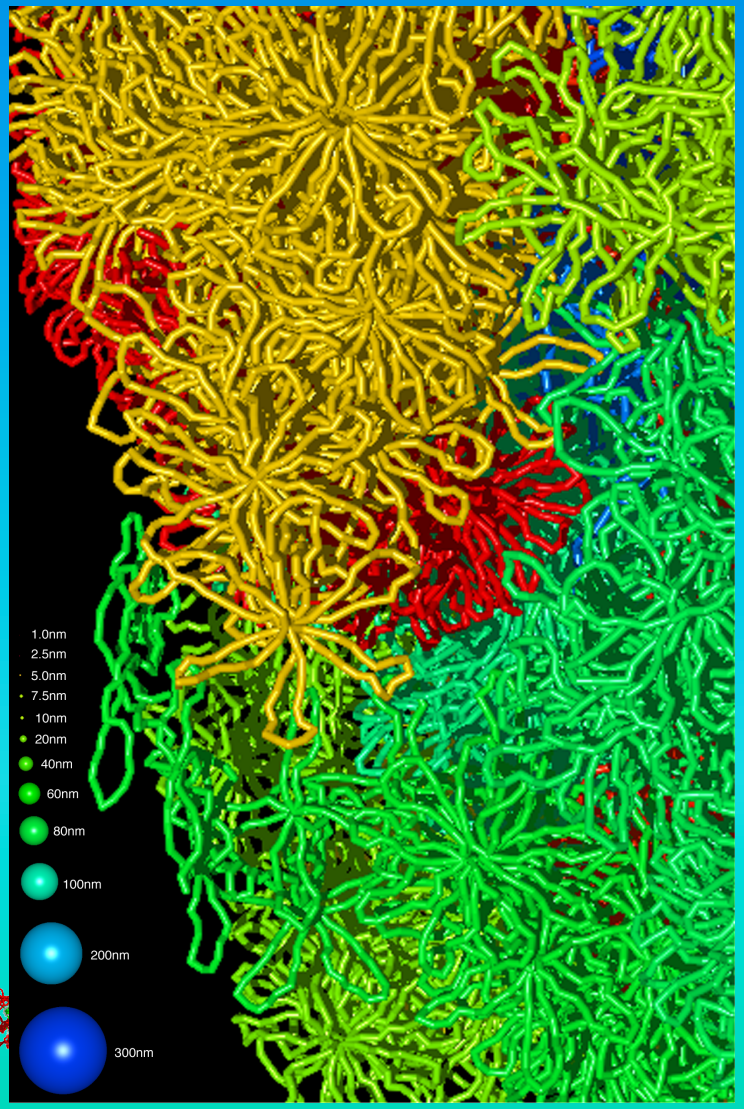

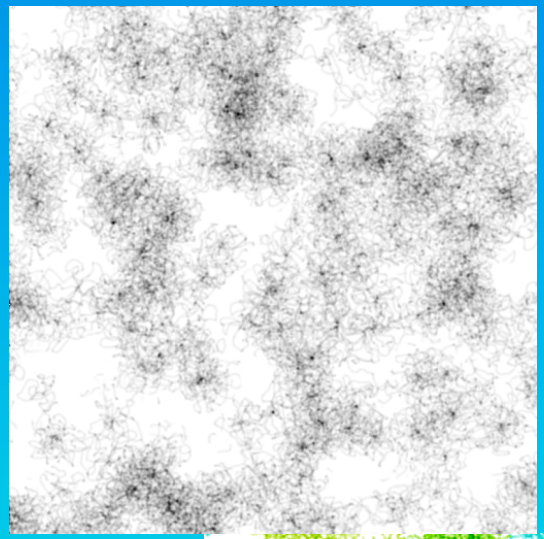

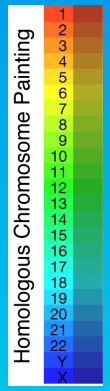

MLS models model with 126 kbp loops and linkers in a 10 μm nucleus.

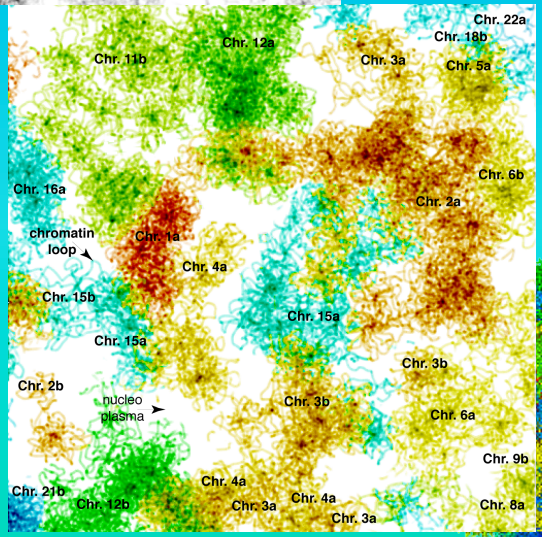

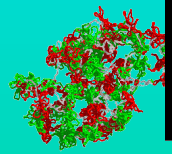

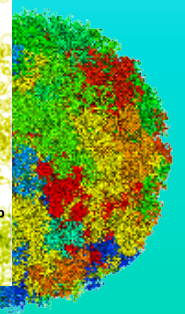

In vivo Morphology & Chromatin Distribution

The stable expression of fusions between histones and autofluorescent proteins and the integration into nucleosomes allows the minimal invasive investigation of the structure and dynamics of chromatin.

The clustered morphology in detail favour an MLS like chromatin topology.

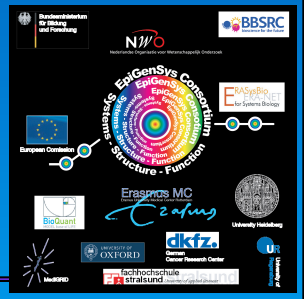

HeLa, H2A-YFP

Cos7, H1.0-GFP

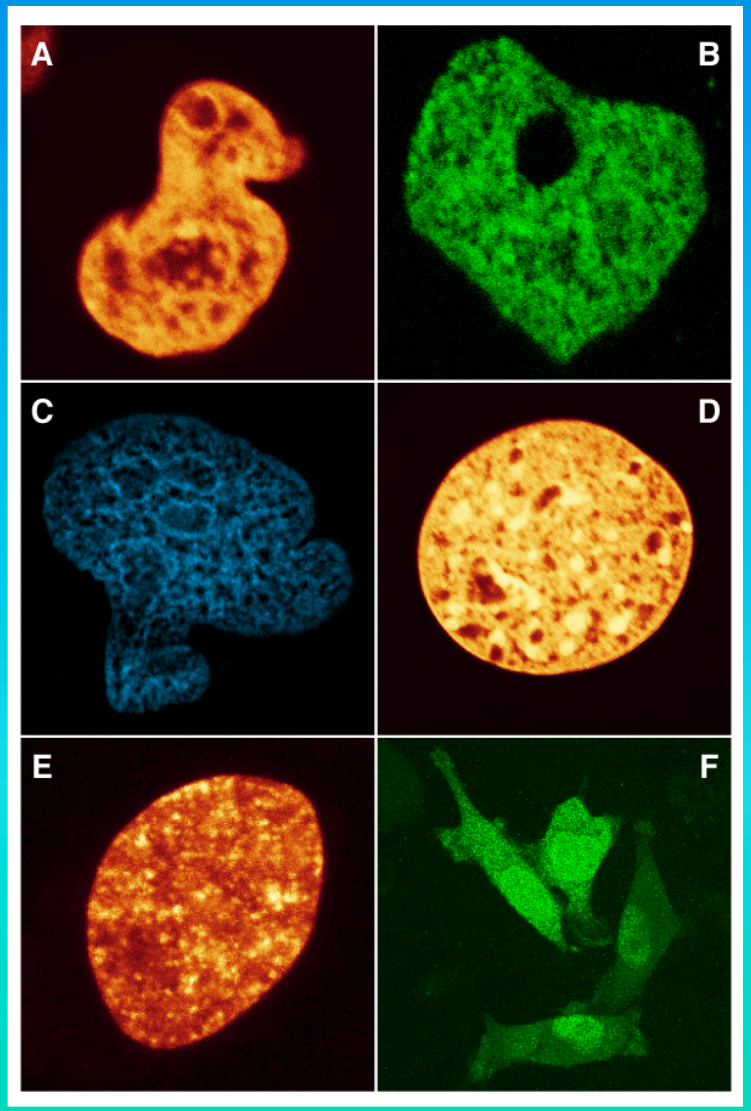

LCLC 103H, H2A-CFP

ID13, H2A-YFP

HeLa, mH2A1.2-YFP

HeLa, H2A-YFP, natural promoter

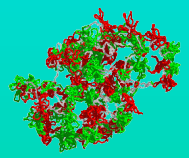

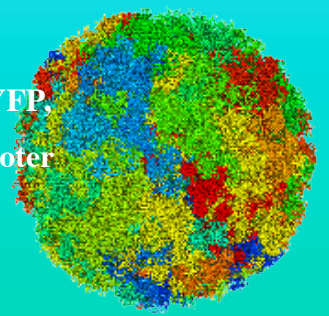

Scaling of the Chromatin Morphology & Distribution

The local (inverse-) mass dimension distribution distinguishs between the models in detail and show also a multi-scaling behaviour with globular feature for the MLS model like the scaling of the fiber topology. With the mass dimension as function of intensity separates very well between different nuclei *in vivo*.

Consequently, the chromatin morphology is causally and quantitatively connected to the fiber topology.

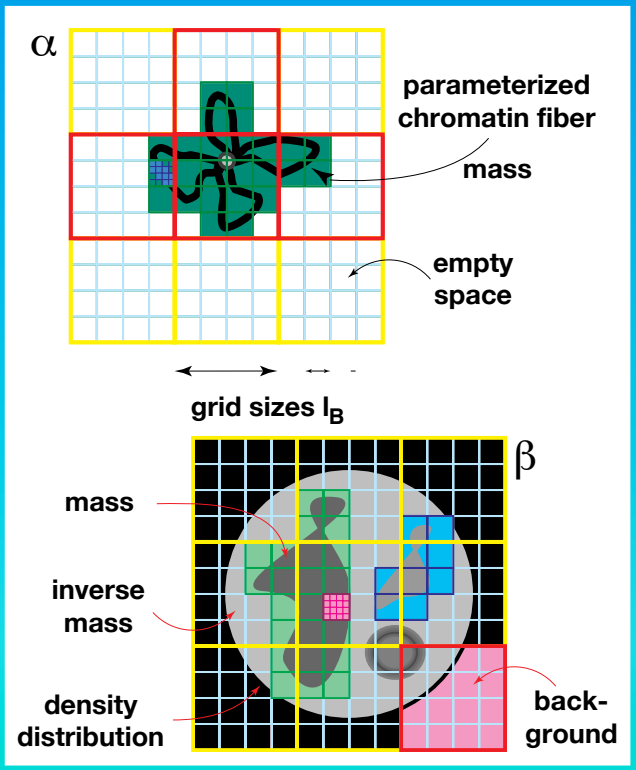

(inverse-) mass dimension distribution

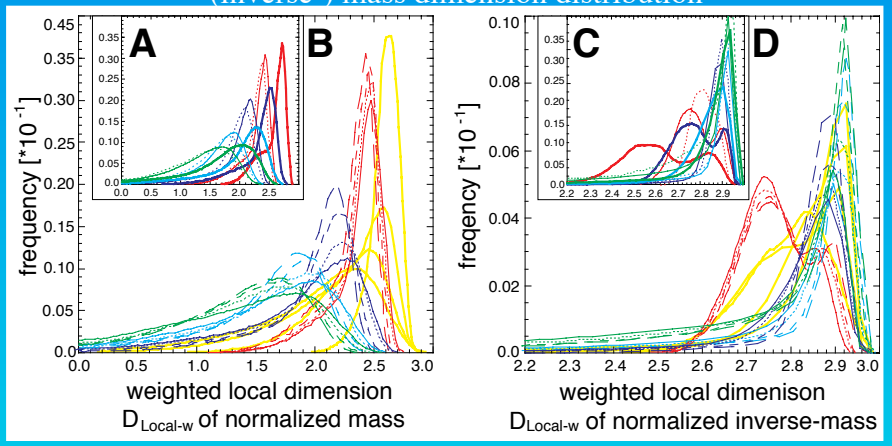

mass dimension as function of image intensity

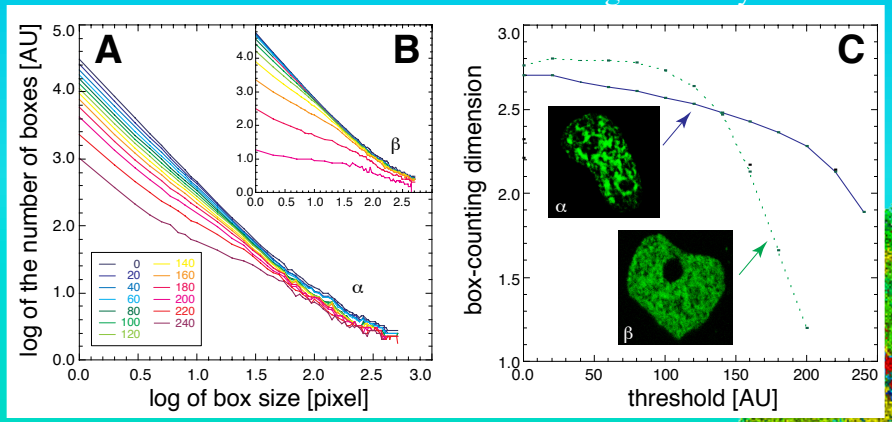

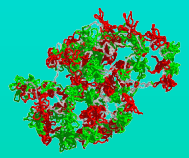

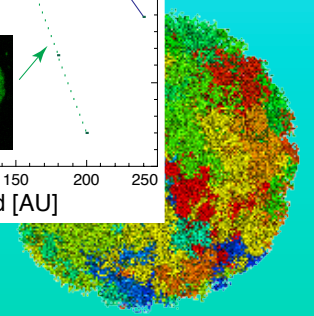

Quantified TSA induced Morpholoy Changes

Trichostatin A induced histone acetylation can be quantified by *in vivo* H2A-GFP confocal images and image correlation spectroscopy (iFCS), which is a scaling analysis, and reveals the opening of chromatin, and thus reorganization changes on scales from 0.2 to ~1μm, consistent with MLS models.

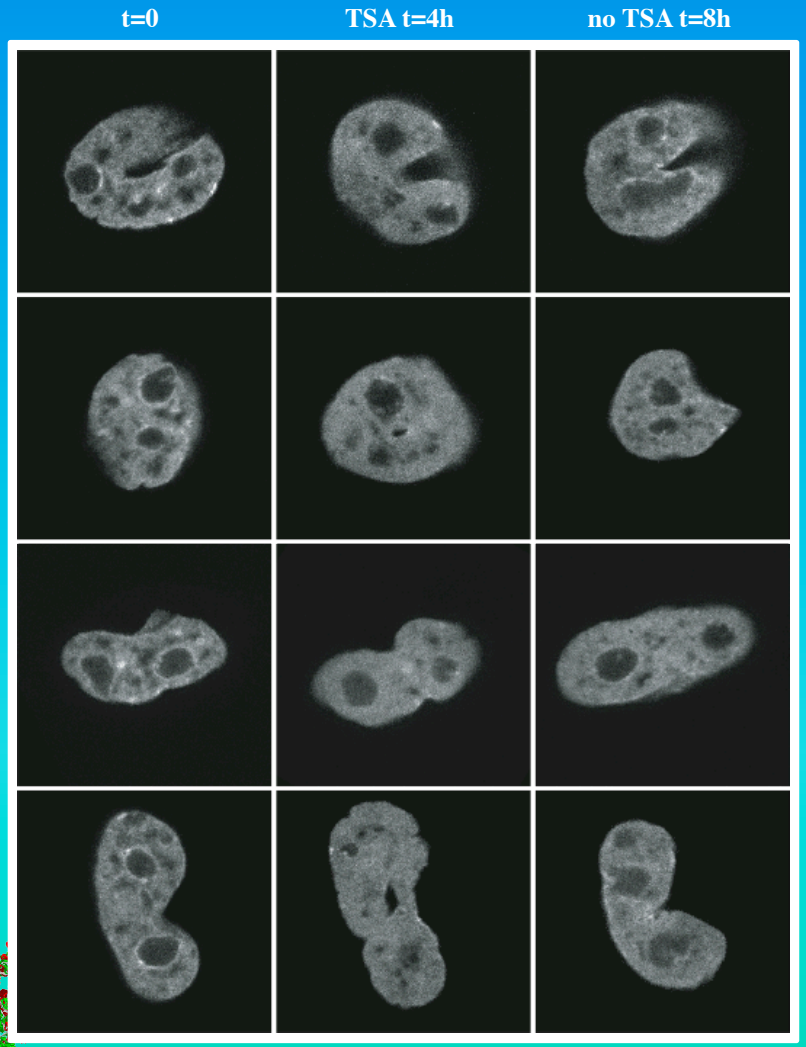

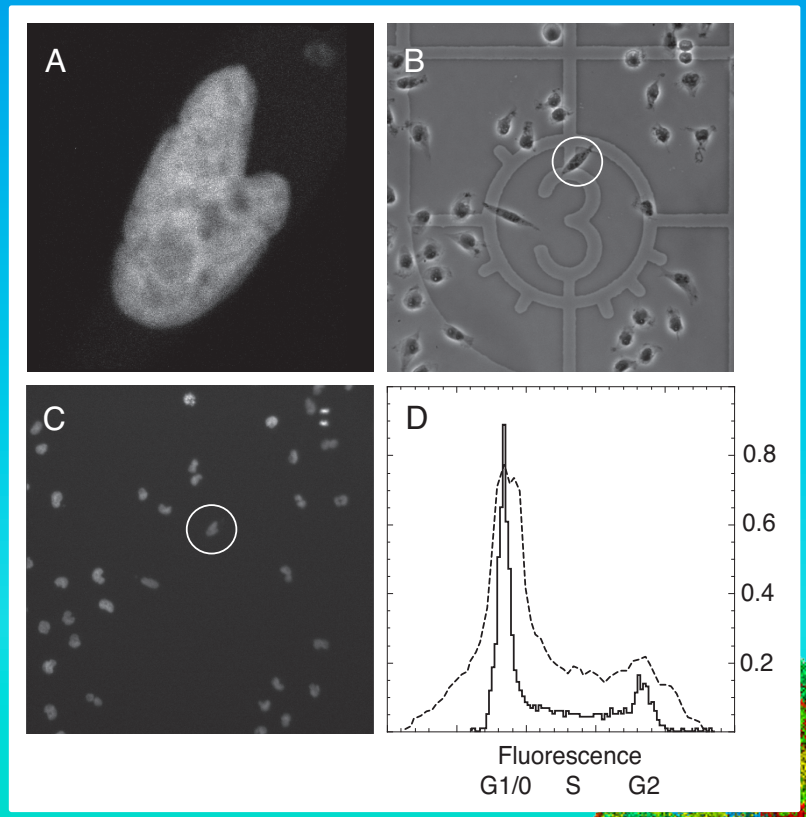

Quantified TSA induced Morpholoy Changes

Trichostatin A induced histone acetylation can be quantified by *in vivo* H2A-GFP confocal images and image correlation spectroscopy (iFCS), which is a scaling analysis, and reveals the opening of chromatin, and thus reorganization changes on scales from 0.2 to ~1μm, consistent with MLS models.

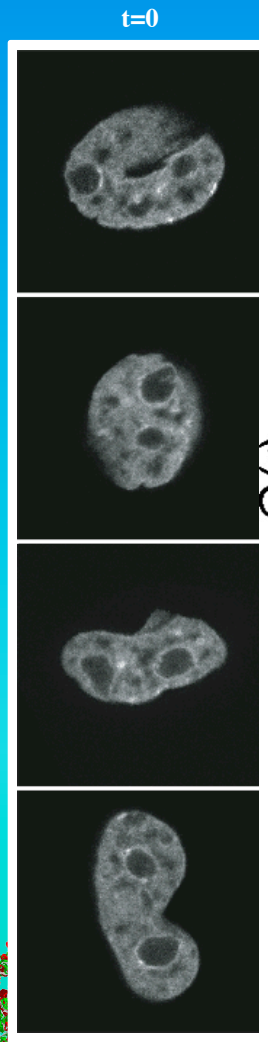

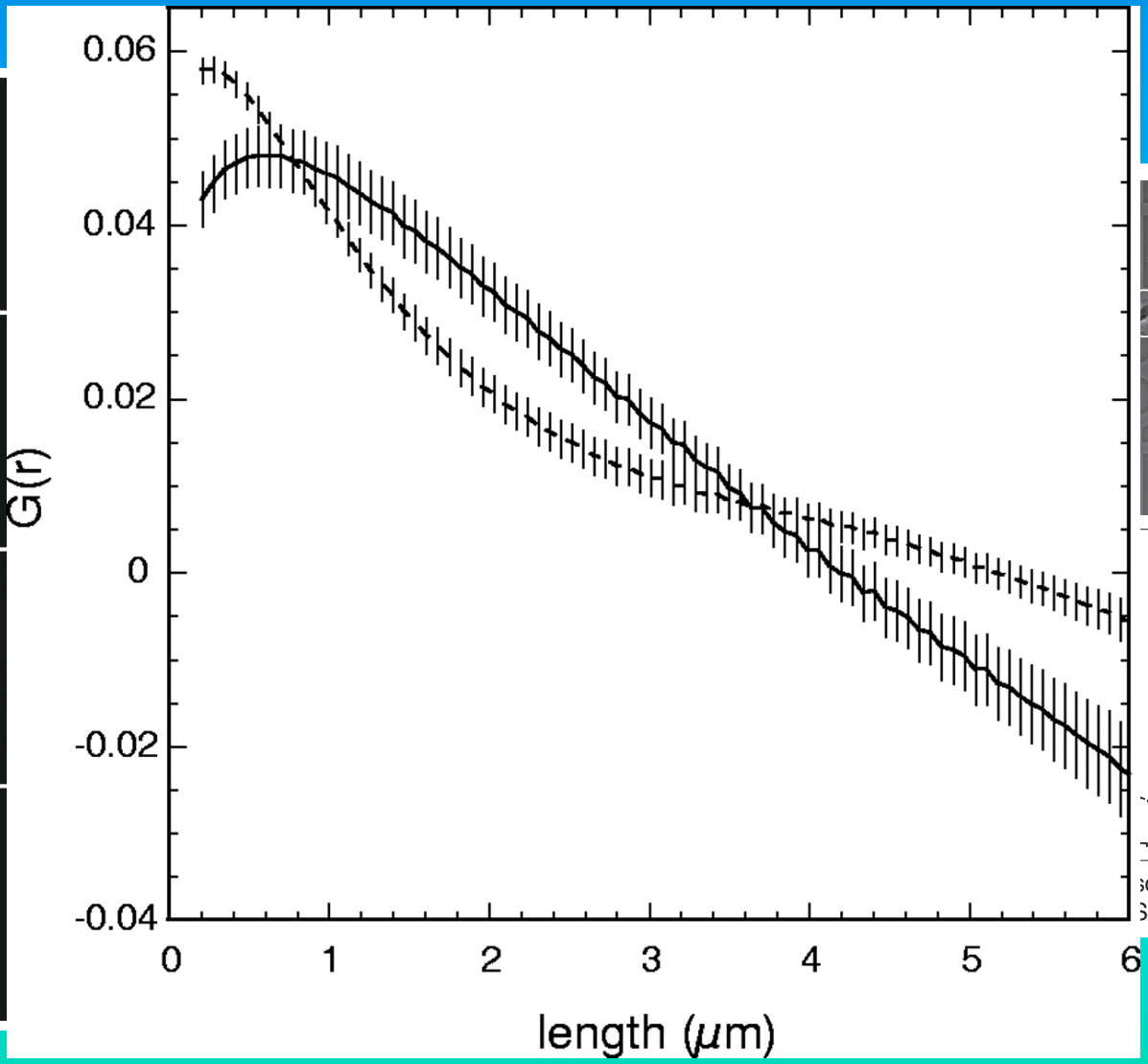

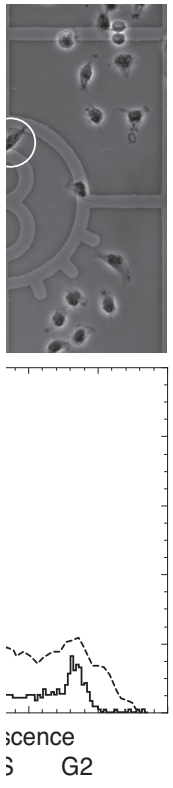

Quantified TSA induced Morpholoy Changes

Trichostatin A induced histone acetylation can be quantified by *in vivo* H2A-GFP confocal images and image correlation spectroscopy (iFCS), which is a scaling analysis, and reveals the opening of chrom and thus reorganization changes on scales from 0.2 to ~1μm, consistent with MLS model

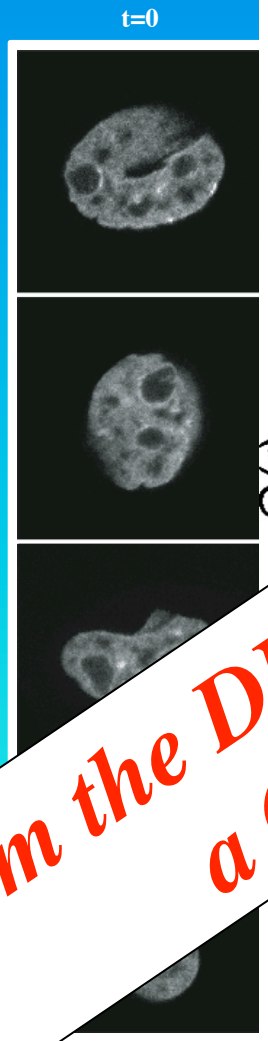

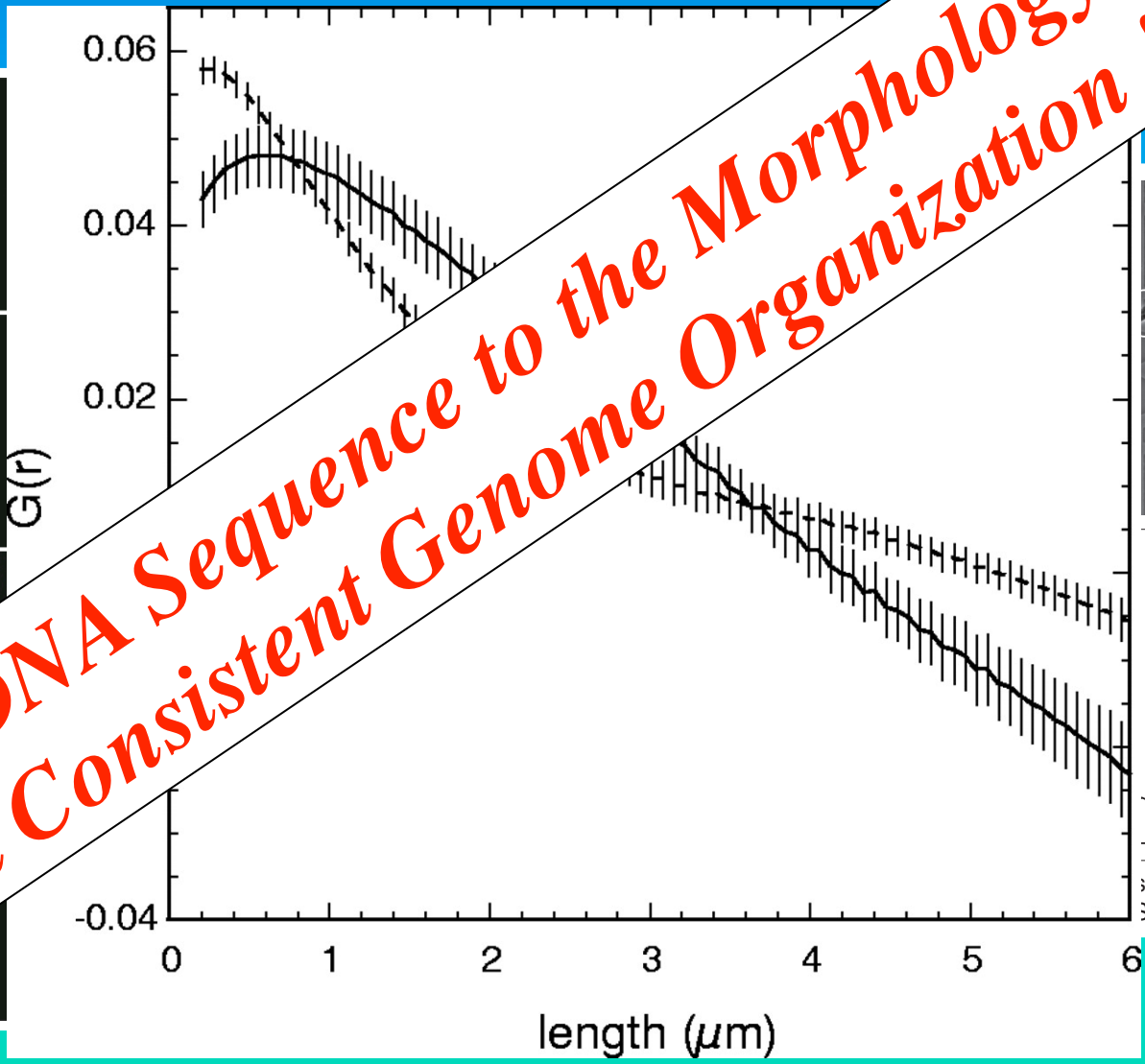

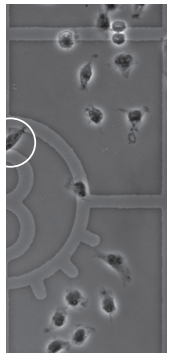

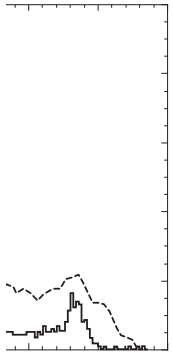

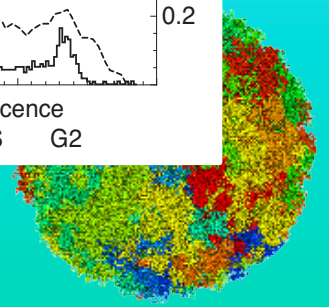

From the DNA Sequence to the Morphology there is a Consistent Genome Organization !

Counting Nucleosomes *In Vivo*

Counting nucleosomes in living cells with a combination of fluorescence correlation spectroscopy (FCS) and confocal laser scanning microscopy (CLSM) reveals not only the free unbound histone component but also the concentration in absolute numbers of bound histones. Thus, the absolute concentration distribution of histones can be determined and reveals again the typical expected distribution of aggregated chromatin loops.

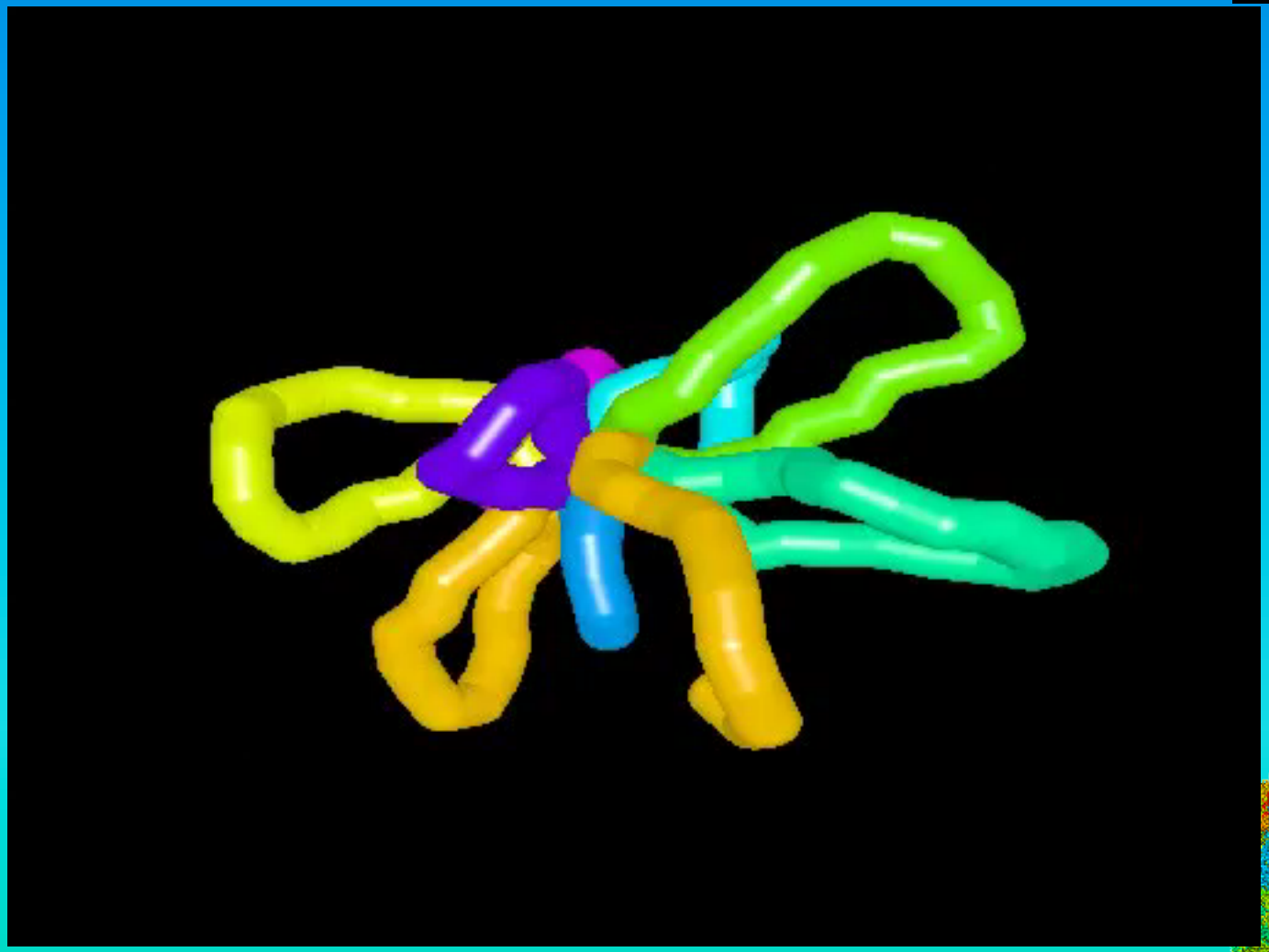

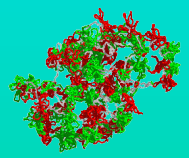

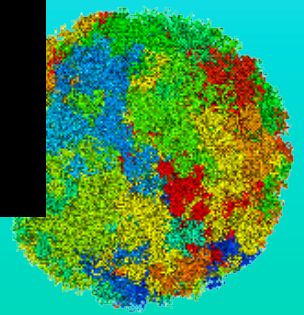

Counting Nucleosomes *In Vivo*

Counting nucleosomes in living cells with a combination of fluorescence correlation spectroscopy (FCS) and confocal laser scanning microscopy (CLSM) reveals not only the free unbound histone component but also the concentration in absolute numbers of bound histones. Thus, the absolute concentration distribution of histones can be determined and reveals again the typical expected distribution of aggregated chromatin loops.

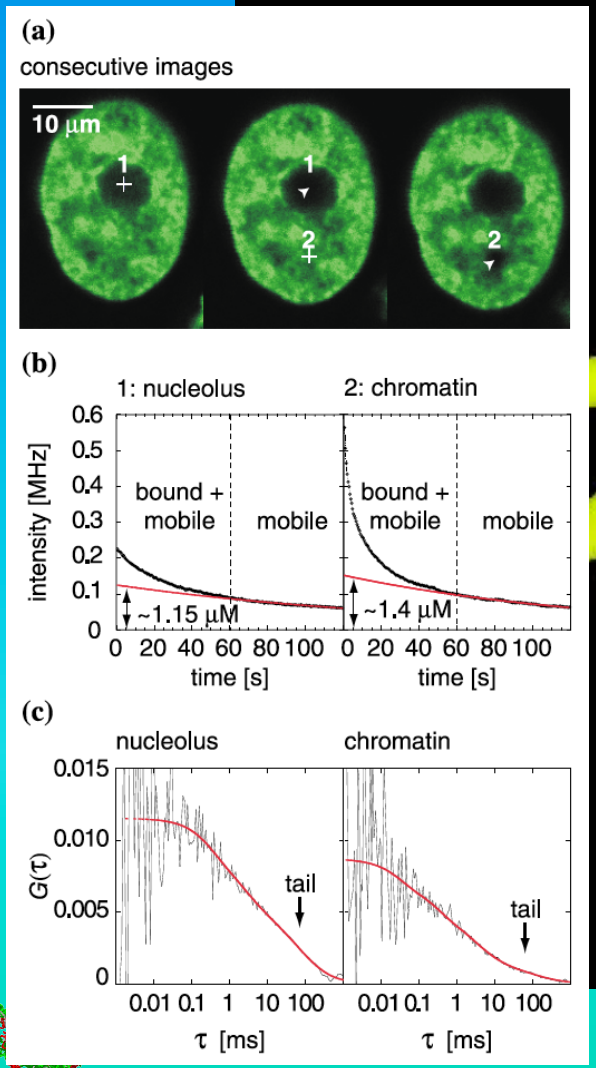

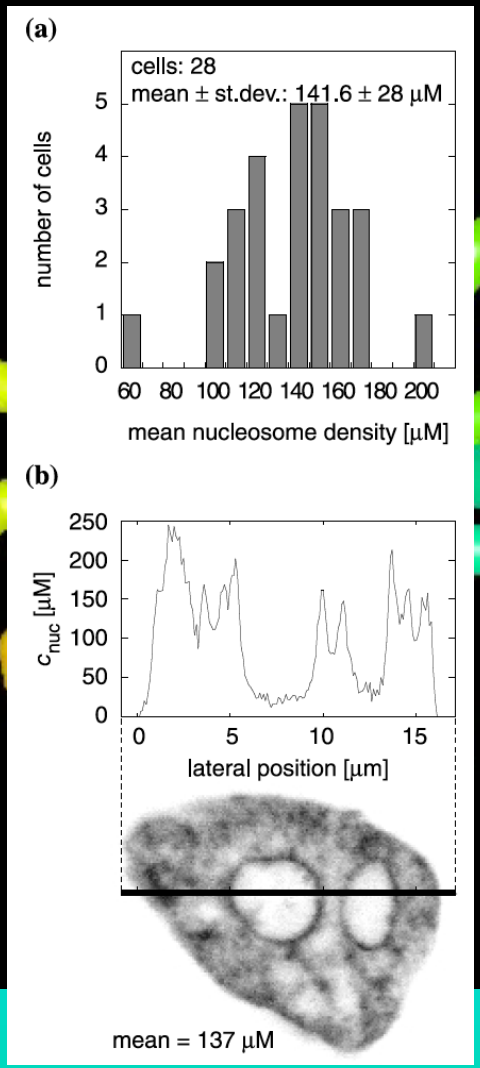

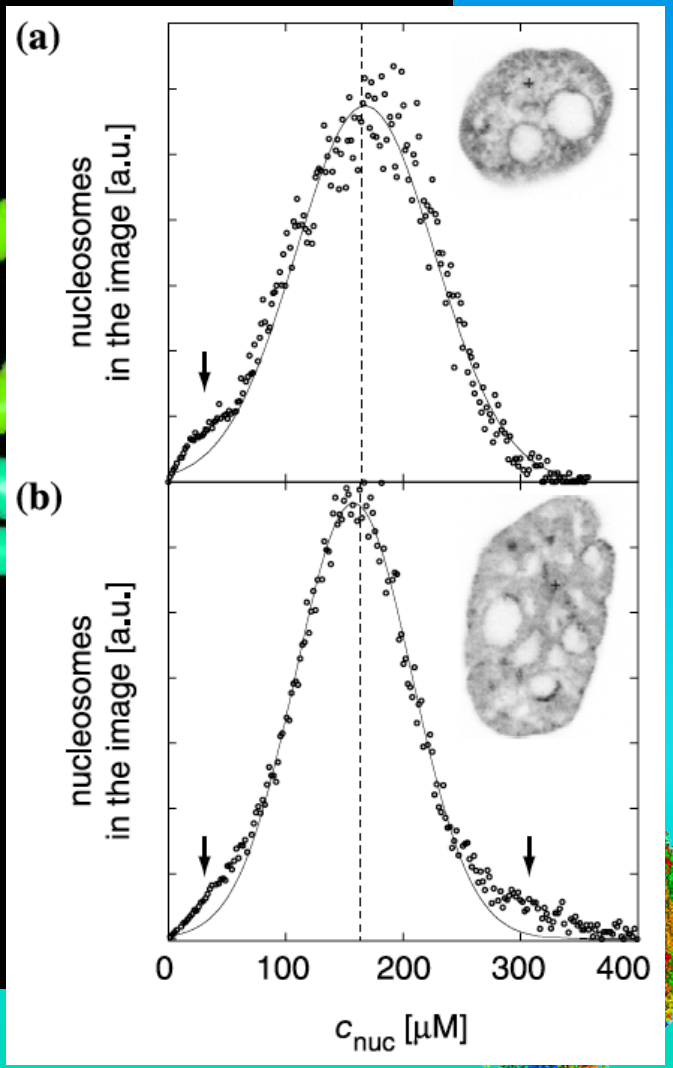

Counting Nucleosomes *In Vivo*

Counting nucleosomes in living cells with a combination of fluorescence correlation spectroscopy (FCS) and confocal laser scanning microscopy (CLSM) reveals not only the free unbound histone component but also concentration in absolute numbers of bound histones. Thus, the absolute concentration distribution of can be determined and reveals again the typical expected distribution of aggregated chromati

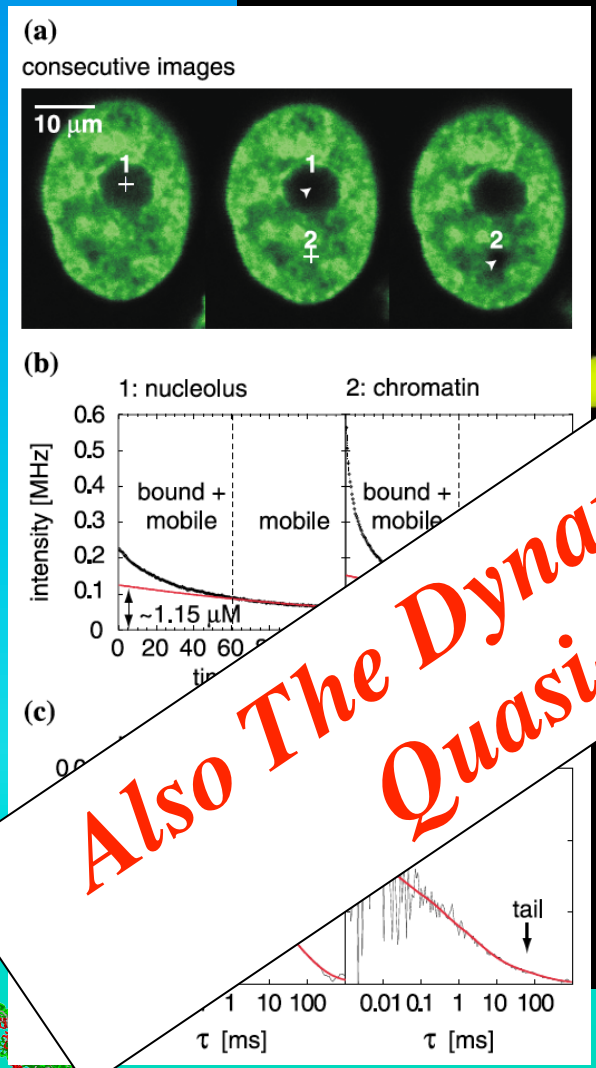

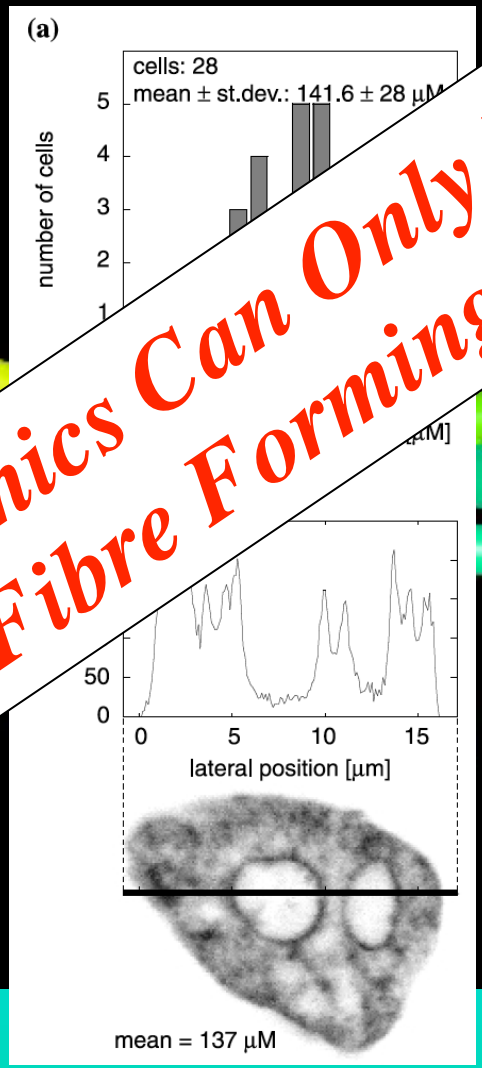

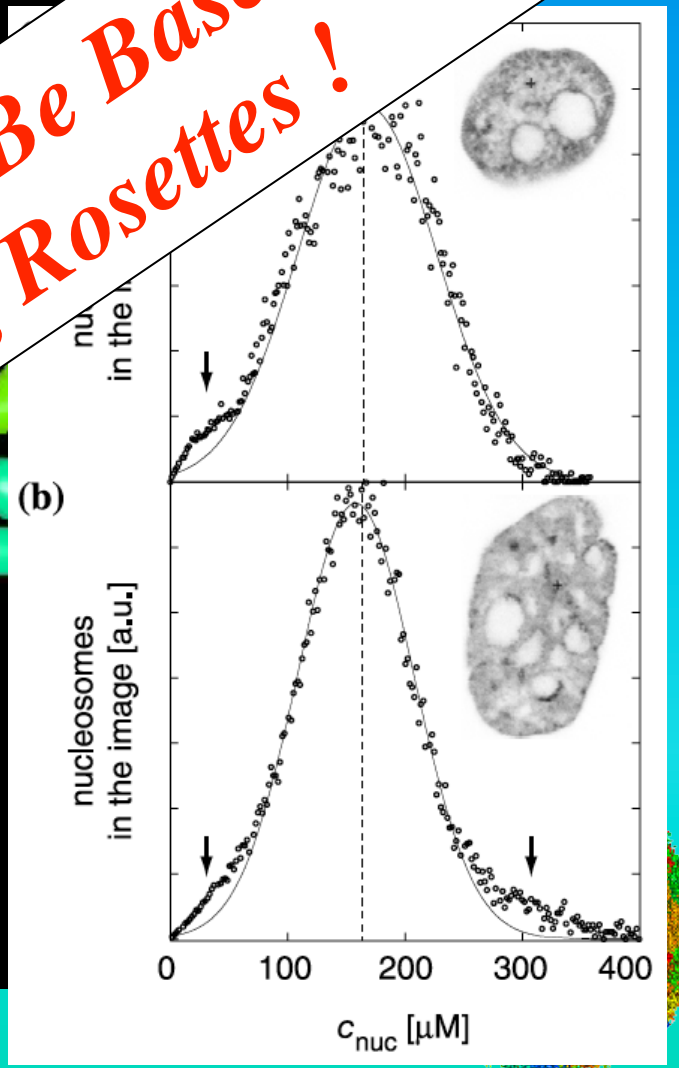

Also The Dynamics Can Only Be Based On A Quasi-Fibre Forming Rosettes !

DNA Fragment Distribution after Ione-Irradiation

The length distribution of DNA fragments after irradiation with e. g. C or Ca with an inhomogeneous spatial double strand breackage probability depends on the detailed folding topology of the chromatin fiber and the RW/GL and MLS models differ largely.

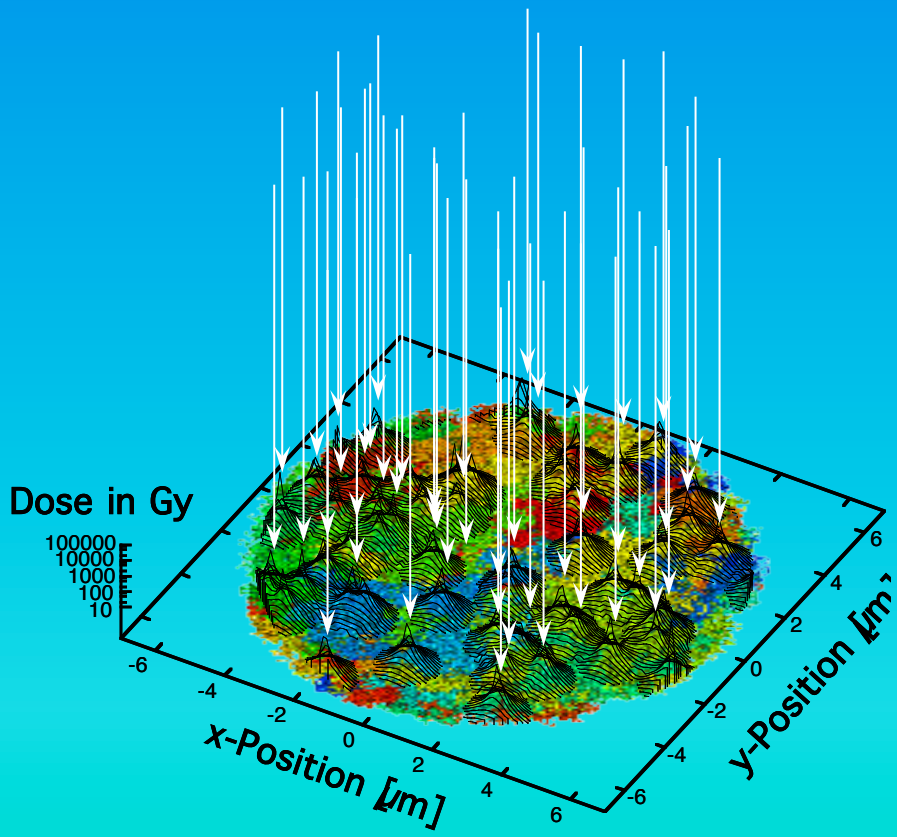

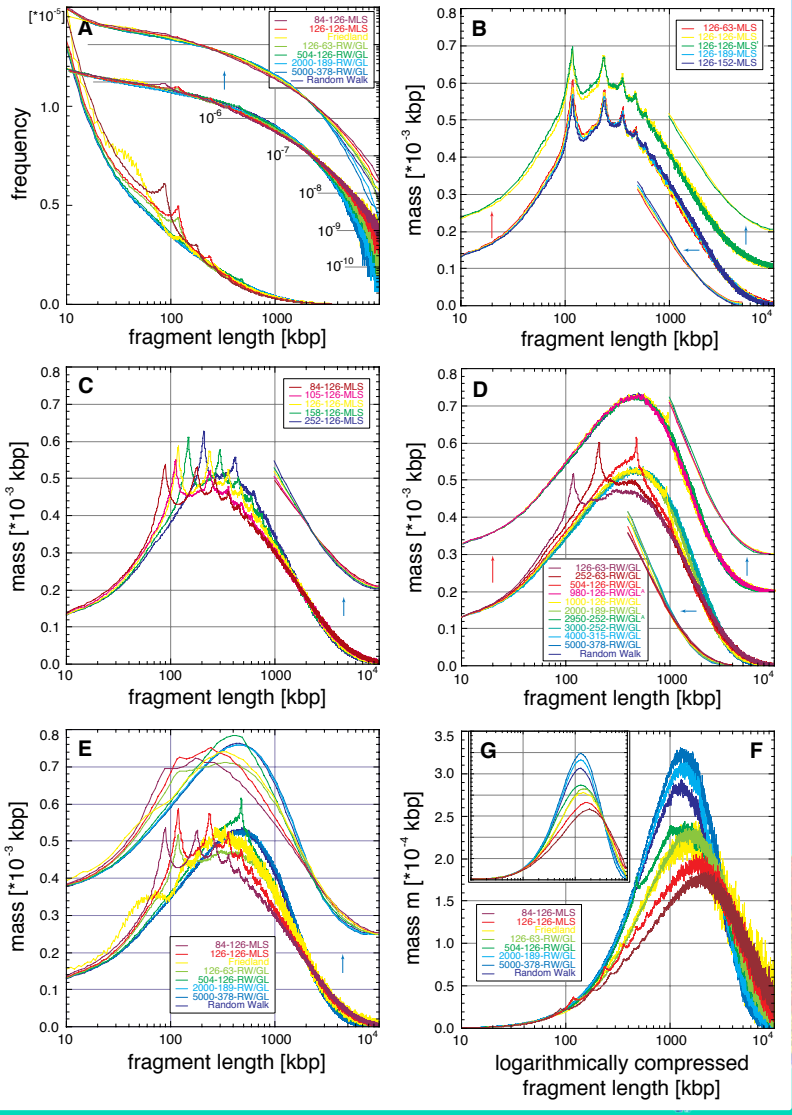

DNA Fragment Distribution after Ione-Irradiation

The length distribution of DNA fragments after irradiation with e. g. C or Ca with an inhomogeneous spatial double strand breackage probability depends on the detailed folding topology of the chromati fiber and the RW/GL and MLS models differ largely.

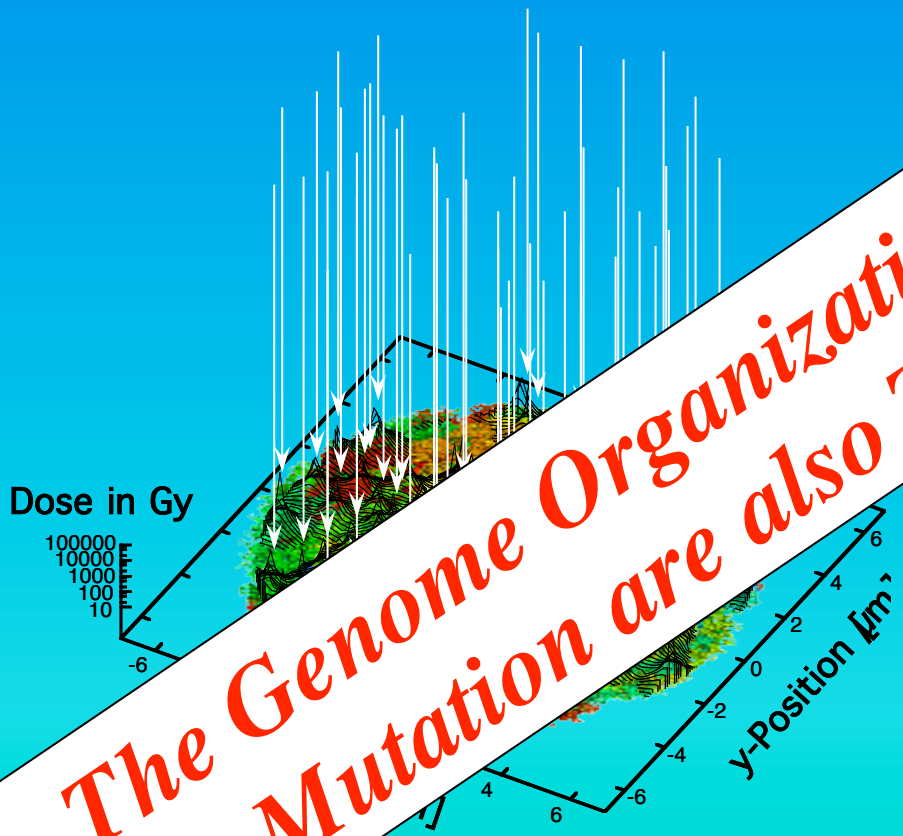

The Genome Organization and Evolution by Mutation are also Tightly Entangled !

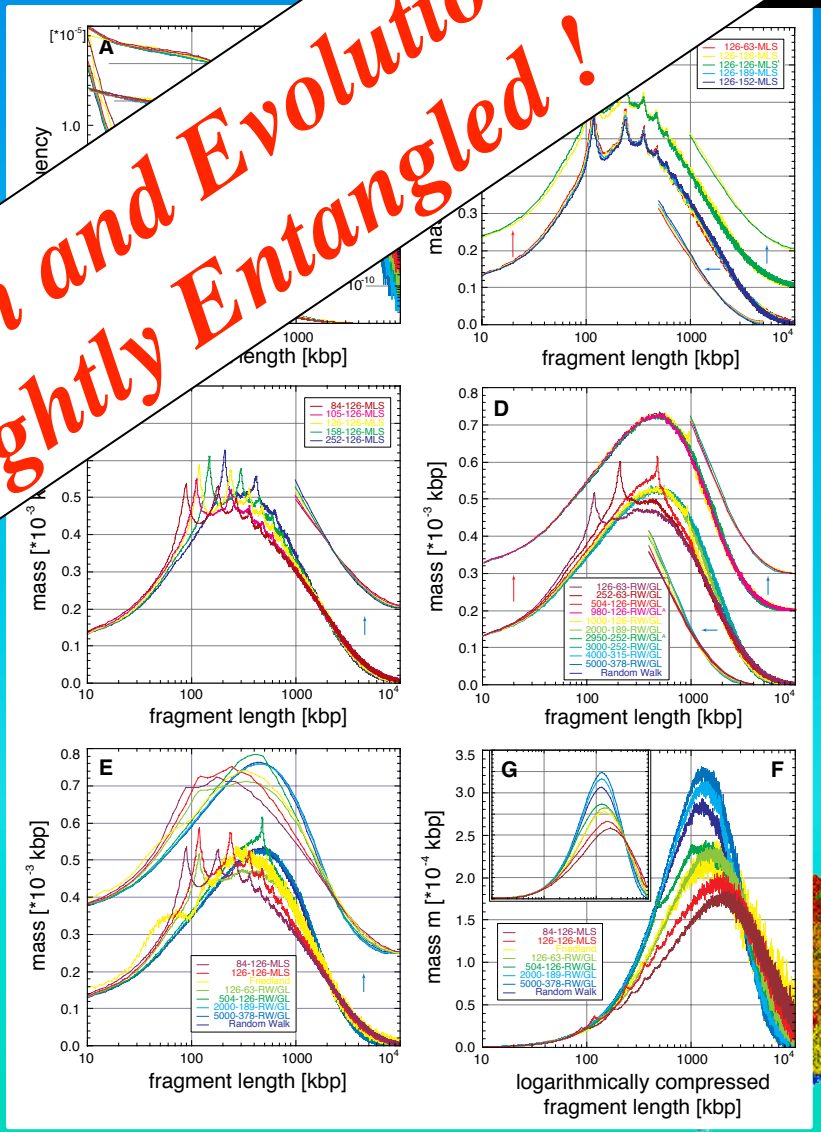

Conclusion

The compacted chromatin quasi-fibre, folds into loop-aggregates connected by a linker !

Every structural level of nuclear organization including its dynamics is connected and represented in all the other levels in a holistic systems genomics manner.

- **The 3D genomes architecture consists of chromatin quasi-fibres (5±1 nuc. / 11 nm, L_p of 80-120 nm), forming stable loop aggregates/rosettes (~40-100 kbp loops, ~60 kbp linkers).**
- **The dynamics of genomes follows the 3D genome architecture in detail and determines in an inseparable entanglement with the architecture genome function.**
- **From the single base pair to the entire cell nucleus, all genomic levels represent all other levels and by modification a code is present and used to store genetic information.**
- **Genomes have a consensus organization with only small variation from the basic theme on each compaction level of the genome and these small variations determine genome function.**
- **Genome organization and function cannot be determined or understood from a single organizational level but only in a holistic systems genomics manner integrating all parts of the system.**
- **The genome behaves on the basis of a genomic statistical mechanics with a genomic uncertainty principle attached !**

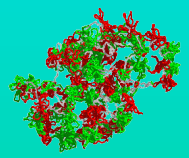

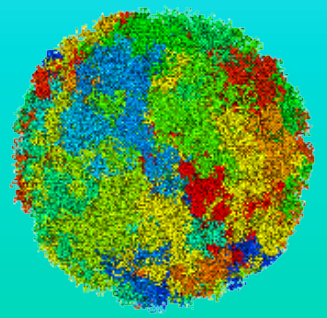

Acknowledgements

Thanks go to all the lab local lab members, those people who supported this work in the last decades, the institutions providing their infrastructure, and the national and international computing infrastructures.

Special thanks go to the reviewers, the EraSysBio+ initiative and the national and EU funding bodies.

Erasmus MC

Nick Kepper
Michael Lesnussa
Anis Abuseiris
A.M. Ali Imam
Petros Kolovos
Harmen J. G. van de Werken
Jessica Zuin
Christel E. M. Kockx
Rutger W. W. Brouwer
Wilfred F. J. van Ijken
Kerstin S. Wendt
Frank G. Grosveld

Cell Biology & Biophysics

EMBL

Malte Wachsmuth

EpiGenSys

EraSysBio+ Consortium Labs

Peter R. Cook
Gernot Längst
Tobias A. Knoch
Karsten Rippe
Gero Wedemann

Erasmus Medical Center and BioQuant & German Cancer Research Center

High-Performance Computing Center Stuttgart, University of Stuttgart; Supercomputing Center Karlsruhe, University of Karlsruhe; Computing Center, Deutsches Krebsforschungszentrum Heidelberg (DKFZ)

Erasmus Medical Center, Hogeschool Rotterdam, The Fraunhofer Society, The German MediGRID and Services@MediGRID Projects, The German D-Grid Initiatives, The German Ministry for Science and Technology, The Dutch Science Organization (NCF), The European EGEE Initiative, The European EDGES Consortium, The German Society for Human Ecology, The International Society for Human Ecology, The European Commission

Acknowledgements

Thanks go also to all those people who supported this work in the last decades,
the institutions providing their infrastructure, and the national and international computing infrastructures.

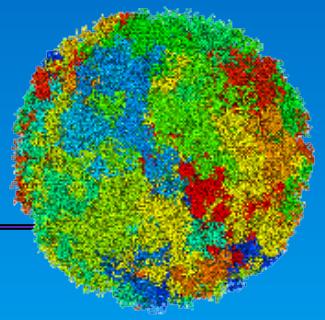

Cell Biology & Biophysics
EMBL
Malte Wachsmuth

Biophysics, LMU
Thomas Weidemann

CALTECH
Katalin Fejes-Toth

Genome Org & Function
BioQuant/DKFZ
Karsten Rippe

Biophysical Genomics,
Cell Biology, Erasmus MC
Petros Kolovos
Anis Abuseiris
Michael Lesnussa
Rob de Graaf
Nick Kepper
Frank Grossveld

LMU Munich
Peter Quicken
Anna Friedl

Biological Sciences, UCSD
Suchit Jhunjhunwala
Menno van Zelm
Cornelis Murre

Clinical Genetics
Erasmus MC
Bert Eussen
Annelies de Klein

University Braunschweig
Markus Göker

The Cremer Labs
Joachim Rauch
Irina Solovei
Michael Hausmann
Christoph Cremer
Thomas Cremer

Molecular Genetics
DKFZ
Karsten Richter
Peter Lichter

Biophysics of Macromolecules
DKFZ
Gabriele Müller
Waldemar Waldeck
Jörg Langowski

Supercomputing Center
Karlsruhe
Rudolph Lohner

Erasmus Medical Center and BioQuant & German Cancer Research Center

High-Performance Computing Center Stuttgart, University of Stuttgart; Supercomputing Center Karlsruhe, University of Karlsruhe; Computing Center, Deutsches Krebsforschungszentrum Heidelberg (DKFZ)

Erasmus Medical Center, Hogeschool Rotterdam, The Fraunhofer Society, The German MediGRID and Services@MediGRID, The German D-Grid Initiatives, The German Ministry for Science and Technology, The Dutch Science Organization (NOW), The European EGEE Initiative, The European EDGES Consortium, The German Society for Human Ecology, The International Society for Human Ecology,
The European Commission

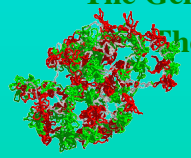

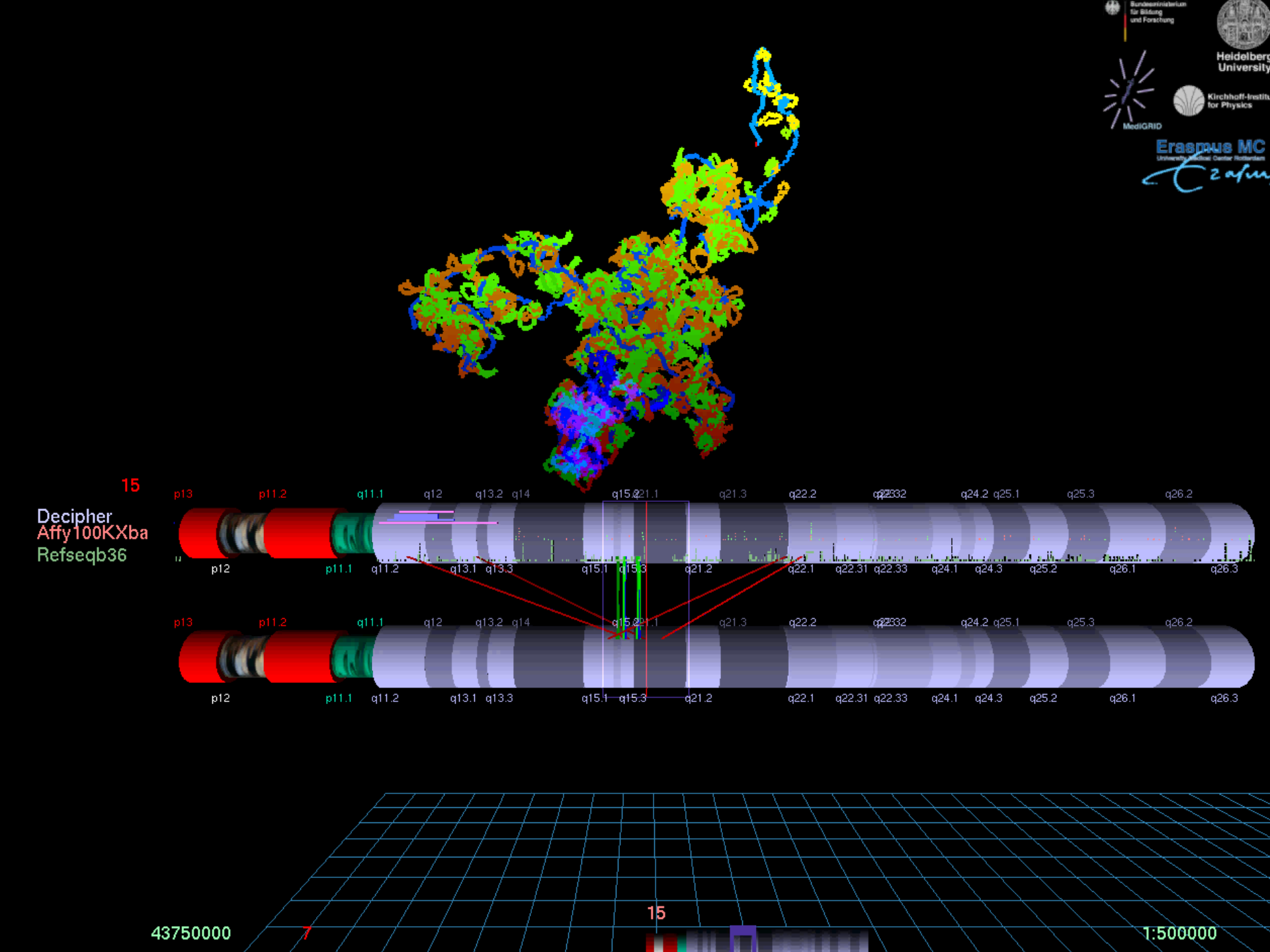
Heidelberg University
Kirchhoff-Institute for Physics
MediGRID
Erasmus MC
15
Decipher
Affy100KXba
Refseqb36
p13 p11.2 q11.1 q12 q13.2 q14 q15.2 q21.1 q21.3 q22.2 q24.2 q25.1 q25.3 q26.2
p12 p11.1 q11.2 q13.1 q13.3 q15.1 q15.3 q21.2 q22.1 q22.31 q22.33 q24.1 q24.3 q25.2 q26.1 q26.3
43750000
15
1:500000

The
Detailed 3D Multi-Loop Aggregate/Rosette Chromatin Architecture
and
Functional Dynamic Organization
of the
Human and Mouse Genome

Knoch, T. A.

New York University, New York, New York, USA, 11th December, 2014.

Abstract

The dynamic three-dimensional chromatin architecture of genomes and the obvious co-evolutionary connection to its function – the storage and expression of genetic information – is still, after ~170 years, a central question of current research. With a systems genomics approach using a novel selective high-throughput chromosomal interaction capture (T2C) technique together with quantitative polymer simulations and scaling analysis of genomic structures and the DNA sequence, we determined the architecture of genomes with unprecedented molecular resolution and dynamic range from single base pair entire chromosomes: for several genetic loci of different species, cell type, and functional states we find a chromatin quasi-fibre exists with 5±1 nucleosome per 11 nm, which folds into 40-100 kbp loops forming aggregates/rosettes which are connected by a ~50 kbp chromatin linker. Polymer simulations using Monte Carlo and Brownian dynamics approaches confirm T2C results and allow to predict and to explain additional experimental findings. This agrees also with novel dynamics information from fluorescence correlation spectroscopy (FCS) analysis of chromatin relaxations *in vivo*. Beyond, we find a fine-structured multi-scaling behaviour of both the architecture and the DNA sequence, which shows for the first time the tight entanglement between architecture and sequence. Since, T2C allows reaching an optimal combination of resolution, interaction frequency range, multiplexing, and an unseen signal-to-noise ratio at molecular resolution this, hence, opens the door to architectural sequencing of genomes. Additionally, we have reached the level of genome mechanics, i.e. corresponding statistical mechanics and uncertainty principles appear and need to be considered.
Hence, we determined the three-dimensional architecture and dynamics of genomes for the first time in a consistent system genomics manner from several angles which are all in agreement as well as additionally also with the heuristics of the research of the last 170 years. This will lead to a detailed understanding of genomes with fundamental new insights and huge novel perspectives for diagnosis and treatment.

Corresponding author email contact: TA.Knoch@taknoch.org

Keywords:

Genome, genomics, genome organization, genome architecture, structural sequencing, architectural sequencing, systems genomics, coevolution, holistic genetics, genome mechanics, genome statistical mechanics, genomic uncertainty principle, multilism genotype-phenotype, genome function, genetics, gene regulation, replication, transcription, repair, homologous recombination, simultaneous co-transfection, cell division, mitosis, metaphase, interphase, cell nucleus, nuclear structure, nuclear organization, chromatin density distribution, nuclear morphology, chromosome territories, subchromosomal domains, chromatin loop aggregates, chromatin rosettes, chromatin loops, chromatin quasi fibre, chromatin density, persistence length, spatial distance measurement, histones, H1.0, H2A, H2B, H3, H4, mH2A1.2, DNA sequence, complete sequenced genomes, molecular transport, obstructed diffusion, anomalous diffusion, percolation, long-range correlations, fractal analysis, scaling analysis, exact yard-stick dimension, box-counting dimension, lacunarity dimension, local nuclear dimension, nuclear diffuseness, parallel super computing, grid computing, volunteer computing, polymer model, analytic mathematical model, Brownian Dynamics, Monte Carlo, fluorescence *in situ* hybridization (FISH), targeted chromatin capture (T2C) confocal laser scanning microscopy, fluorescence correlation spectroscopy, spatial precision distance microscopy, super-resolution microscopy, two dimensional fluorescence correlations spectroscopy (2D-FCS) auto-fluorescent proteins, CFP, GFP, YFP, DsRed, fusion protein, *in vivo* labelling, information browser, visual data base access, holistic viewing system, integrative data management, extreme visualization, three-dimensional virtual environment, virtual paper tool, human ecology, e-human grid ecology, society, social systems, e-social challenge, inverse tragedy of the commons, grid phenomenon, micro-sociality, macro-sociality, autopoietic tragedy of social sub-systems, micro subsystems, macro subsystems, micro operationality, macro operationality, grid psychology micro riskmanagement, macro riskmanagement.

Literature References

Knoch, T. A. Dreidimensionale Organisation von Chromosomen-Domänen in Simulation und Experiment. (Three-dimensional organization of chromosome domains in simulation and experiment.) *Diploma Thesis*, Faculty for Physics and Astronomy, Ruperto-Carola University, Heidelberg, Germany, 1998, and TAK Press, Tobias A. Knoch, Mannheim, Germany, ISBN 3-00-010685-5 and ISBN 978-3-00-010685-9 (soft cover, 2rd ed.), ISBN 3-00-035857-9 and ISBN 978-3-00-0358857-0 (hard cover, 2rd ed.), ISBN 3-00-035858-7, and ISBN 978-3-00-035858-6 (DVD, 2rd ed.), 1998.

Knoch, T. A., Münkel, C. & Langowski, J. Three-dimensional organization of chromosome territories and the human cell nucleus - about the structure of a self replicating nano fabrication site. *Foresight Institute - Article Archive*, Foresight Institute, Palo Alto, *CA, USA,* http://www. foresight.org, 1- 6, 1998.

Knoch, T. A., Münkel, C. & Langowski, J. Three-Dimensional Organization of Chromosome Territories and the Human Interphase Nucleus. *High Performance Scientific Supercomputing*, editor Wilfried Juling, Scientific Supercomputing Center (SSC) Karlsruhe, University of Karlsruhe (TH), 27- 29, 1999.

Knoch, T. A., Münkel, C. & Langowski, J. Three-dimensional organization of chromosome territories in the human interphase nucleus. *High Performance Computing in Science and Engineering 1999*, editors Krause, E. & Jäger, W., High-Performance Computing Center (HLRS) Stuttgart, University of Stuttgart, Springer Berlin-Heidelberg-New York, ISBN 3-540-66504-8, 229-238, 2000.

Bestvater, F., **Knoch, T. A.**, Langowski, J. & Spiess, E. GFP-Walking: Artificial construct conversions caused by simultaneous cotransfection. *BioTechniques* 32(4), 844-854, 2002.

Gil-Parado, S., Fernández-Montalván, A., Assfalg-Machleidt, I., Popp, O., Bestvater, F., Holloschi, A., **Knoch, T. A.**, Auerswald, E. A., Welsh, K., Reed, J. C., Fritz, H., Fuentes-Prior, P., Spiess, E., Salvesen, G. & Machleidt, W. Ionomycin-activated calpain triggers apoptosis: A probable role for Bcl-2 family members. *J. Biol. Chem.* 277(30), 27217-27226, 2002.

Knoch, T. A. (editor), Backes, M., Baumgärtner, V., Eysel, G., Fehrenbach, H., Göker, M., Hampl, J., Hampl, U., Hartmann, D., Hitzelberger, H., Nambena, J., Rehberg, U., Schmidt, S., Weber, A., & Weidemann, T. Humanökologische Perspectiven Wechsel - Festschrift zu Ehren des 70. Geburtstags von Prof. Dr. Kurt Egger. Human Ecology Working Group, Ruperto-Carola University of Heidelberg, Heidelberg, Germany, 2002.

Knoch, T. A. Approaching the three-dimensional organization of the human genome: structural-, scaling- and dynamic properties in the simulation of interphase chromosomes and cell nuclei, long- range correlations in complete genomes, *in vivo* quantification of the chromatin distribution, construct conversions in simultaneous co-transfections. *Dissertation*, Ruperto-Carola University, Heidelberg, Germany, and TAK†Press, Tobias A. Knoch, Mannheim, Germany, ISBN 3-00-009959-X and ISBN 978-3-00-009959-5 (soft cover, 3rd ed.), ISBN 3-00-009960-3 and ISBN 978-3-00-009960-1 (hard cover, 3rd ed.), ISBN 3-00-035856-9 and ISBN 978-3-00-010685-9 (DVD, 3rd ed.) 2002.

Westphal, G., van den Berg-Stein, S., Braun, K., **Knoch, T. A.**, Dümmerling, M., Langowski, J., Debus, J. & Friedrich, E. Detection of the NGF receptors TrkaA and p75NTR and effect of NGF on the growth characteristics of human tumor cell lines. *J. Exp. Clin. Canc. Res.* 21(2), 255-267, 2002.

Westphal, G., Niederberger, E., Blum, C., Wollman, Y., **Knoch, T. A.**, Dümmerling, M., Rebel, W., Debus, J. & Friedrich, E. Erythropoietin Receptor in Human Tumor Cells: Expression and Aspects Regarding Functionality. *Tumori* 88(2), 150-159, 2002.

Gil-Parado, S., Popp, O., **Knoch, T. A.**, Zahler, S., Bestvater, F., Felgenträger, M., Holoshi, A., Fernández-Montalván, A., Auerswald, E. A., Fritz, H., Fuentes-Prior, P., Machleidt, W. & Spiess, E. Subcellular localization and subunit interactions of over-expressed human µ-calpain. *J. Biol. Chem. 278(18),* 16336-15346, 2003.

Knoch, T. A. Towards a holistic understanding of the human genome by determination and integration of its sequential and three-dimensional organization. *High Performance Computing in Science and Engineering 2003*, editors Krause, E., Jäger, W. & Resch, M., High-Performance Computing Center (HLRS) Stuttgart, University of Stuttgart, Springer Berlin-Heidelberg-New York, ISBN 3- 540-40850-9, 421-440, 2003.

Wachsmuth, M., Weidemann, T., Müller, G., Urs W. Hoffmann-Rohrer, **Knoch, T. A.**, Waldeck, W. & Langowski, J. Analyzing intracellular binding and diffusion with continuous fluorescence photobleaching. *Biophys. J.* 84(5), 3353-3363, 2003.

Weidemann, T., Wachsmuth, M., **Knoch, T. A.**, Müller, G., Waldeck, W. & Langowski, J. Counting nucleosomes in living cells with a combination of fluorescence correlation spectroscopy and confocal imaging. *J. Mol. Biol.* 334(2), 229-240, 2003.

Fejes Tóth, K., **Knoch**, **T. A.**, Wachsmuth, M., Frank-Stöhr, M., Stöhr, M., Bacher, C. P., Müller, G. & Rippe, K. Trichostatin A induced histone acetylation causes decondensation of interphase chromatin. *J. Cell Science* 177, 4277-4287, 2004.

Ermler, S., Krunic, D., **Knoch, T. A.**, Moshir, S., Mai, S., Greulich-Bode, K. M. & Boukamp, P. Cell cycle-dependent 3D distribution of telomeres and telomere repeat-binding factor 2 (TRF2) in HaCaT and HaCaT-myc cells. *Europ. J. Cell Biol.* 83(11-12), 681-690, 2004.

Kost, C., Gama de Oliveira, E., **Knoch, T. A.** & Wirth, R. Spatio-temporal permanence and plasticity of foraging trails in young and mature leaf-cutting ant colonies (*Atta spp.*). *J. Trop. Ecol.* 21(6), 677- 688, 2005.

Winnefeld, M., Grewenig, A., Schnölzer, M., Spring, H., **Knoch, T. A.**, Gan, E. C., Rommelaere, J. & Cziepluch, C. Human SGT interacts with BAG-6/Bat-3/Scythe and cells with reduced levels of either protein display persistence of few misaligned chromosomes and mitotic arrest. *Exp. Cell Res.* 312, 2500-2514, 2006.

Sax, U., Weisbecker, A., Falkner, J., Viezens, F., Yassene, M., Hartung, M., Bart, J., Krefting, D., **Knoch, T. A.** & Semler, S. Grid-basierte Services für die elektronische Patientenakte der Zukunft. *E- HEALTH-COM - Magazin für Gesundheitstelematik und Telemedizin*, 4(2), 61-63, 2007.

de Zeeuw, L. V., **Knoch, T. A.,** van den Berg, J. & Grosveld, F. G. Erasmus Computing Grid - Het bouwen van een 20 TeraFLOP virtuelle supercomputer. *NIOC proceedings 2007 - het perspective of lange termijn*. editor Frederik, H. NIOC, Amsterdam, The Netherlands, 52-59, 2007.

Rauch, J., **Knoch, T. A.** , Solovei, I., Teller, K. Stein, S., Buiting, K., Horsthemke, B., Langowski, J., Cremer, T., Hausmann, M. & Cremer, C. Lightoptical precision measurements of the Prader- Willi/Angelman Syndrome imprinting locus in human cell nuclei indicate maximum condensation changes in the few hundred nanometer range. *Differentiation* 76(1), 66-82, 2008.

Sax, U., Weisbecker, A., Falkner, J., Viezens, F., Mohammed, Y., Hartung, M., Bart, J., Krefting, D., **Knoch, T. A.** & Semler, S. C. Auf dem Weg zur individualisierten Medizin - Grid-basierte Services für die EPA der Zukunft. *Telemedizinführer Deutschland 2008*, editor Jäckel, A. Deutsches Medizinforum, Minerva KG, Darmstadt, ISBN 3-937948-06-6, ISBN-13 9783937948065, 47-51, 2008.

Drägestein, K. A., van Capellen, W. A., van Haren, J. Tsibidis, G. D., Akhmanova, A., **Knoch, T. A.**, Grosveld, F. G. & Galjart, N. Dynamic behavior of GFP-CLIP-170 reveals fast protein turnover on microtubule plus ends. *J. Cell Biol. 180(4)*, 729-737, 2008.

Jhunjhunwala, S., van Zelm, M. C., Peak, M. M., Cutchin, S., Riblet, R., van Dongen, J. J. M., Grosveld, F. G., **Knoch, T. A.**[+] & Murre, C.[+] The 3D-structure of the Immunoglobulin Heavy Chain Locus: implications for long-range genomic interactions. *Cell 133(2)*, 265-279, 2008.

Krefting, D., Bart, J., Beronov, K., Dzhimova, O., Falkner, J., Hartung, M., Hoheisel, A., **Knoch, T. A.**, Lingner, T., Mohammed, Y., Peter, K., Rahm, E., Sax, U., Sommerfeld, D., Steinke, T., Tolxdorff, T., Vossberg, M., Viezens, F. & Weisbecker, A. MediGRID - Towards a user friendly secured grid infrastructure. *Future Generation Computer Systems 25(3)*, 326-336, 2008.

Knoch, T. A., Lesnussa, M., Kepper, F. N., Eussen, H. B., & Grosveld, F. G. The GLOBE 3D Genome Platform - Towards a novel system-biological paper tool to integrate the huge complexity of genome organization and function. *Stud. Health. Technol. Inform. 147*, 105-116, 2009.

Knoch, T. A., Baumgärtner, V., de Zeeuw, L. V., Grosveld, F. G., & Egger, K. e-Human Grid Ecology: Understanding and approaching the Inverse Tragedy of the Commons in the e-Grid Society. *Stud. Health. Technol. Inform. 147*, 269-276, 2009.

Dickmann, F., Kaspar, M., Löhnardt, B., **Knoch, T. A.,** & Sax, U. Perspectives of MediGRID. *Stud. Health. Technol. Inform. 147*, 173-182, 2009.

Knoch, T. A., Göcker, M., Lohner, R., Abuseiris, A. & Grosveld, F. G. Fine-structured multi-scaling long-range correlations in completely sequenced genomes - features, origin and classification. *Eur. Biophys. J. 38(6)*, 757-779, 2009.

Dickmann, F., Kaspar, M., Löhnhardt, B., Kepper, N., Viezens, F., Hertel, F., Lesnussa, M., Mohammed, Y., Thiel, A., Steinke, T., Bernarding, J., Krefting, D., **Knoch, T. A.** & Sax, U. Visualization in health-grid environments: a novel service and business approach. *LNCS 5745*, 150-159, 2009.

Dickmann, F., Kaspar, M., Löhnhardt, B., Kepper, N., Viezens, F., Hertel, F., Lesnussa, M., Mohammed, Y., Thiel, A., Steinke, T., Bernarding, J., Krefting, D., **Knoch, T. A.** & Sax, U. Visualization in health-grid environments: a novel service and business approach. *Grid economics and business models - GECON 2009 Proceedings, 6th international workshop, Delft, The Netherlands.* editors Altmann, J., Buyya, R. & Rana, O. F., GECON 2009, LNCS 5745, Springer-Verlag Berlin Heidelberg, ISBN 978-3-642-03863-1, 150-159, 2009.

Estrada, K.[*], Abuseiris, A.[*], Grosveld, F. G., Uitterlinden, A. G., **Knoch, T. A.**[+] & Rivadeneira, F.[+] GRIMP: A web- and grid-based tool for high-speed analysis of large-scale genome-wide association using imputed data. *Bioinformatics 25(20), 2750-2752*, 2009.

de Wit, T., Dekker, S., Maas, A., Breedveld, G., **Knoch, T. A.,** Langeveld, A., Szumska, D., Craig, R., Bhattacharya, S., Grosveld, F. G.[+] & Drabek, D. Tagged mutagenesis of efficient minos based germ line transposition. *Mol. Cell Biol 30(1)*, 66-77, 2010.

Kepper, N., Schmitt, E., Lesnussa, M., Weiland, Y., Eussen, H. B., Grosveld, F. G., Hausmann, M. & **Knoch T. A.,** Visualization, Analysis, and Design of COMBO-FISH Probes in the Grid-Based GLOBE 3D Genome Platform. *Stud. Health Technol. Inform. 159*, 171-180, 2010.

Kepper, N., Ettig, R., Dickmann, F., Stehr, R., Grosveld, F. G., Wedemann, G. & **Knoch, T. A.** Parallel high-performance grid computing: capabilities and opportunities of a novel demanding service and business class allowing highest resource efficiency. *Stud. Health Technol. Inform. 159*, 264-271, 2010.

Skrowny, D., Dickmann, F., Löhnhardt, B., **Knoch, T. A.** & Sax, U. Development of an information platform for new grid users in the biomedical field. *Stud. Health Technol. Inform. 159*, 277-282, 2010.

Knoch, T. A., Baumgärtner, V., Grosveld, F. G. & Egger, K. Approaching the internalization challenge of grid technologies into e-Society by e-Human "Grid" Ecology. *Economics of Grids, Clouds, Systems, and Services – GECON 2010 Proceedings*, 7th International Workshop, Ischia, Italy, editors Altman, J., & Rana, O. F., Lecture Notes in Computer Science (LNCS) 6296, Springer Berlin Heidelberg New York, ISSN 0302-9743, ISBN-10 3-642-15680-0, ISBN-13 978-3-642-15680-9, 116-128, 2010.

Dickmann, F., Brodhun, M., Falkner, J., **Knoch, T. A.** & Sax, U. Technology transfer of dynamic IT outsourcing requires security measures in SLAs. *Economics of Grids, Clouds, Systems, and Services – GECON 2010 Proceedings*, 7th International Workshop, Ischia, Italy, editors Altman, J., & Rana, O. F., Lecture Notes in Computer Science (LNCS) 6296, Springer Berlin Heidelberg New York, ISSN 0302-9743, ISBN-10 3-642-15680-0, ISBN-13 978-3-642-15680-9, 1-115, 2010.

Knoch, T. A. Sustained Renewability: approached by systems theory and human ecology. *Renewable Energy 2*, editors M. Nayeripour & M. Keshti, Intech, ISBN 978-953-307-573-0, 21-48, 2011.

Kolovos, P., **Knoch, T. A.**, F. G. Grosveld, P. R. Cook, & Papantonis, A. Enhancers and silencers: an integrated and simple model for their function. *Epigenetics and Chromatin 5(1)*, 1-8, 2012.

Dickmann, F., Falkner, J., Gunia, W., Hampe, J., Hausmann, M., Herrmann, A., Kepper, N., **Knoch, T. A.**, Lauterbach, S., Lippert, J., Peter, K., Schmitt, E., Schwardmann, U., Solodenko, J., Sommerfeld, D., Steinke, T., Weisbecker, A. & Sax, U. Solutions for Biomedical Grid Computing - Case Studies from the D-Grid Project Services@MediGRID. *JOCS 3(5)*, 280-297, 2012.

Estrada, K., Abuseiris, A., Grosveld, F. G., Uitterlinden, A. G., **Knoch, T. A.** & Rivadeneira, F. GRIMP: A web- and grid-based tool for high-speed analysis of large-scale genome-wide association using imputed data. *Dissection of the complex genetic architecture of human stature and osteoporosis.* cummulative dissertation, editor Estrada K., Erasmus Medical Center, Erasmus University Rotterdam, Rotterdam, The Netherlands, ISBN 978-94-6169-246-7, 25-30, 1st June 2012.

van de Corput, M. P. C., de Boer, E., **Knoch, T. A.**, van Cappellen, W. A., Quintanilla, A., Ferrand, L., & Grosveld, F. G. Super-resolution imaging reveals 3D folding dynamics of the β-globin locus upon gene activation. *J. Cell Sci. 125 (Pt 19)*, 4630-4639, 2012.

da Silva, P. S. D., Delgado Bieber, A. G., Leal, I. R., **Knoch, T. A.**, Tabarelli, M., Leal, I. R., & Wirth, R. Foraging in highly dynamic environments: leaf-cutting ants adjust foraging trail networks to pioneer plant availability. *Entomologia Experimentalis et Applicata 147*, 110-119. 2013.

Zuin, J., Dixon, J. R., van der Reijden, M. I. J. A., Ye, Z., Kolovos, P., Brouwer, R. W. W., van de Corput, M. P. C., van de Werken, H. J. G., **Knoch, T. A.**, van IJcken, W. F. J., Grosveld, F. G., Ren, B. & Wendt, K. S. Cohesin and CTCF differentially affect chromatin architecture and gene expression in human cells. *PNAS 111(3)*, 9906-1001, 2014.

Kolovos, P., Kepper, N., van den Werken, H. J. G., Lesnussa, M., Zuin, J., Brouwer, R. W. W., Kockx, C. E. M., van IJcken, W. F. J., Grosveld, F. G. & **Knoch, T. A.** Targeted Chromatin Capture (T2C): A novel high resolution high throughput method to detect genomic interactions and regulatory elements. *Epigenetics & Chromatin 7:10*, 1-17, 2014.

Diermeier, S., Kolovos, P., Heizinger, L., Schwartz, U., Georgomanolis, T., Zirkel, A., Wedemann, G., Grosveld, F. G., **Knoch, T. A.**, Merkl, R., Cook, P. R., Längst, G. & Papantonis, A. TNFα signalling primes chromatin for NF-kB binding and induces rapid and widespread nucleosome repostioning. *Genome Biology 15(12)*, 536-548, 2014.

Knoch, T. A., Wachsmuth, M., Kepper, N., Lesnussa, M., Abuseiris, A., A. M. Ali Imam, Kolovos, P., Zuin, J., Kockx, C. E. M., Brouwer, R. W. W., van de Werken, H. J. G., van IJcken, W. F. J., Wendt, K. S. & Grosveld, F. G. The detailed 3D multi-loop aggregate/rosette chromatin architecture and functional dynamic organization of the human and mouse genomes. *bioXriv preprint*, 16.07.2016.

Kolovos, P., Georgomanolis, T., Koeferle, A., Larkin, J. D., Brant, J., Nikolić, M., Gusmao, E. G., Zirkel, A., **Knoch, T. A.**, van IJcken, W. F. J., Cook, P. R., Costa, I. G., Grosveld, F. G. & Papantonis, A. Binding of nuclear kappa-B to non-canonical consensus sites reveals its multimodal role during the early inflammatory response. *Genome Research* 26(11), 1478-1489, 2016.

Wachsmuth, M., **Knoch, T. A.** & Rippe, K. Dynamic properties of independent chromatin domains measured by correlation spectroscopy in living cells. *Epigenetics & Chromatin 9:57*, 1-20, 2016.

Knoch, T. A., Wachsmuth, M., Kepper, N., Lesnussa, M., Abuseiris, A., A. M. Ali Imam, Kolovos, P., Zuin, J., Kockx, C. E. M., Brouwer, R. W. W., van de Werken, H. J. G., van IJcken, W. F. J., Wendt, K. S. & Grosveld, F. G. The detailed 3D multi-loop aggregate/rosette chromatin architecture and functional dynamic organization of the human and mouse genomes. *Epigenetics & Chromatin 9:58*, 1-22, 2016.